https://www.mdc-berlin.de/de/veroeffentlichungstypen/clinical-journal-club

Als gemeinsame Einrichtung von MDC und Charité fördert das Experimental and Clinical Research Center die Zusammenarbeit zwischen Grundlagenwissenschaftlern und klinischen Forschern. Hier werden neue Ansätze für Diagnose, Prävention und Therapie von Herz-Kreislauf- und Stoffwechselerkrankungen, Krebs sowie neurologischen Erkrankungen entwickelt und zeitnah am Patienten eingesetzt. Sie sind eingeladen, uns beizutreten. Bewerben Sie sich!

Was ist das?

An 83-year-old woman with type 2 diabetes mellitus presented with a 6-month history of painful rash. Physical examination findings are shown. The glycated hemoglobin level was 9.1% (reference value, <5.8), which had increased from a level of 6.6% measured 4 months earlier. What is the most likely diagnosis?

Acquired acrodermatitis enteropathica

Necrolytic acral erythema

● Necrolytic migratory erythema

Staphylococcal scalded skin syndrome

Stevens-Johnson syndrome

Necrolytic migratory erythema, which occurs in most patients with glucagonoma, is thought to result from a glucagon-induced catabolism that leads to amino acid deficiency, zinc depletion, and epidermal necrolysis. The patient first underwent a computed tomography of the abdomen that reveled a mass in the tail of the pancreas. Histopathological analysis from a biopsy sample of the mass was consistent with a neuroendocrine tumor. Immunohistochemical staining was positive for glucagon and a skin biopsy confirmed diagnosis.

Das **Necrolytic migratory erythema (NME)** (deutsch: *Erythema necrolyticum migrans*) ist ein charakteristischer, schmerzhafter Hautausschlag, der am häufigsten als Teil des **Glukagonom-Syndroms** auftritt. Er gilt oft als das erste sichtbare Warnzeichen für einen seltenen, glucagonproduzierenden Tumor der Bauchspeicheldrüse (Glukagonom).

Der Ausschlag verläuft typischerweise in Zyklen von etwa 7 bis 14 Tagen:

- **Beginn:** Es entstehen rote, juckende oder brennende Flecken, die sich ringförmig ausbreiten.
- **Verlauf:** Im Zentrum bilden sich Blasen, die aufplatzen und verkrusten. Die Ränder wandern weiter nach außen (migratorisch), während die Mitte unter Pigmentveränderungen abheilt.
- **Lokalisation:** Besonders betroffen sind Regionen mit hoher Reibung wie Leiste, Genitalbereich, Gesäß und die unteren Gliedmaßen, aber auch das Gesicht (um den Mund).
- **Begleitsymptome:** Häufig treten zusätzlich eine glatte, schmerzhafte Zunge (Glossitis), Entzündungen der Mundwinkel (Anguläre Cheilitis) sowie Nagelanomalien auf.

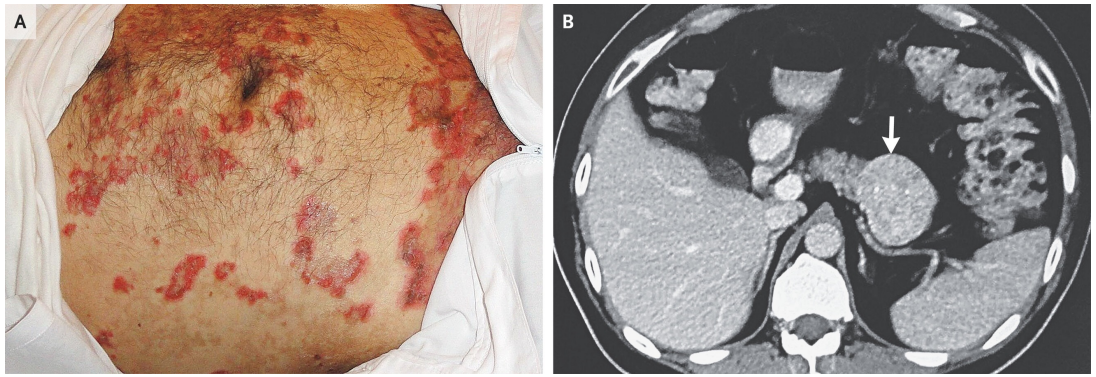

Das **Glukagonom-Syndrom** ist ein seltenes Krankheitsbild, das durch einen glukagonproduzierenden neuroendokrinen Tumor der Bauchspeicheldrüse (Glukagonom) verursacht wird. Durch die massive Überproduktion des Hormons Glukagon gerät der Stoffwechsel aus dem Gleichgewicht.

Leitsymptome (Die "4 Ds")
Klinisch ist das Syndrom oft durch eine charakteristische Kombination von Symptomen gekennzeichnet:

- **Dermatitis**: Das auffälligste Zeichen ist das **Erythema necrolyticum migrans**. Dabei handelt es sich um einen juckenden, schmerzhaften Hautausschlag mit Bläschenbildung, der oft ringförmig wandert und bevorzugt an Beinen, Gesäß und im Genitalbereich auftritt.
- **Diabetes mellitus**: Glukagon ist der Gegenspieler von Insulin und erhöht den Blutzuckerspiegel, was zu einem meist leicht ausgeprägten Diabetes führt.
- **Depression**: Psychische Veränderungen wie Depressionen oder Reizbarkeit sind häufige Begleiterscheinungen.
- **Deep Vein Thrombosis (Tiefe Venenthrombose)**: Es besteht ein deutlich erhöhtes Risiko für Blutgerinnsel und Lungenembolien.

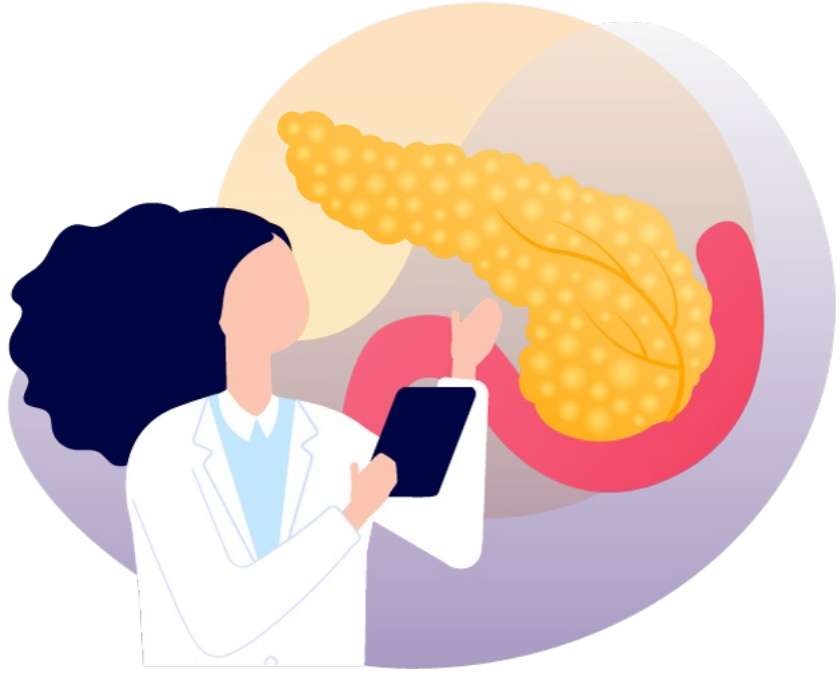

Advanced bladder cancer (Stage 3B-4) has spread beyond the bladder muscle into nearby tissue, lymph nodes, or distant organs. Common symptoms include pain in the back/pelvis, weight loss, and hematuria. Key treatments include combination chemotherapy, immunotherapy (e.g., avelumab), and sometimes surgery or radiotherapy for symptom management, according to.

Key Aspects of Advanced Bladder Cancer

- **Definition & Stages:**
  - **Locally Advanced (Stage 3):** Cancer has grown through the bladder wall into nearby tissue (uterus, prostate, vagina) or into several pelvic lymph nodes.
  - **Metastatic (Stage 4):** The cancer has spread to distant lymph nodes, bones, lungs, or liver.

- **Treatment Options:**
  - **Chemotherapy:** Often the first-line treatment (e.g., cisplatin-based) to kill cancer cells throughout the body.
  - **Immunotherapy:** Drugs such as avelumab, pembrolizumab, or atezolizumab are used to boost the immune system to fight the cancer.
  - **Radiation Therapy:** Primarily used to manage symptoms like pain or bleeding, or in combination with chemotherapy, as shown in.
  - **Surgery:** Sometimes used to remove the bladder (radical cystectomy) or to relieve symptoms.

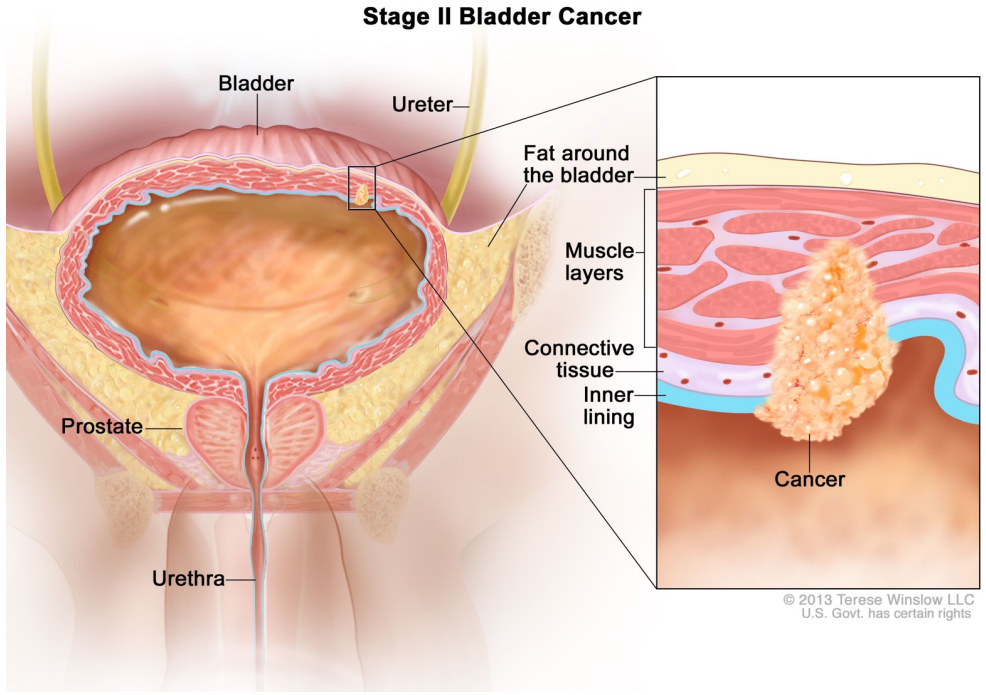

Enfortumab-Vedotin (Handelsname **Padcev**) ist ein modernes Krebsmedikament, das als **Antikörper-Wirkstoff-Konjugat (ADC)** bezeichnet wird. Es wurde speziell für die Behandlung von fortgeschrittenem oder metastasiertem **Urothelkarzinom** (Blasenkrebs) entwickelt.

Wirkungsweise

Das Medikament funktioniert wie eine „zielsuchende Rakete“:

- **Ziel**: Der Antikörper bindet gezielt an das Protein **Nectin-4**, das auf der Oberfläche vieler Blasenkrebszellen in hohen Mengen vorkommt.
- **Wirkstoff**: Nach der Bindung wird ein hochwirksames Zellgift (Monomethyl-Auristatin E, MMAE) direkt in die Krebszelle eingeschleust und zerstört diese von innen.

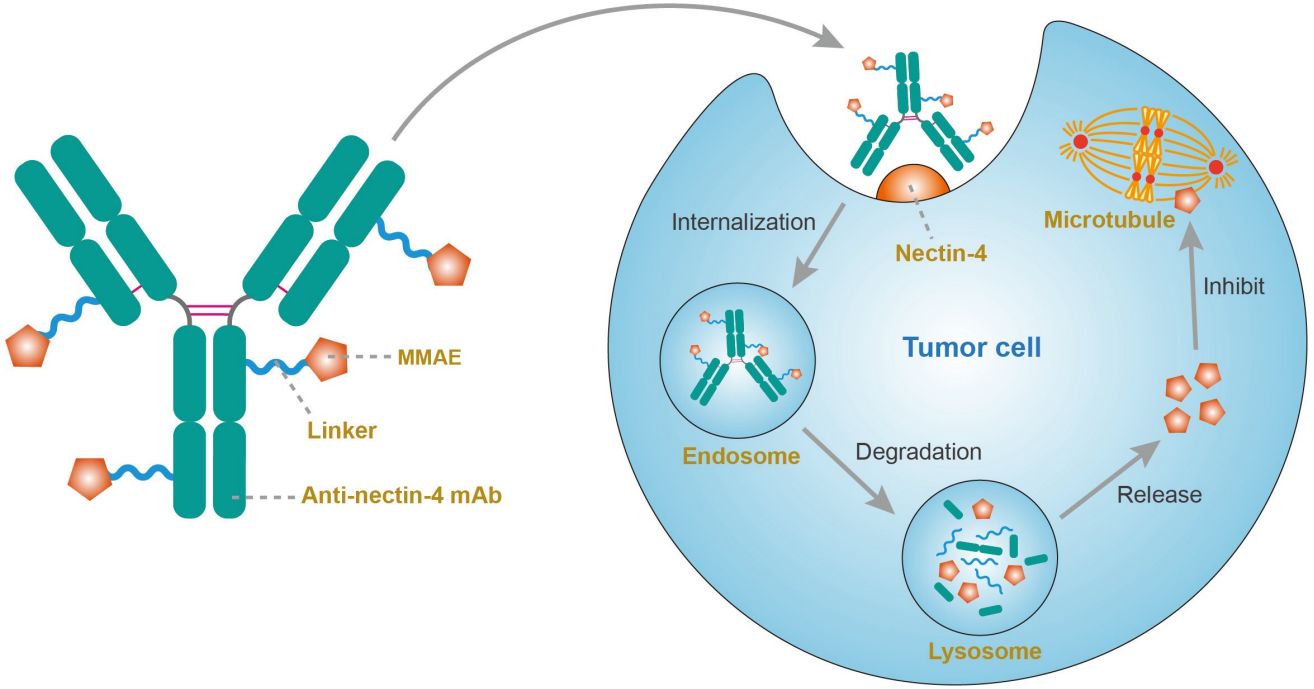

Plus

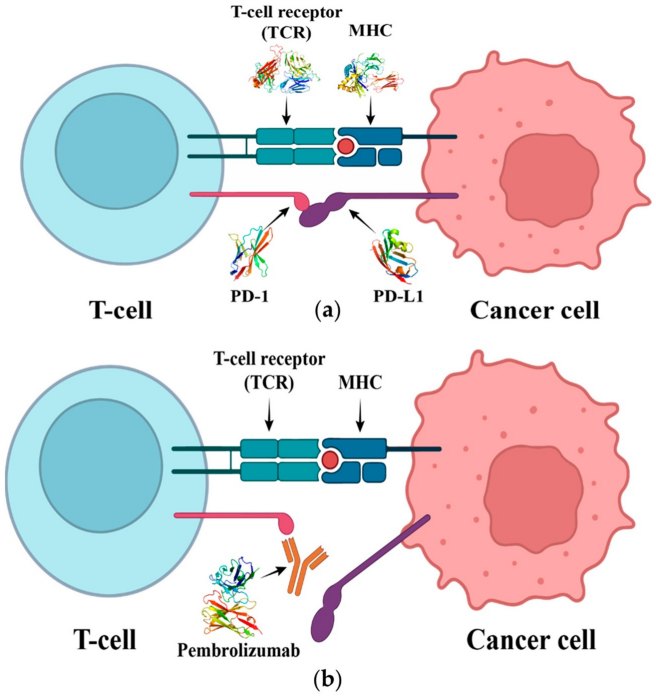

Perioperative Enfortumab Vedotin and Pembrolizumab in Bladder Cancer

Patients with muscle-invasive bladder cancer who are ineligible for cisplatin-based chemotherapy proceed directly to radical cystectomy with pelvic lymph-node dissection. Perioperative therapy may improve outcomes in this population.
In this phase 3, open-label trial, participants with muscle-invasive bladder cancer who were ineligible for or declined cisplatin-based chemotherapy were randomly assigned to perioperative (neoadjuvant and adjuvant) enfortumab vedotin, an antibody–drug conjugate directed at nectin-4, plus pembrolizumab and surgery (9 total cycles of enfortumab vedotin [1.25 mg per kilogram of body weight on days 1 and 8] plus 17 total cycles of pembrolizumab [200 mg on day 1 every 3 weeks], with surgery after 3 cycles) or surgery alone (control). The primary end point was event-free survival. Key secondary end points were overall survival and pathological complete response (absence of viable tumor after surgical resection). Other secondary end points included safety.

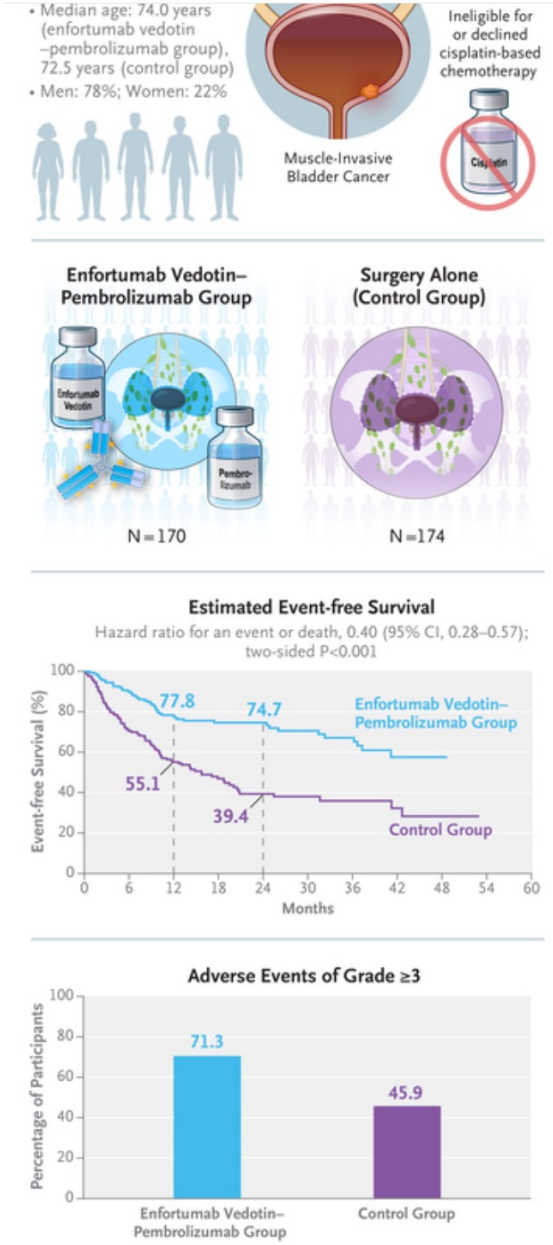

Neoadjuvant cisplatin-based chemotherapy (with or without neoadjuvant and adjuvant durvalumab or adjuvant nivolumab) and radical cystectomy with pelvic lymph node dissection is the standard of care for patients with muscle-invasive bladder cancer. However, nearly half the patients with muscle-invasive bladder cancer are ineligible for cisplatin-based chemotherapy and proceed directly to surgery.

Cisplatin ineligibility is commonly defined as meeting at least one of the following Galsky criteria: impaired renal function (creatinine clearance, <60 ml per minute), Eastern Cooperative Oncology Group (ECOG) performance-status score of 2 or higher (range, 0 to 5, with higher scores reflecting greater disability), New York Heart Association class III heart failure (range, I [asymptomatic] to IV [symptomatic at rest]), or grade 2 or higher peripheral neuropathy or audiometric hearing loss. Patients who meet these criteria are generally older, have more coexisting conditions, and have poorer outcomes than those who are eligible for cisplatin, with a reported median event-free survival of 12.1 months and 36.1% probability of remaining event-free at 3 years (although available data are limited).

The combination of enfortumab vedotin (a nectin-4–directed antibody–drug conjugate) and pembrolizumab (an anti–programmed cell death protein 1 [PD-1] antibody) showed robust antitumor activity in patients with locally advanced or metastatic urothelial carcinoma irrespective of cisplatin eligibility and represents the current first-line standard of care.

Participants

Eligible participants were adults (≥18 years of age) with clinically nonmetastatic muscle-invasive bladder cancer (stage T2 to T4a with N0M0, or T1 to T4a with N1M0) with predominantly (≥50%) urothelial histologic features, as confirmed by central pathological review. Baseline disease staging was determined through central review of both pathological findings and imaging. Participants had ECOG performance-status scores of 0 to 2, could undergo surgery, and were ineligible for or declined cisplatin-based neoadjuvant chemotherapy. Cisplatin ineligibility was defined according to the Galsky criteria, with modification to omit peripheral neuropathy). Participants provided written informed consent, and a tumor sample was obtained through transurethral resection within 60 days before enrollment for central pathological assessment of histologic features and programmed death ligand 1 (PD-L1) expression.

End Points and Assessments

The primary end point was event-free survival as assessed by blinded independent central review (central review) in the enfortumab vedotin–pembrolizumab group as compared with the control group.

Characteristic	Enfortumab Vedotin–Pembrolizumab (N=170)	Control (N=174)
Age		
Median (range) — yr	74.0 (47–87)	72.5 (46–87)
Distribution — no. (%)		
<65 yr	29 (17.1)	29 (16.7)
65 to <75 yr	63 (37.1)	77 (44.3)
≥75 yr	78 (45.9)	68 (39.1)
Male sex — no. (%)	137 (80.6)	131 (75.3)
ECOG performance-status score — no. (%)†		
0	102 (60.0)	95 (54.6)
1	47 (27.6)	53 (30.5)
2	21 (12.4)	26 (14.9)
Region — no. (%)		
United States	21 (12.4)	23 (13.2)
European Union	78 (45.9)	77 (44.3)
Rest of the world	71 (41.8)	74 (42.5)
Race or ethnic group — no. (%)‡		
American Indian or Alaska Native	0	1 (0.6)
Asian	31 (18.2)	25 (14.4)
Black	2 (1.2)	2 (1.1)
Multiple	4 (2.4)	7 (4.0)
White	132 (77.6)	136 (78.2)
Missing	1 (0.6)	3 (1.7)
Cisplatin eligibility status — no. (%)		
Ineligible	142 (83.5)	139 (79.9)
Eligible but declined	28 (16.5)	35 (20.1)
PD-L1 status — no. (%)§		
CPS <10	87 (51.2)	90 (51.7)
CPS ≥10	80 (47.1)	83 (47.7)
Missing	3 (1.8)	1 (0.6)
Tumor stage — no. (%)¶		
T2N0	30 (17.6)	32 (18.4)
T3N0 or T4aN0	133 (78.2)	132 (75.9)
T1 to T4a with N1	7 (4.1)	10 (5.7)
Creatinine clearance — no. (%)		
<30 ml/min	0	1 (0.6)
30 to <60 ml/min	102 (60.0)	101 (58.0)
≥60 ml/min	68 (40.0)	72 (41.4)
Histologic features — no. (%)		
Urothelial carcinoma with no variant histologic features	152 (89.4)	161 (92.5)
Urothelial carcinoma with glandular differentiation	6 (3.5)	3 (1.7)
Urothelial carcinoma with squamous differentiation	9 (5.3)	6 (3.4)
Urothelial carcinoma with other variant histologic features	3 (1.8)	4 (2.3)
Smoking status — no. (%)		
Never smoked	55 (32.4)	44 (25.3)
Former smoker	82 (48.2)	86 (49.4)
Current smoker	33 (19.4)	44 (25.3)

Adverse Events.

Adverse Event	Enfortumab Vedotin–Pembrolizumab (N=167)	Control (N=159)
	no. of participants with one or more events (%)	
Adverse events of any cause		
Any grade	167 (100)	103 (64.8)
Grade ≥3	119 (71.3)	73 (45.9)
Led to enfortumab vedotin dose reduction	28 (16.8)	NA
Led to discontinuation of any trial drug	81 (48.5)	NA
Led to death	13 (7.8)	9 (5.7)
Serious†	97 (58.1)	65 (40.9)
Drug-related adverse events as determined by the investigator		
Any grade	154 (92.2)	NA
Grade ≥3	76 (45.5)	NA
Led to enfortumab vedotin dose reduction	26 (15.6)	NA
Led to discontinuation of any trial drug	62 (37.1)	NA
Led to death	2 (1.2)	NA
Serious†	33 (19.8)	NA
Adverse events of special interest		
Any grade for pembrolizumab‡	72 (43.1)	NA
Grade ≥3 for pembrolizumab‡	30 (18.0)	NA
Drug-related any grade for enfortumab vedotin	123 (73.7)	NA
Drug-related grade ≥3 for enfortumab vedotin	27 (16.2)	NA

Event-free Survival.

Shown are the Kaplan–Meier estimates of event-free survival as assessed by blinded independent central review in the intention-to-treat population, which included all participants who had undergone randomization. Event-free survival was defined as the time from randomization to the first occurrence of radiographic progression precluding surgery, biopsy-proven residual muscle-invasive bladder cancer in participants who did not undergo surgery, inability of the surgeon to complete curative-intent surgery owing to an unresectable tumor or newly discovered metastatic disease, local or distant recurrence after surgery as assessed by imaging or biopsy, or death from any cause, whichever occurred first. Participants in the enfortumab vedotin (EV)–pembrolizumab (pembro) group received perioperative enfortumab vedotin and pembrolizumab and underwent surgery, and participants in the control group underwent surgery only. Tick marks indicate censored data. NR denotes not reached.

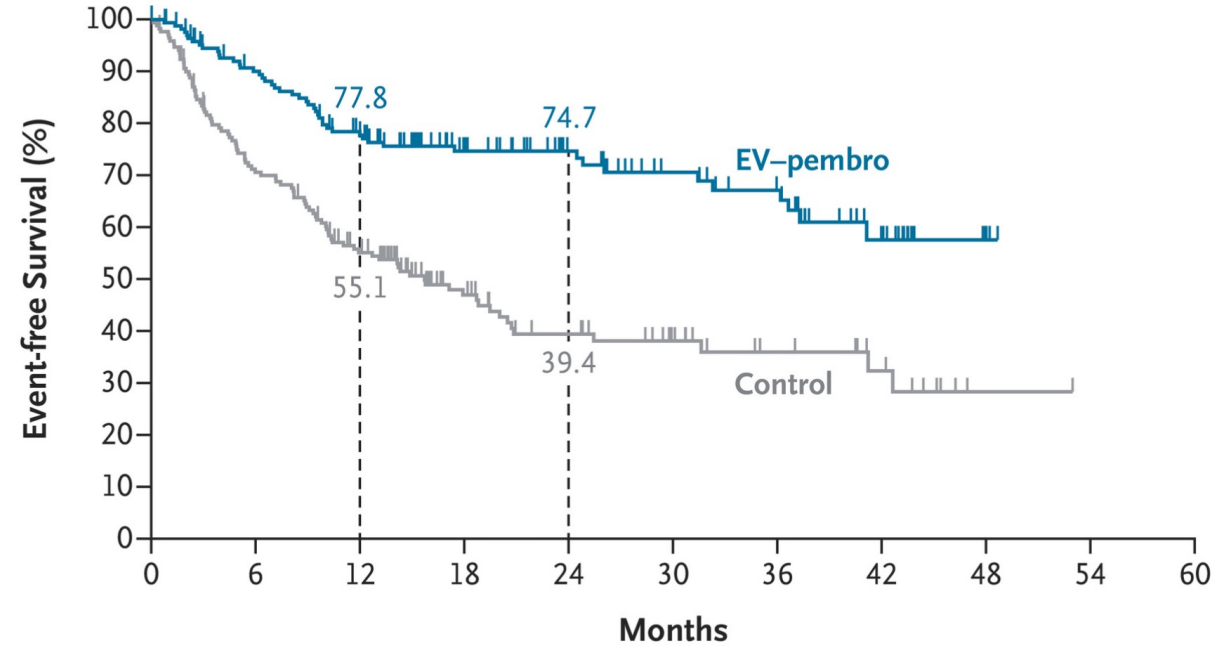

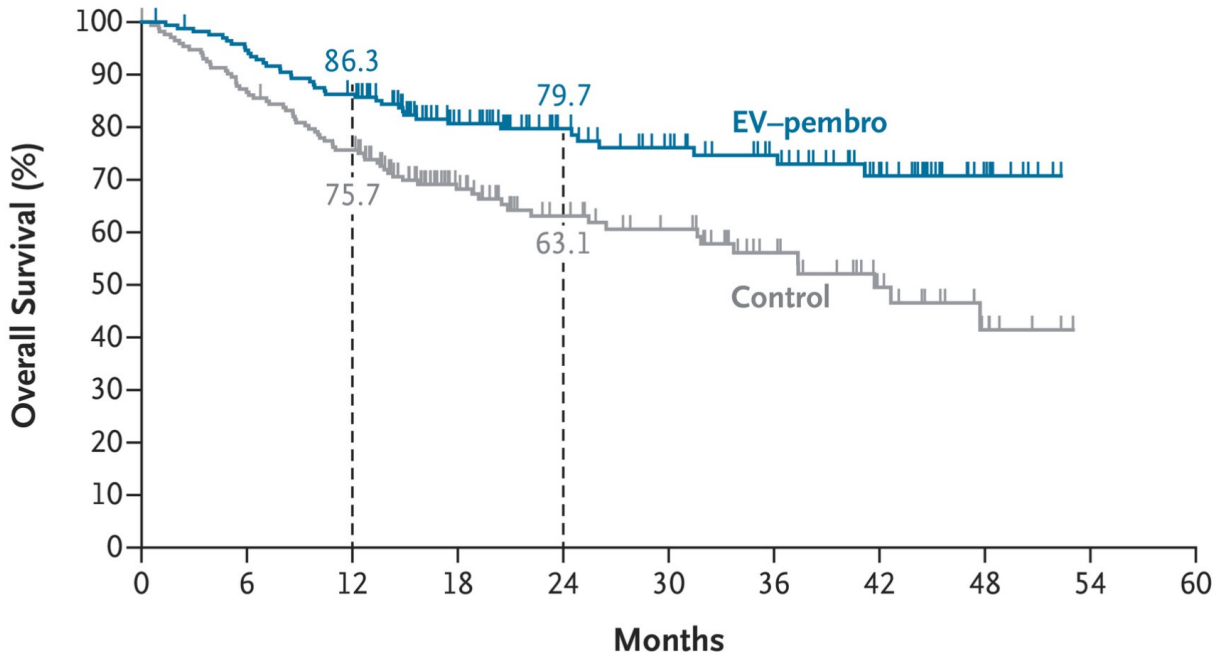

Overall Survival.

Shown are the Kaplan–Meier estimates of overall survival in the intention-to-treat population. Overall survival was defined as the time from randomization to death from any cause. Tick marks indicate censored data.

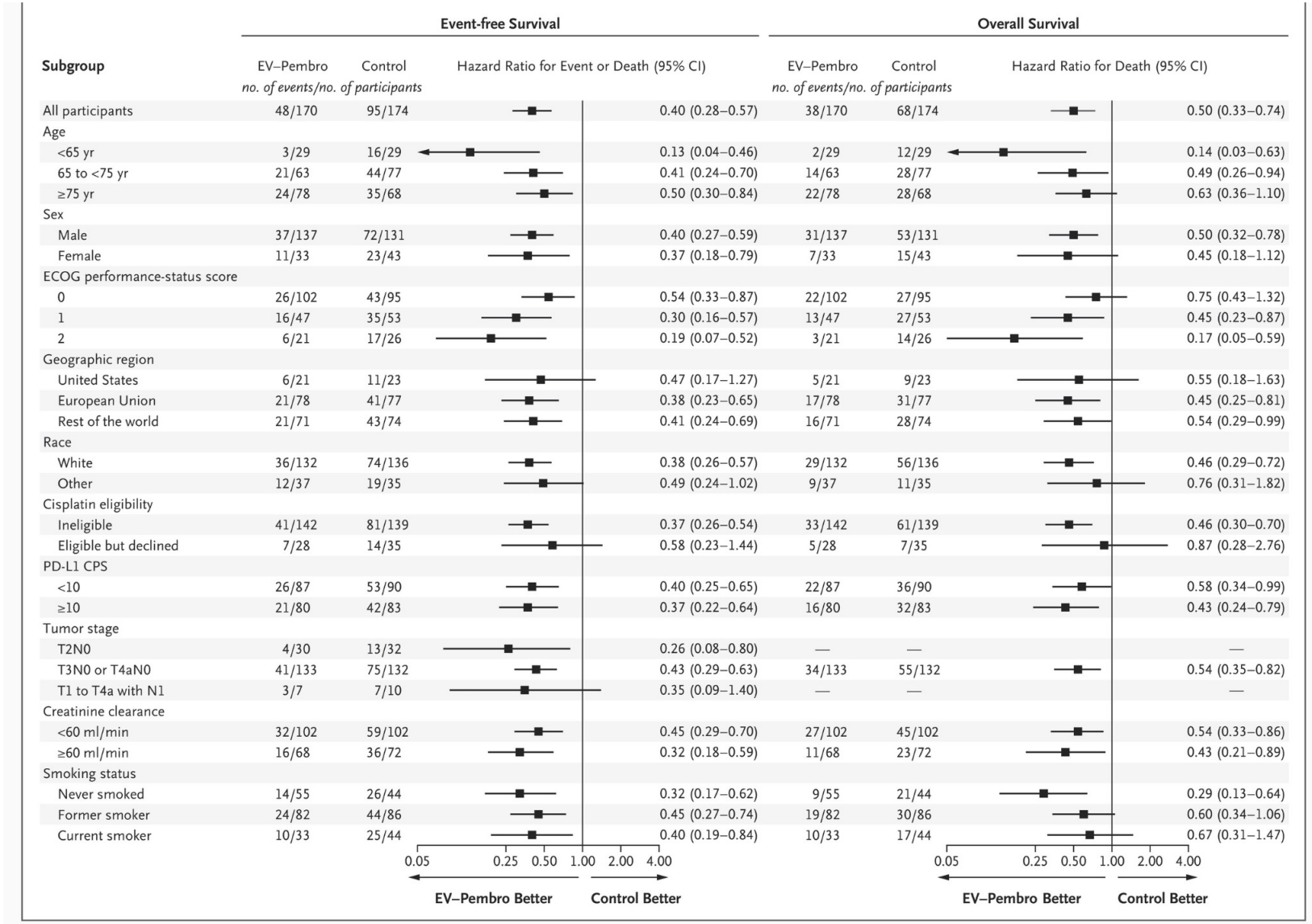

Event-free Survival and Overall Survival According to Subgroups.

Forest plots show the risk of an event or death as assessed by blinded independent central review (at left) and the risk of death (at right) in key subgroups in the intention-to-treat population. Hazard ratios and 95% confidence intervals for the subgroups were estimated with an unstratified Cox proportional-hazards model. Subgroup analyses were not adjusted for multiplicity. Subgroup categories with fewer than 10 events across both treatment groups were not included in the forest plots, including the category of missing data in the programmed death ligand 1 (PD-L1) combined positive score (CPS) and race subgroups for both event-free and overall survival and the tumor-stage categories of T2N0 and T1 to T4a with N1 for overall survival. Eastern Cooperative Oncology Group (ECOG) performance-status scores range from 0 to 5, with 0 indicating no symptoms and higher scores indicating greater disability. The CPS is defined as the number of PD-L1–staining cells, including tumor cells, lymphocytes, and macrophages, divided by the total number of viable tumor cells multiplied by 100.

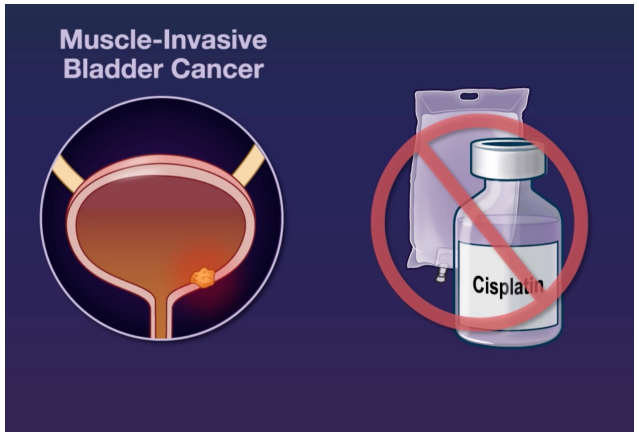
Muscle-Invasive Bladder Cancer
Cisplatin

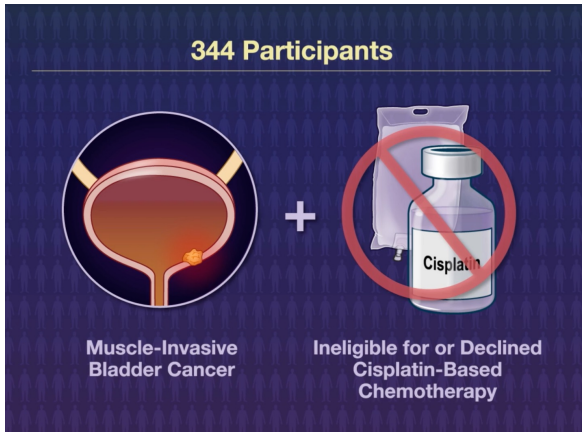
344 Participants
Muscle-Invasive Bladder Cancer
Ineligible for or Declined Cisplatin-Based Chemotherapy

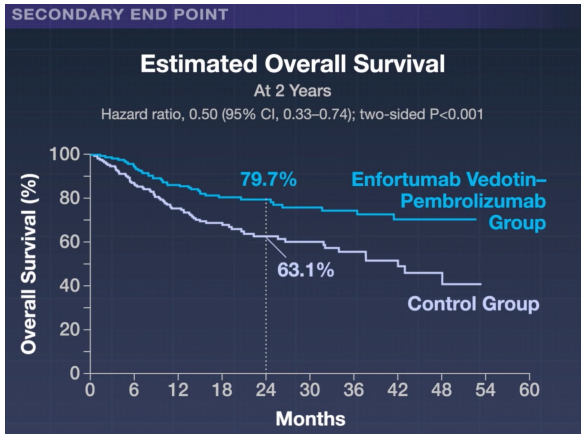
SECONDARY END POINT
Estimated Overall Survival
At 2 Years
Hazard ratio, 0.50 (95% CI, 0.33–0.74); two-sided P<0.001
Overall Survival (%)
79.7%
Enfortumab Vedotin–Pembrolizumab Group
63.1%
Control Group
Months

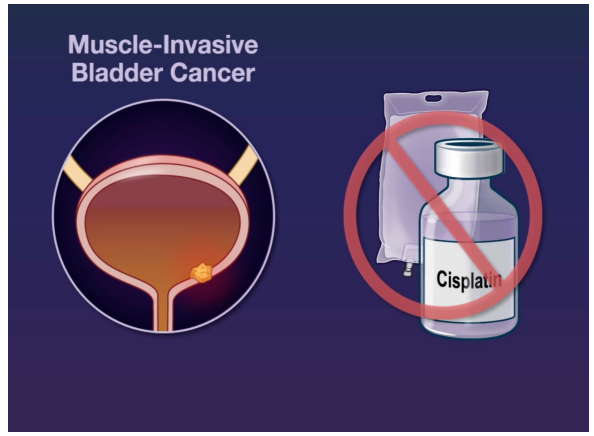
Muscle-Invasive Bladder Cancer
Cisplatin

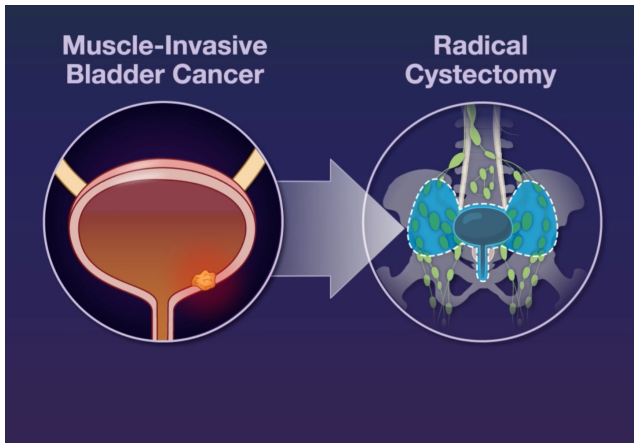
Muscle-Invasive Bladder Cancer
Radical Cystectomy

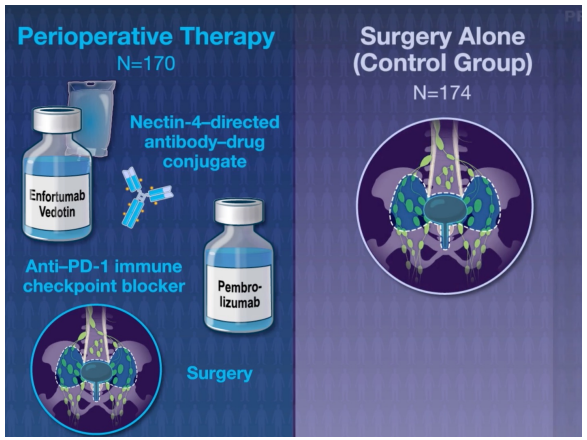
Perioperative Therapy
N=170
Nectin-4–directed antibody–drug conjugate
Enfortumab Vedotin
Anti–PD-1 immune checkpoint blocker
Pembro-lizumab
Surgery
Surgery Alone (Control Group)
N=174

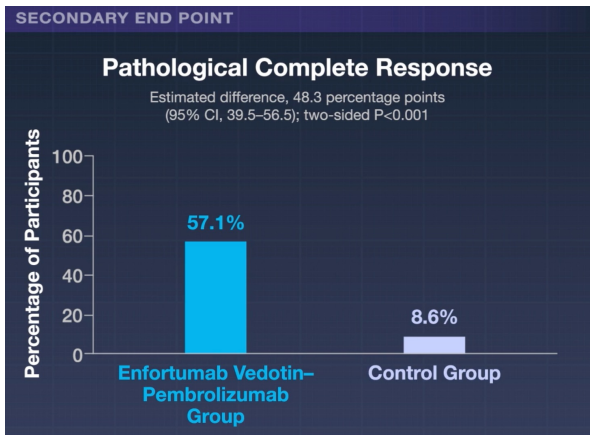
SECONDARY END POINT
Pathological Complete Response
Estimated difference, 48.3 percentage points
(95% CI, 39.5–56.5); two-sided P<0.001
Percentage of Participants
57.1%
8.6%
Enfortumab Vedotin–Pembrolizumab Group
Control Group

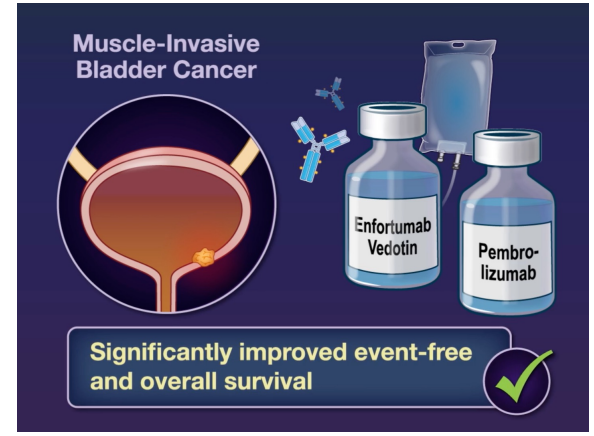
Muscle-Invasive Bladder Cancer
Enfortumab Vedotin
Pembro-lizumab
Significantly improved event-free and overall survival

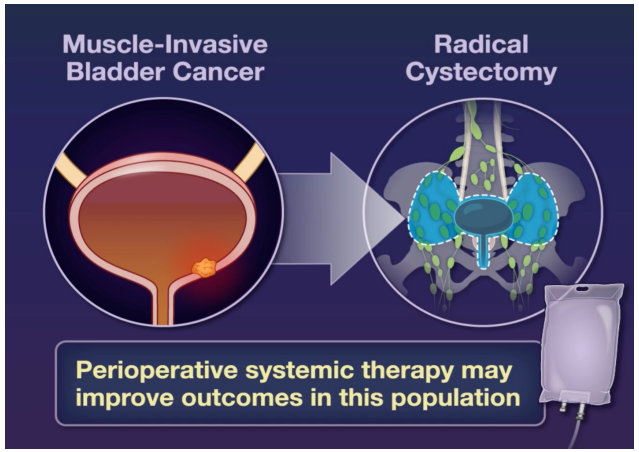
Muscle-Invasive Bladder Cancer
Radical Cystectomy
Perioperative systemic therapy may improve outcomes in this population

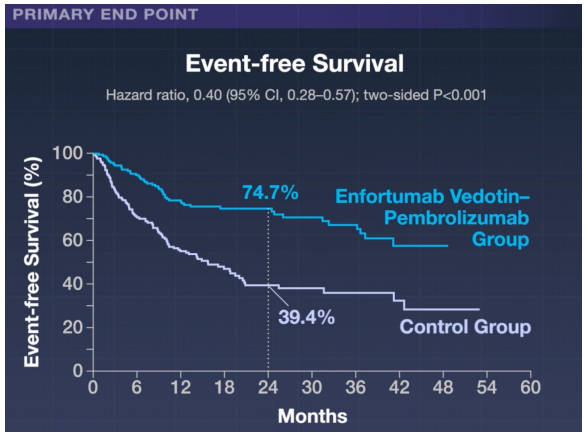
PRIMARY END POINT
Event-free Survival
Hazard ratio, 0.40 (95% CI, 0.28–0.57); two-sided P<0.001
Event-free Survival (%)
74.7%
Enfortumab Vedotin–Pembrolizumab Group
39.4%
Control Group
Months

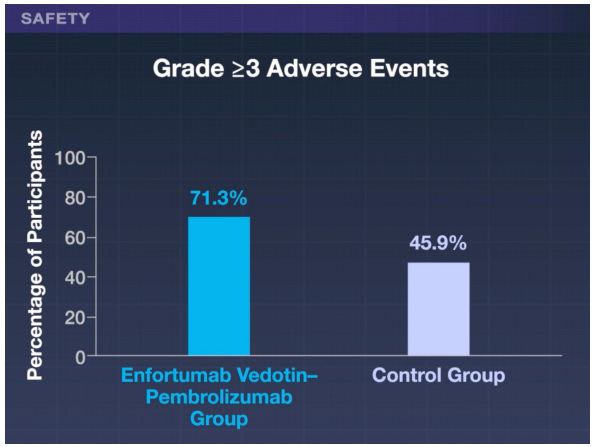
SAFETY
Grade ≥3 Adverse Events
Percentage of Participants
71.3%
45.9%
Enfortumab Vedotin–Pembrolizumab Group
Control Group

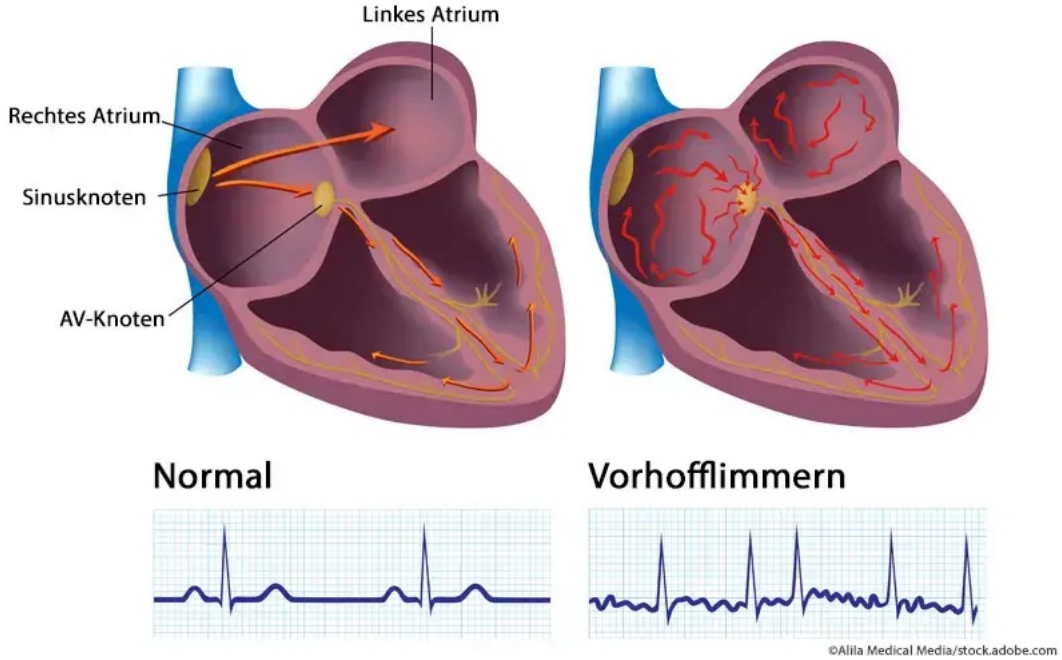
Linkes Atrium
Rechtes Atrium
Sinusknoten
AV-Knoten
Normal
Vorhofflimmern
©Alila Medical Media/stock.adobe.com

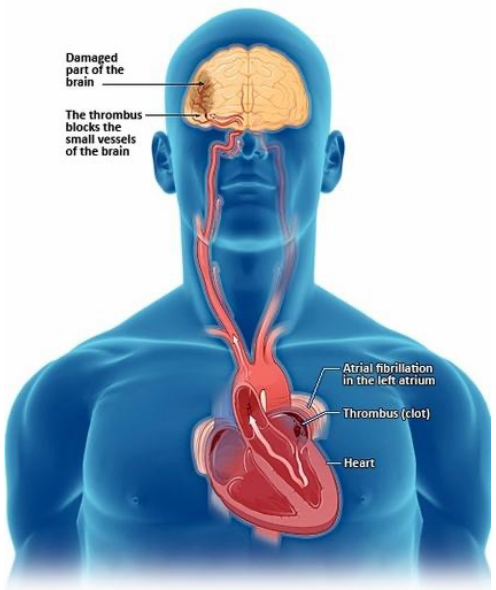
Damaged part of the brain
The thrombus blocks the small vessels of the brain
Atrial fibrillation in the left atrium
Thrombus (clot)
Heart

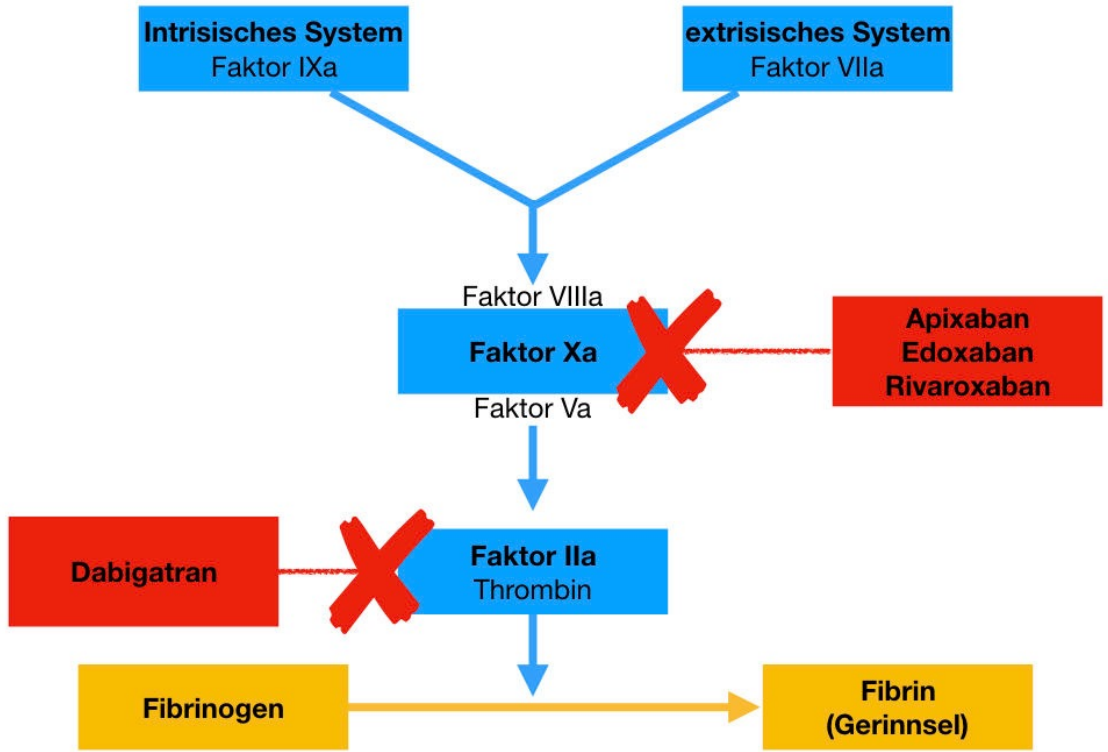
Intrisisches System
Faktor IXa
extrisisches System
Faktor VIIa
Faktor VIIIa
Faktor Xa
Faktor Va
Apixaban
Edoxaban
Rivaroxaban
Dabigatran
Faktor IIa
Thrombin
Fibrinogen
Fibrin
(Gerinnsel)

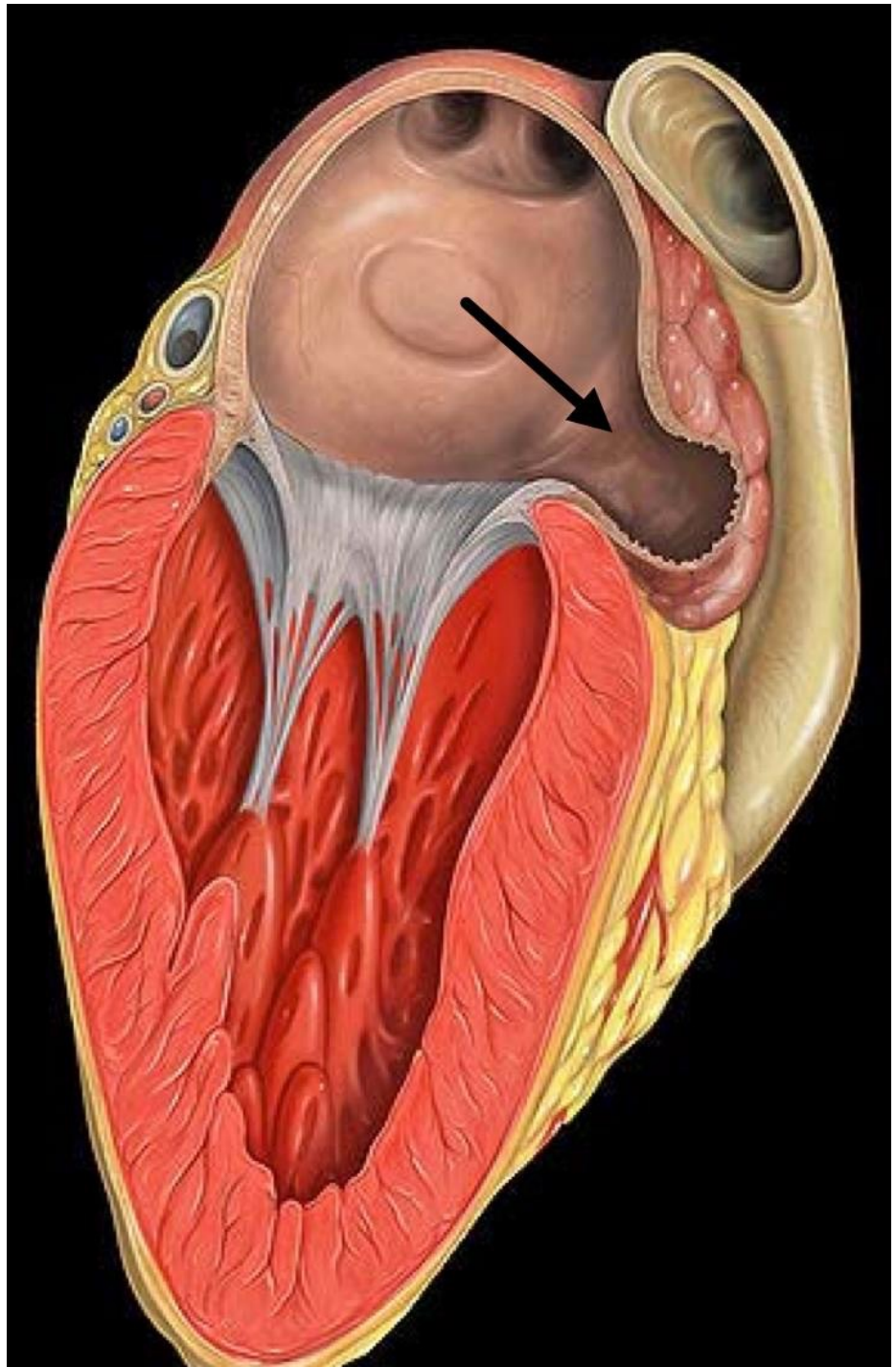

Nicht nicht unterlegen

Amplatzer-Okkluder sind spezialisierte, minimalinvasive Implantate aus Nitinolgeflecht zum Verschluss von Herzdefekten wie PFO, ASD, VSD oder dem LAA. Sie werden mittels Kathetertechnik über die Leistenvene eingeführt, woraufhin sie mit dem Gewebe verwachsen. Sie reduzieren Schlaganfallrisiken und behandeln angeborene Herzfehler effektiv.

Amplatzer™ Amulet™ LAA Occluder:
Verschließt das linke Vorhofohr (Left Atrial Appendage) zur Schlaganfallprophylaxe bei Vorhofflimmern.

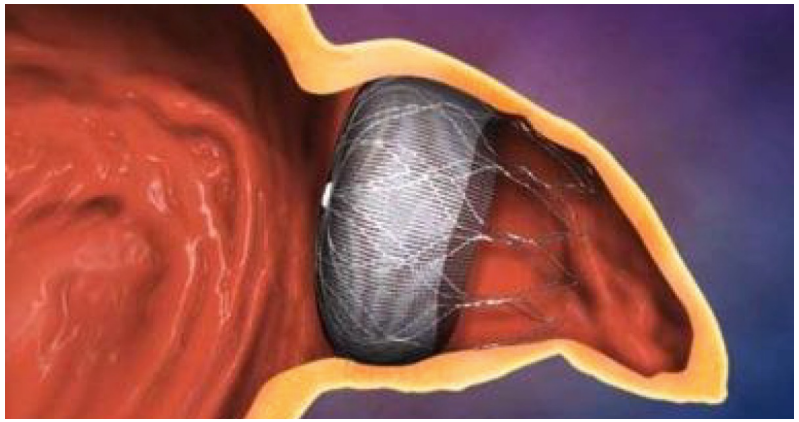

Left Atrial Appendage Closure or Medical Therapy in Atrial Fibrillation

Catheter-based closure of the left atrial appendage is an alternative to oral anticoagulation for stroke prevention in patients with atrial fibrillation. The effectiveness of this strategy, as compared with physician-directed best medical care, in patients at high risk for stroke and bleeding is unknown. In this multicenter randomized trial conducted in Germany, we assigned patients with atrial fibrillation and a high risk of stroke and bleeding to undergo left atrial appendage closure or to receive physician-directed best medical care (including direct oral anticoagulants, if eligible). The primary end point, tested for noninferiority, was a composite of stroke (ischemic or hemorrhagic), systemic embolism, major bleeding, or cardiovascular or unexplained death, assessed in a time-to-event analysis. The noninferiority margin was a hazard ratio of 1.3.

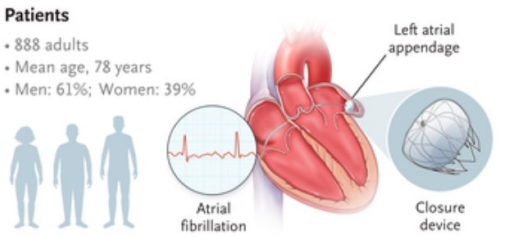

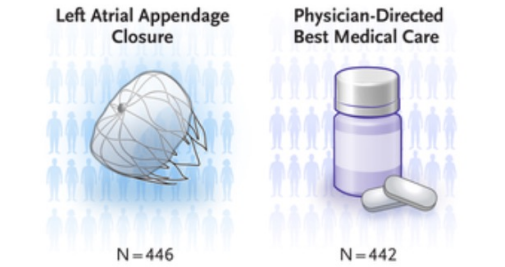

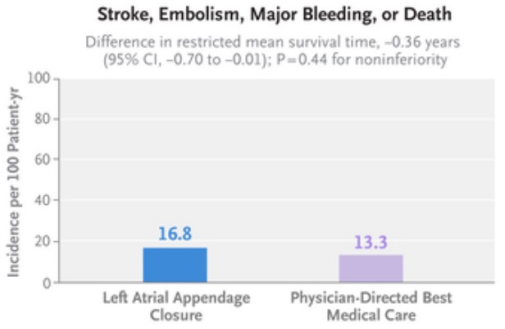

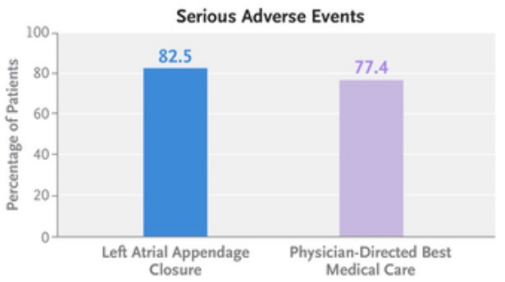

Catheter-based closure of the left atrial appendage has been suggested to provide protection against stroke, systemic embolism, and cardiovascular death that is similar to that provided by anticoagulation therapy in moderate-sized clinical trials. Device-based strategies are associated with a certain degree of periprocedural risk but have the potential to reduce bleeding events. Data comparing left atrial appendage closure to contemporary medical therapy are scarce, especially with regard to patients who are at high risk for stroke and bleeding, the patient population that is considered to potentially derive the greatest benefit. Therefore, we designed the CLOSURE-AF (Catheter-Based Left Atrial Appendage Closure in Patients with Atrial Fibrillation at High Risk of Stroke and Bleeding as Compared with Best Medical Therapy) trial to compare left atrial appendage closure with physician-directed best medical care (including DOACs when considered feasible) in patients with atrial fibrillation and a high risk of stroke and bleeding.

Trial Population

Patients were eligible for inclusion if they had atrial fibrillation and were at a high risk for stroke and bleeding or had contraindications to long-term anticoagulation therapy. High risk of stroke was defined as a CHA_2DS_2-VASc score of 2 or higher (range, 0 to 9, with higher scores indicating a greater risk of stroke).

Patients assigned to undergo left atrial appendage closure (the device group) could receive a Watchman or Amplatzer device. The LAmbre device (LifeTech) was available at selected sites as a bailout device. All participating sites were required to have documented experience with catheter-based left atrial appendage closure, and operators were required to be certified for all devices used. Postimplantation antithrombotic treatment was individualized according to the patient's bleeding risk. After deployment of the device, therapy with a dual antiplatelet agent was recommended for at least 3 months. If transesophageal echocardiography showed complete left atrial appendage closure or only a small residual leak (<5 mm) without device-related thrombus, discontinuation of dual antiplatelet therapy was recommended. Discontinuation of single antiplatelet therapy with aspirin was recommended after 6 months unless a clear indication existed for continuing therapy. In patients with excessive bleeding risk, dual antiplatelet therapy could be shortened to 6 weeks, and aspirin could be stopped after 3 months.

End Points

The primary end point was a patient-relevant composite end point of stroke (ischemic or hemorrhagic), systemic embolism, major bleeding (BARC type 3 or higher), or cardiovascular or unexplained death, assessed in a time-to-event analysis.

Figure S1: Therapy recommendations of CLOSURE-AF

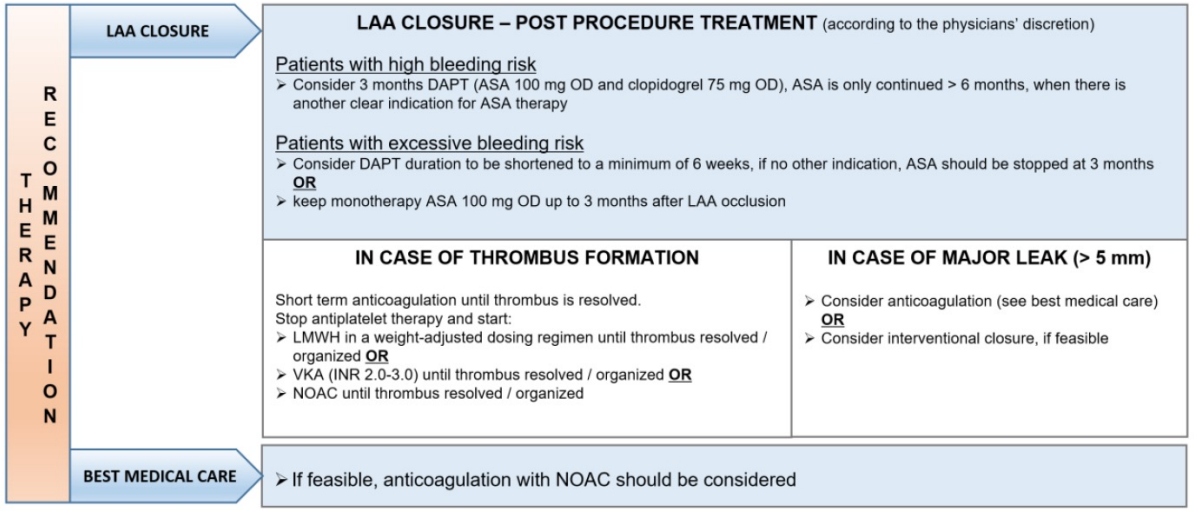

Figure S3: Antithrombotic medication in both treatment arms

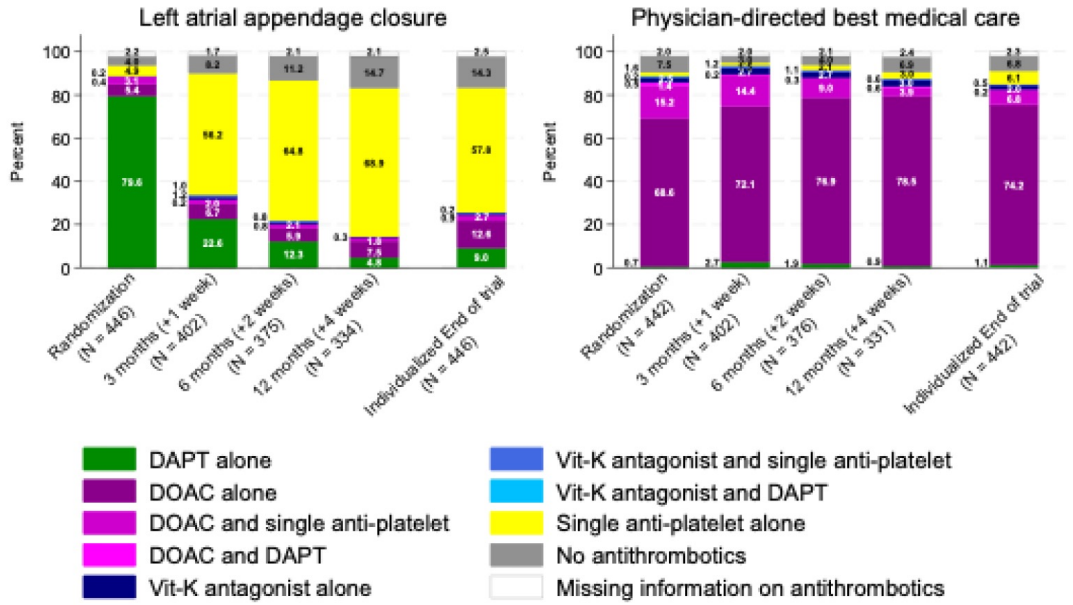

After deployment of the device, therapy with a dual antiplatelet agent was recommended for at least 3 months. If transesophageal echocardiography showed complete left atrial appendage closure or only a small residual leak (<5 mm) without device-related thrombus, discontinuation of dual antiplatelet therapy was recommended. Discontinuation of single antiplatelet therapy with aspirin was recommended after 6 months unless a clear indication existed for continuing therapy. In patients with excessive bleeding risk, dual antiplatelet therapy could be shortened to 6 weeks, and aspirin could be stopped after 3 months.

The treating physician decided what qualified as best medical care, with DOAC as the default therapy in patients who were deemed to be eligible for anticoagulation therapy. When anticoagulation therapy was ruled out, an antiplatelet or no-antithrombotic therapy was selected. The patients who did not qualify for anticoagulation therapy were not prospectively identified. All the patients were followed for a minimum of 6 months, with visits at 3, 6, 12, 18, and 24 months and yearly thereafter until the end of the trial. Clinical information was recorded at each follow-up visit, including medication, adverse events, and quality of life.

The atrial fibrillation patients

Characteristic	Left Atrial Appendage Closure (N=446)	Physician-Directed Best Medical Care (N=442)	Total (N=888)
Age — yr	78.5±6.8	77.3±7.3	77.9±7.1
Female sex — no. (%)	172 (38.6)	171 (38.7)	343 (38.6)
Race — no. (%)†			
White	415 (93.0)	416 (94.1)	831 (93.6)
Black	2 (0.4)	1 (0.2)	3 (0.3)
Not reported	29 (6.5)	25 (5.7)	54 (6.1)
CHA_2DS_2-VASc score‡	5.2±1.5	5.1±1.6	5.2±1.5
HAS-BLED score§	3.1±0.9	3.0±0.9	3.0±0.9
Diabetes — no. (%)	175 (39.2)	186 (42.1)	361 (40.7)
Hypertension — no. (%)	417 (93.5)	417 (94.3)	834 (93.9)
Dyslipidemia — no./total no. (%)	269/433 (62.1)	241/422 (57.1)	510/855 (59.6)
Smoking — no./total no. (%)	30/415 (7.2)	50/411 (12.2)	80/826 (9.7)
Coronary heart disease — no./total no. (%)	257/441 (58.3)	232/439 (52.8)	489/880 (55.6)
Cardiomyopathy — no./total no. (%)	78/439 (17.8)	75/438 (17.1)	153/877 (17.4)
Peripheral artery disease — no./total no. (%)	59/445 (13.3)	49/439 (11.2)	108/884 (12.2)
Stroke or transient ischemic attack — no./total no. (%)	142/445 (31.9)	151/442 (34.2)	293/887 (33.0)
History of major bleeding — no. (%)¶			
BARC type 3a or 3b	132 (29.6)	138 (31.2)	270 (30.4)
BARC type 3c	56 (12.6)	53 (12.0)	109 (12.3)
Recurrent nonmajor bleeding — no./total no. (%)	46/404 (11.4)	56/408 (13.7)	102/812 (12.6)
Stage IV chronic kidney disease — no. (%)‖	114 (25.6)	100 (22.6)	214 (24.1)

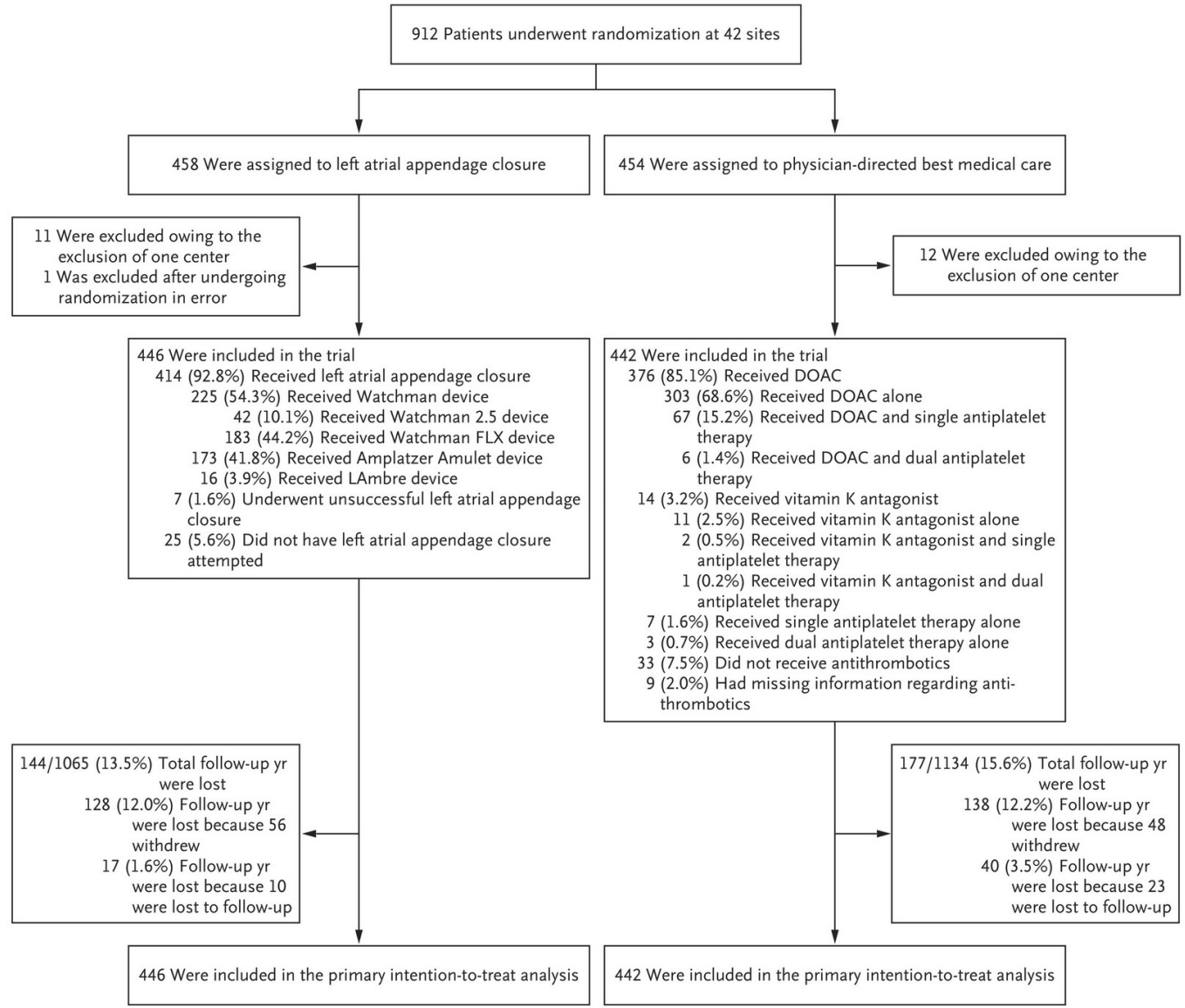

Primary and Secondary End Points.

End Point	Left Atrial Appendage Closure (N=446)	Physician-Directed Best Medical Care (N=442)	Adjusted Difference in Restricted Mean Survival Time in Years (95% CI)‡
Primary end point — no. of patients with event/no. of patient-yr of follow-up (incidence per 100 patient-yr)‡	155/920.8 (16.8)	127/957.0 (13.3)	−0.36 (−0.70 to −0.01)
Per-protocol analysis — no. of patients	411	392	
Per-protocol analysis — no. of patients with event/no. of patient-yr of follow-up (incidence per 100 patient-yr)	144/870.0 (16.6)	108/864.5 (12.5)	−0.40 (−0.76 to −0.04)
Secondary end points — no. of patients with event/no. of patient-yr of follow-up (incidence per 100 patient-yr)			
Systemic embolism	3/1042.7 (0.3)	1/1045.4 (0.1)	−0.02 (−0.08 to 0.03)
Ischemic or hemorrhagic stroke	27/1019.0 (2.6)	27/1015.1 (2.7)	0.01 (−0.17 to 0.20)
Major bleeding	70/941.5 (7.4)	61/978.7 (6.2)	−0.12 (−0.40 to 0.15)
Cardiovascular or unexplained death	99/1045.2 (9.5)	81/1045.4 (7.7)	−0.19 (−0.50 to 0.11)
Death from any cause	155/1045.2 (14.8)	141/1045.4 (13.5)	−0.13 (−0.48 to 0.21)
Myocardial infarction	14/1021.8 (1.4)	20/1016.9 (2.0)	0.07 (−0.08 to 0.22)
Transient ischemic attack	9/1029.1 (0.9)	10/1028.6 (1.0)	0.02 (−0.10 to 0.13)
Ischemic stroke	18/1022.8 (1.8)	15/1022.8 (1.5)	−0.04 (−0.18 to 0.11)
Hemorrhagic stroke	10/1039.5 (1.0)	13/1037.4 (1.3)	0.04 (−0.08 to 0.17)
Stroke or systemic embolism	29/1016.5 (2.9)	28/1015.0 (2.8)	−0.00 (−0.19 to 0.19)
Hospitalization for bleeding or cardiovascular event	284/535.9 (53.0)	250/633.9 (39.4)	−0.44 (−0.80 to −0.09)
Major adverse cardiac and cerebrovascular event	92/994.1 (9.3)	81/988.6 (8.2)	−0.11 (−0.41 to 0.19)

Procedural Outcomes and Periprocedural Complications with Left Atrial Appendage Closure.

Outcomes or Complication	Total (N=446)
Patients with attempted device implantation — no. (%)	421 (94.4)
Technical and procedural success of device implantation — no./total no. (%)	
Device success when deployed and implanted in the correct position	414/421 (98.3)
Technical success with peridevice leak ≤5 mm and no device-related complications	411/421 (97.6)
Procedural success	406/421 (96.4)
Leak up to day 7 or hospital discharge — no. of patients	
Total	20
Leak <3 mm	16
Leak 3 to 5 mm	1
Leak >5 mm	3
Periprocedural complications by day 7 day or by hospital discharge — no. of patients	
Pericardial tamponade*	5
Major bleeding leading to transfusion (BARC types 3–5)	18
Device embolization, surgical removal	1
Procedure-related transient ischemic attack	1
Peripheral embolism	1
Death within 7 days after implantation	2

A Primary End Point

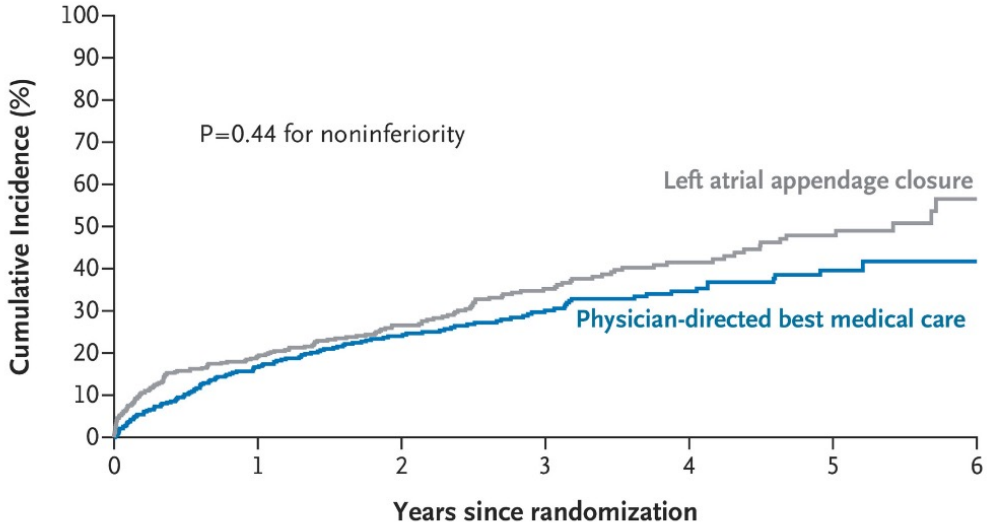

No. at Risk							
Physician-directed best medical care	442	306	203	136	77	40	7
Left atrial appendage closure	446	304	202	117	71	33	9

B Noncardiovascular Death

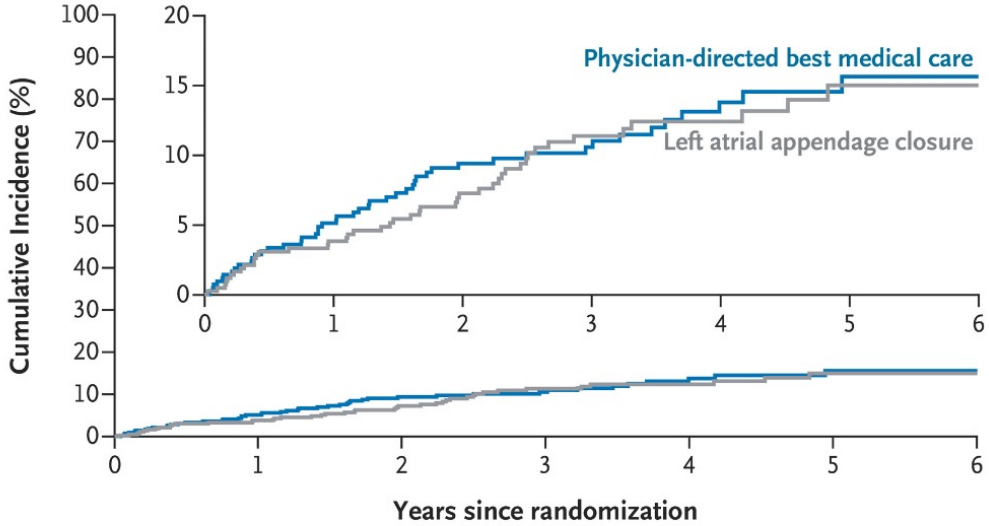

No. at Risk							
Physician-directed best medical care	442	306	203	136	77	40	7
Left atrial appendage closure	446	304	202	117	71	33	9

Incidence of Primary End-Point Event and Noncardiovascular Death.

The primary end point was a composite of stroke (ischemic or hemorrhagic), systemic embolism, major bleeding, or cardiovascular or unexplained death, assessed in a time-to-event analysis.

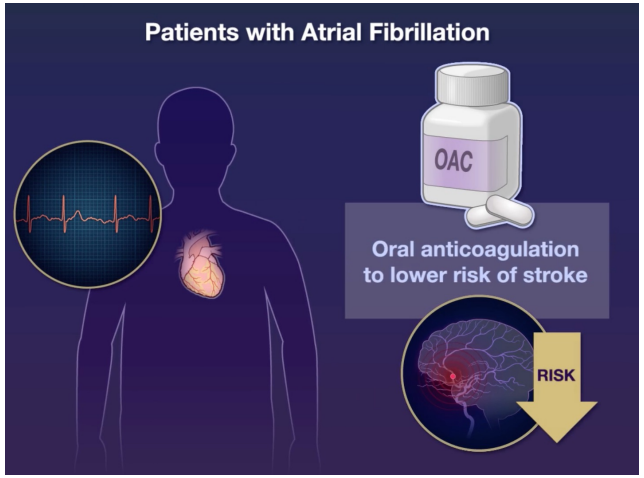

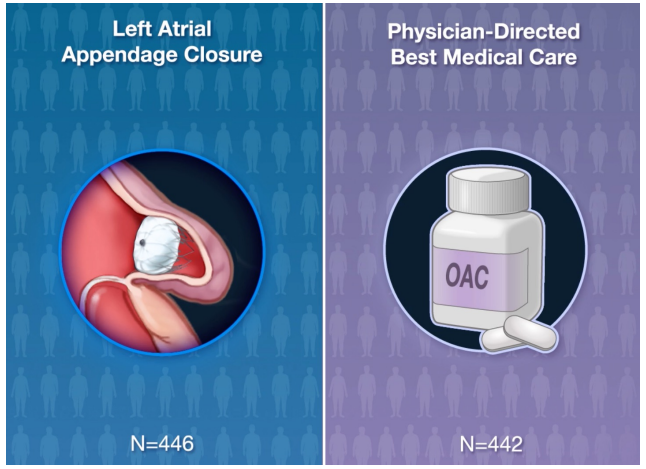

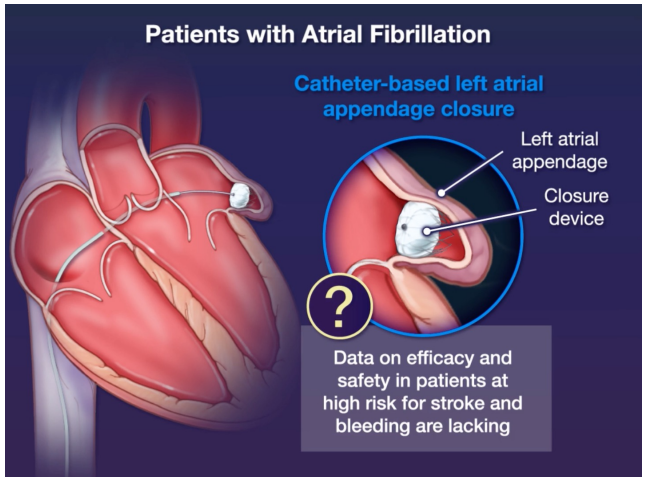

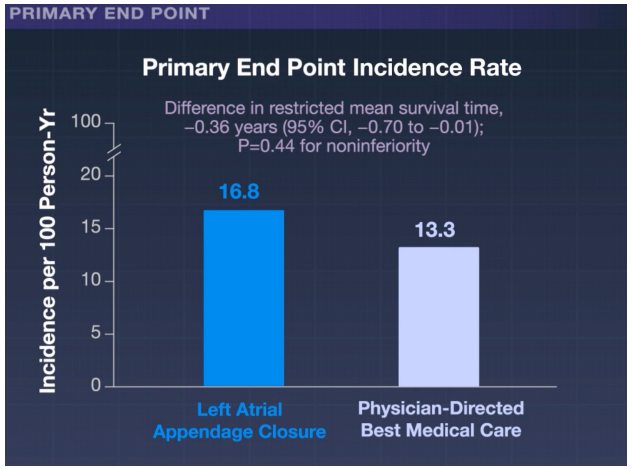

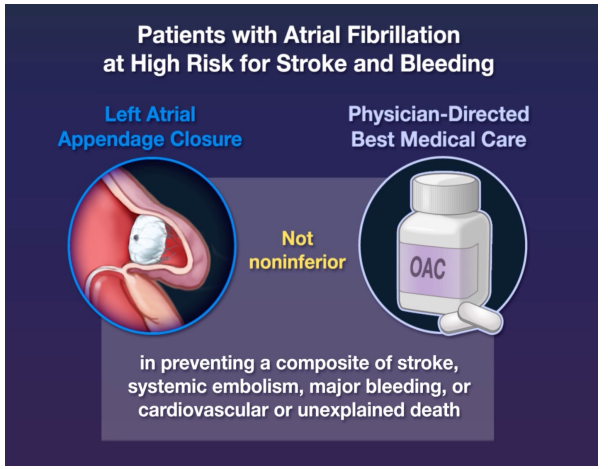

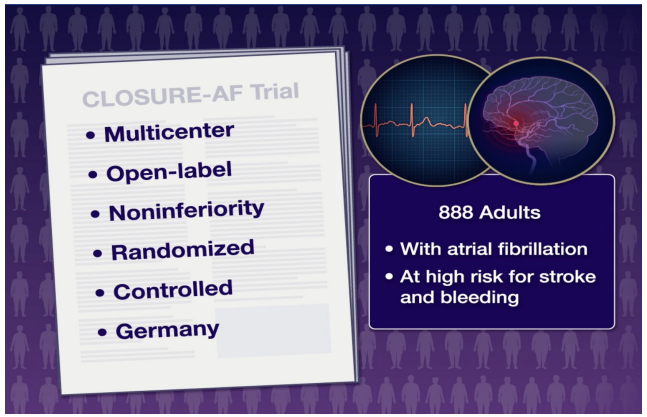

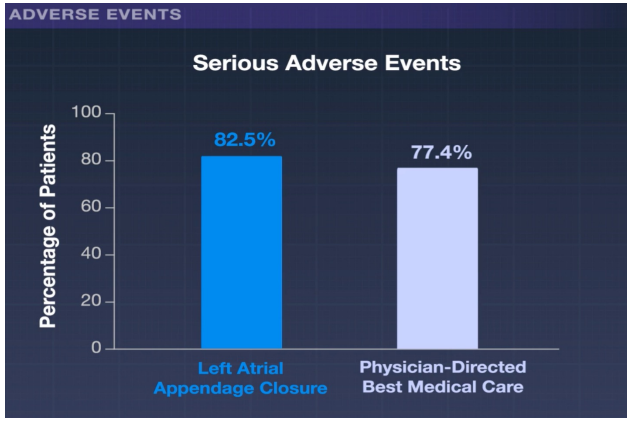

Nicht nicht unterlegen

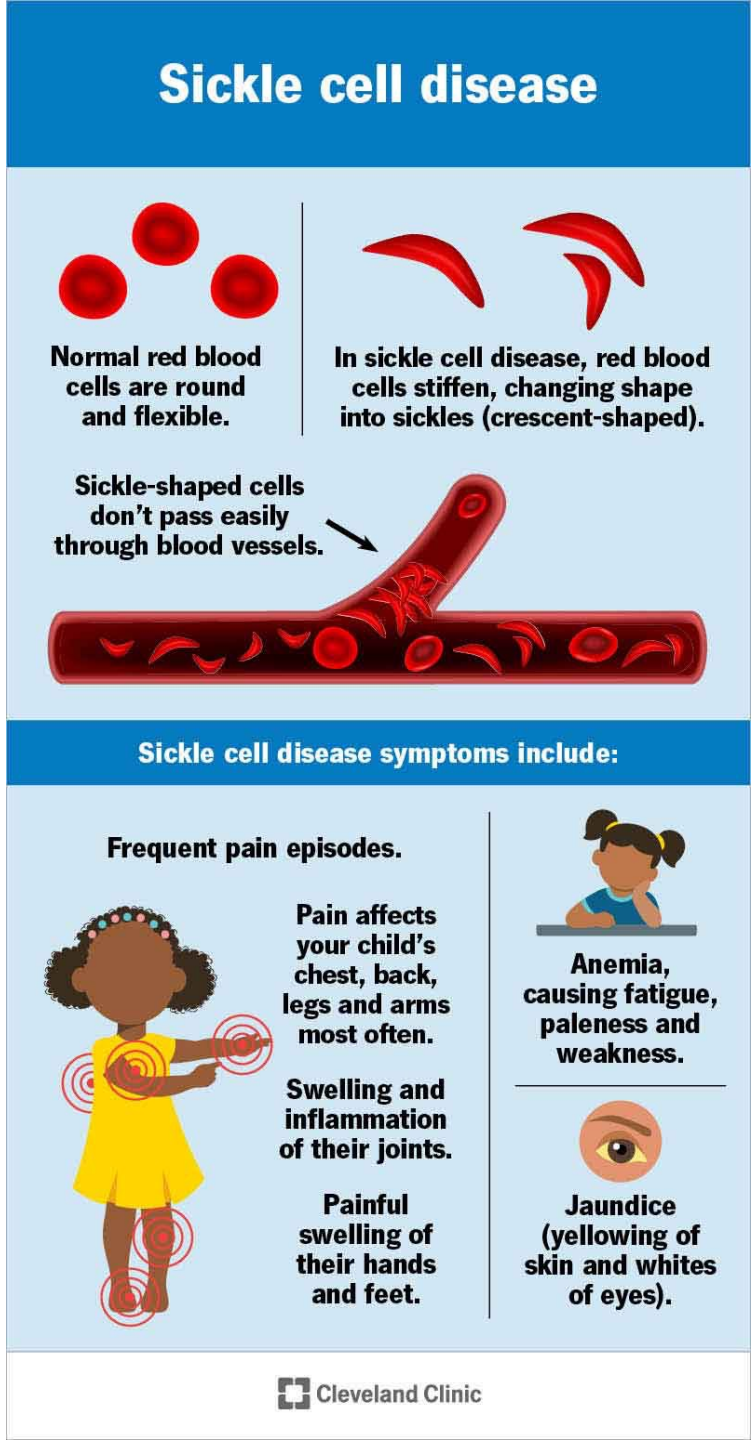

HbA=
2 alpha chains
2 beta chains

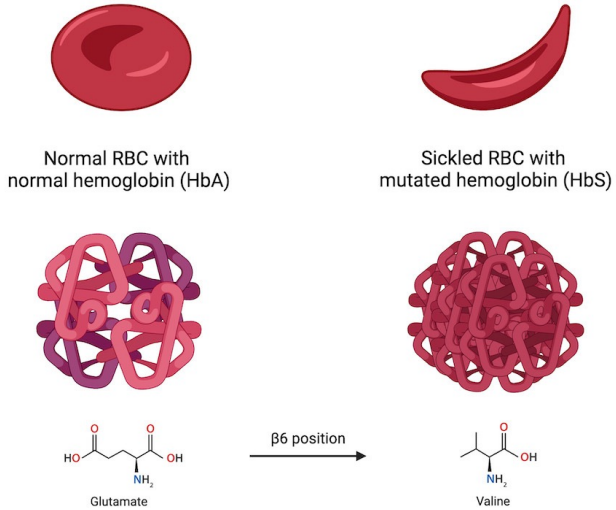

HbS=
2 alpha chains
2 mutated beta chains

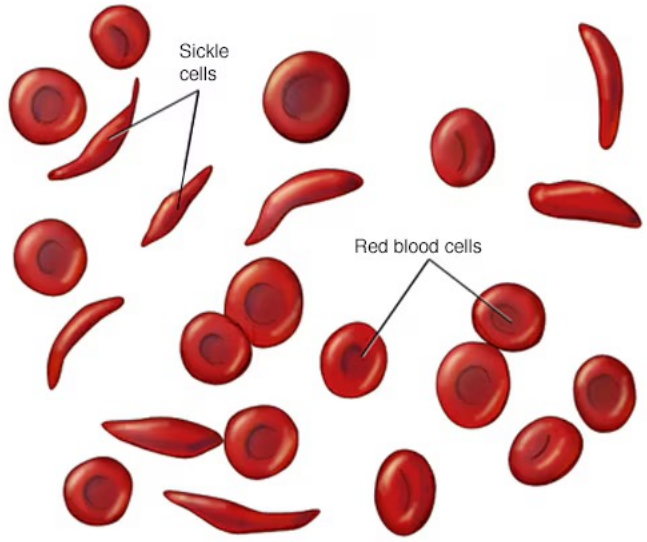

BCL11A (B-Cell CLL/Lymphoma 11A) ist ein entscheidender Transkriptionsfaktor, der die Entwicklung von B-Lymphozyten reguliert und nach der Geburt die Expression von fötalem Hämoglobin (gamma-Hämaglobin) unterdrückt. Die genetische Hemmung von BCL11A wird als therapeutischer Ansatz zur Reaktivierung von HbF bei Sichelzellkrankheit und Beta-Thalassämie genutzt.

Hauptmerkmale und Funktionen:

- **Hämoglobin-Umschaltung:** BCL11A ist der Hauptakteur bei der Repression des fötalen Hämoglobins (HbF) zugunsten des adulten Hämoglobins (HbA).
- **Therapeutischer Ansatz:** Durch CRISPR-Cas9-vermittelte Deaktivierung des BCL11A-Erythroid-Enhancers in CD34+-Stammzellen kann die HbF-Produktion reaktiviert werden, was Patienten transfusionsunabhängig machen kann
- **Hämatopoese & Gehirn:** Neben der Blutbildung (B-Zell-Entwicklung) ist BCL11A essenziell für die neuronale Entwicklung. Mutationen können zu einer intellektuellen Behinderung (BCL11A-ID) führen.
- **Struktur:** Das Protein enthält Zinkfinger-Domänen, die an DNA-Motive binden, und interagiert mit dem SWI/SNF-Chromatin-Remodellierungskomplex.

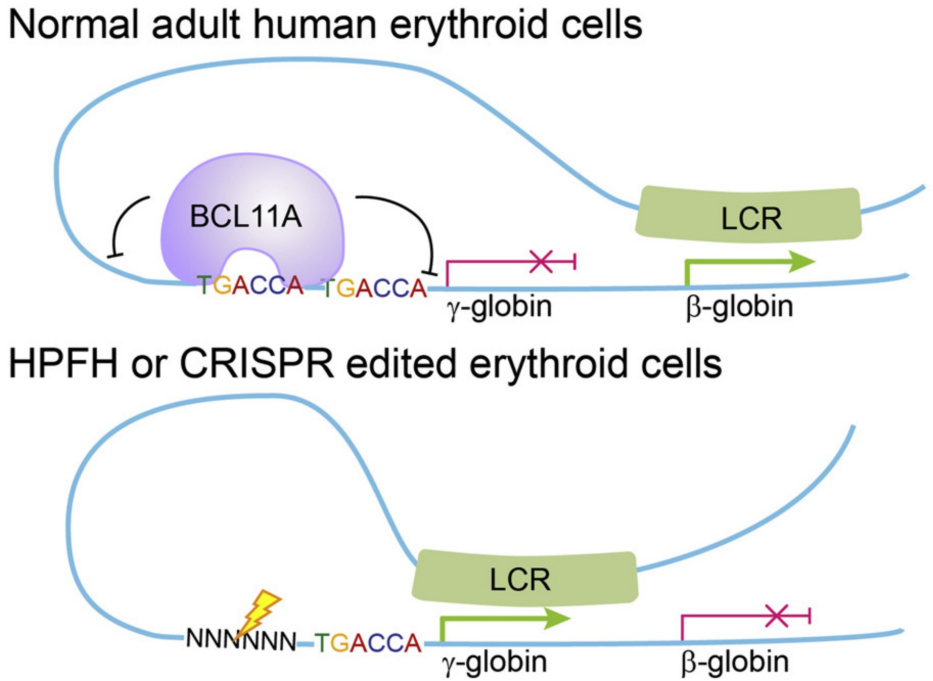

HbF=
2 alpha chains
2 gamma chains

Die Promotoren der Gene **HBG1** und **HBG2** (die für die gamma-Globin-Ketten des fetalen Hämoglobins kodieren) sind zentrale Zielgebiete moderner Gentherapien zur Behandlung von Sichelzellkrankheit und Beta-Thalassämie. In der erwachsenen Blutbildung sind diese Promotoren normalerweise "stummgeschaltet", doch durch gezielte genetische Eingriffe kann die Produktion von fetalem Hämoglobin (HbF) reaktiviert werden, um defektes adultes Hämoglobin zu ersetzen.

LCR bezieht sich im Zusammenhang mit **BCL11A** auf die **Locus Control Region** des Beta-Globin-Genclusters.

Hemoglobin F (HbF) has a higher affinity for oxygen compared to Hemoglobin A (HbA), which generally results in a lower oxygen delivery to tissues at a given partial pressure, potentially affecting exercise tolerance. However, in contexts like sickle cell disease, higher HbF levels improve exercise tolerance by reducing polymerization (sickling) of red blood cells.

Key Aspects of Exercise Tolerance (HbF vs. HbA):

- **Oxygen Affinity:** HbF binds oxygen more tightly (higher affinity) than HbA, making it harder for oxygen to be released from HbF into muscles during exercise.
- **Disease Context (Sickle Cell):** In Sickle Cell Disease, high levels of HbF are beneficial for exercise. HbF inhibits the polymerization of deoxygenated sickle hemoglobin (HbS), which reduces the sickling of red blood cells and associated vaso-occlusive crises, thus improving exercise capability.
- **Anaerobic/Aerobic Performance:** Research indicates that hemoglobin variants (like HbE) with different affinities can result in diminished aerobic (VO_2max) and anaerobic capacity compared to normal HbA.

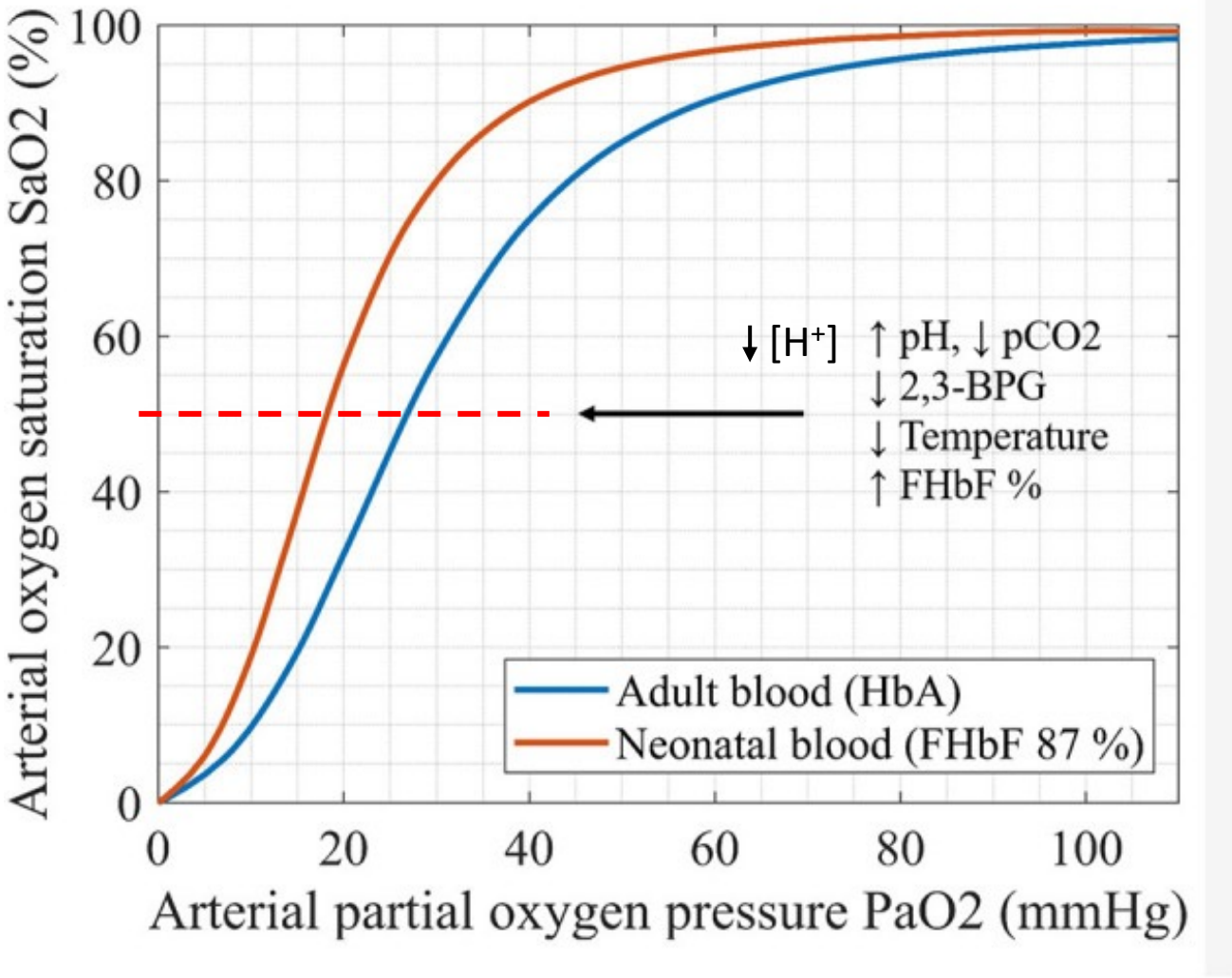

Hemoglobin F is more O_2 saturated at any PO_2

CRISPR-Cas12a Gene Editing of *HBG1* and *HBG2* Promoters to Treat Sickle Cell Disease

Abstract

Renizgamglogene autogedtemcel (reni-cel) is an investigational clustered regularly interspaced short palindromic repeats (CRISPR)–Cas12a gene-edited autologous hematopoietic stem-cell therapy. The therapy was designed to disrupt the BCL11A binding sites in the *HBG1* and *HBG2* promoters to reactivate fetal hemoglobin production for the treatment of sickle cell disease. We conducted a phase 1–2, multicenter, open-label, single-group study involving patients with severe sickle cell disease who were 12 to 50 years of age and had had at least two severe vaso-occlusive events per year in the previous 2 years. The patients received a single infusion of reni-cel after myeloablative conditioning with busulfan. The patients were monitored for engraftment, hemoglobin-related measures, allelic editing levels, vaso-occlusive events, and adverse events over a 24-month period. The study was terminated early on the basis of the sponsor's reassessment of clinical development priorities. Results of an analysis that was not prespecified are reported.

Conclusions

Treatment with reni-cel led to normalization of the total hemoglobin level and an increase in the percentage of fetal hemoglobin, with no vaso-occlusive events occurring in 27 of 28 patients after infusion. These results support further investigation of this gene-editing approach in the treatment of severe sickle cell disease.

Renizgamglogene autogedtemcel (reni-cel) is an investigational gene-edited autologous hematopoietic stem-cell therapy designed to reactivate fetal hemoglobin expression. Evidence shows that high fetal hemoglobin levels (>30%) with pancellular distribution are associated with amelioration of sickle cell disease symptoms. Patients with sickle cell disease who coinherit the naturally occurring genetic condition hereditary persistence of fetal hemoglobin (HPFH) have elevated fetal hemoglobin levels and attenuated severity of sickle cell disease. Genomic targets for reactivating fetal hemoglobin expression include the *BCL11A* erythroid enhancer and the γ-globin gene promoters (*HBG1* and *HBG2*), to which the BCL11A repressor binds. Reni-cel, which was designed to functionally mimic HPFH, is composed of CD34+ cells edited by an engineered AsCas12a nuclease at the *HBG1* and *HBG2* promoters to disrupt binding of BCL11A. This target site was selected on the basis of preclinical xenotransplantation data showing that editing the BCL11A binding site at the *HBG1* and *HBG2* promoters enables robust fetal hemoglobin induction without adversely affecting erythropoiesis. An engineered AsCas12a nuclease was selected for reni-cel manufacturing because of its high efficiency and specificity.

A. Patients with SCD produce HbS, which leads to sickle-shaped RBCs and disease symptoms

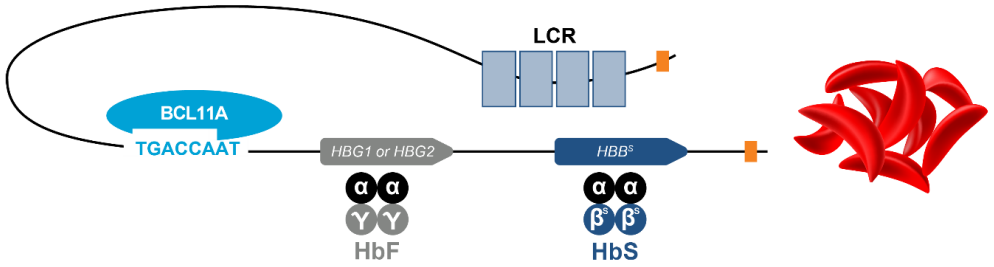

B. Patients treated with reni-cel show increased expression of γ-globin and produce HbF at therapeutically relevant levels

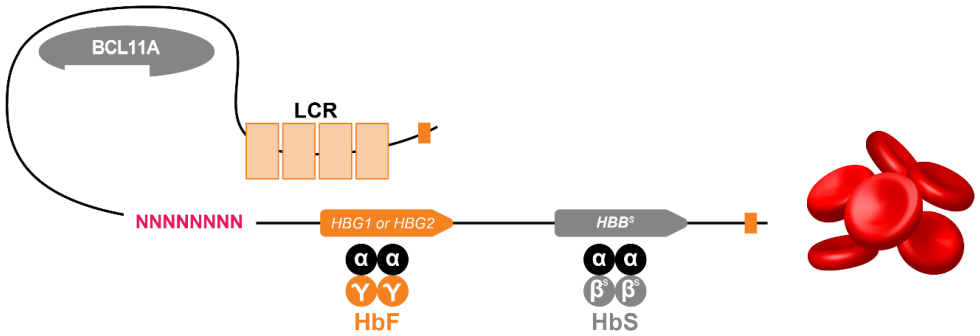

HbF=
2 alpha chains
2 gamma chains

A. At birth, BCL11A binds to the TGACCA motif within the *HBG1* and *HBG2* promoters, preventing interaction of the *HBG1* and *HBG2* gene promoters with the super enhancer LCR. Instead, the LCR loops to the *HBB* gene, leading to its expression and ultimately, to production of HbA. In people with SCD, expression of the *HBB* variant (*HBB*^{S}) leads to production of HbS and sickling of RBCs. **B.** In reni-cel, the *HBG1* and *HBG2* promoters are edited using a highly specific and efficient, engineered AsCas12a gene-editing nuclease to mimic naturally occurring variants found in HPFH and disrupt the BCL11A binding motif. This allows the LCR to loop to the *HBG1* and *HBG2* genes, leading to their expression and ultimately to production of HbF and inhibition of RBC sickling. Note, this is a schematic figure and is not drawn proportionally. For simplicity, only one target site is shown for one of the *HBG* genes. Grey-colored elements indicate downregulated or inactive components. AsCas12a, *Acidaminococcus* sp CRISPR-associated protein 12a; BCL11A, B-cell lymphoma/leukemia 11A; CRISPR, clustered regularly interspaced short palindromic repeats; HbA, adult hemoglobin; *HBB,* β-globin gene; HbF, fetal hemoglobin; *HBG,* γ-globin gene; HbS, sickle hemoglobin; HPFH, hereditary persistence of fetal hemoglobin; LCR, locus control region; RBC, red blood cell; SCD, sickle cell disease.

Patients

Eligible patients were 12 to 50 years of age and had a confirmed diagnosis of sickle cell disease (β^S/β^S, β^S/β^0, β^S/β^+, $\beta^S\beta^D$, or $\beta^S\beta^{OArab}$), a history of at least two severe vaso-occlusive events per year that led to medical attention despite supportive therapies in the 2-year period before the provision of written informed consent, and no available 10/10 HLA-matched related donor. Full eligibility criteria are provided in the study protocol. All the patients or their legal representative provided written informed consent before enrollment.

Reni-cel Manufacturing and Infusion

Before mobilization, patients received prophylactic simple or exchange red-cell transfusions for 8 weeks or more to maintain a sickle hemoglobin level of less than 30% and a hemoglobin level of 9 to 11 g per deciliter. Hydroxyurea and other disease-modifying therapies were discontinued at 60 days or more and at 30 days or more, respectively, before mobilization and transplantation.

Assessment of Clinical Outcomes

Patients were monitored for engraftment, hemoglobin-related measures, hemolysis markers, on-target editing in bone marrow–derived CD34+ cells and peripheral-blood nucleated cells, vaso-occlusive events, and adverse events over a 24-month period.

Patients

Characteristic	Patients (N=28)
Sickle cell disease genotype	
β^S/β^S — no. (%)	27 (96)
β^S/β^0 — no. (%)	1 (4)
Median age (range) — yr	26 (18–41)
Sex — no. (%)	
Female	15 (54)
Male	13 (46)
Race — no. (%)†	
Black or African American	27 (96)
Other	1 (4)
No. of severe vaso-occlusive events per year during prestudy period‡	4.6±2.6
Total hemoglobin level — g/dl	9.8±1.7
Percentage of fetal hemoglobin	2.5±2.5
Median no. of mobilization and apheresis cycles (range)§	2 (1–4)
Median total no. of CD34+ cells collected (range), $\times 10^{-6}$ cells	23.8 (15.2–50.8)
Median total exposure to busulfan over 4 days (range) — mg¶	957.6 (650.0–1596.0)
Median total reni-cel dose (range) — $\times 10^{-6}$ CD34+ cells/kg	4.3 (2.9–10.0)
Median time to neutrophil engraftment (range) — days‖	23 (14–29)
Median time to platelet engraftment (range) — days**	25 (17–51)
Median duration of follow-up (range) — mo	9.5 (0.7–25.2)

Reni-cel Safety and Side-Effect Profile.

Event	Patients (N=28)	No. of Events
	no. (%)	
Any adverse event	28 (100)	618
Any adverse event related to reni-cel†	3 (11)	6
Any adverse event related to busulfan	27 (96)	322
Any serious adverse event	12 (43)	26
Any serious adverse event related to reni-cel	2 (7)	2
Any grade 3 or 4 adverse event	27 (96)	144
Any grade 3 or 4 adverse event related to reni-cel	2 (7)	2
Any adverse event related to reni-cel that led to discontinuation	0	0
Grade 3 or 4 adverse events in ≥2 patients		
Febrile neutropenia	11 (39)	12
Stomatitis	11 (39)	12
Mucosal inflammation	10 (36)	10
Decreased neutrophil count	8 (29)	17
Decreased platelet count	6 (21)	9
Decreased white-cell count	5 (18)	12
Decreased appetite	5 (18)	5
Anemia	4 (14)	4
γ-Glutamyltransferase increased	4 (14)	4
Thrombocytopenia	4 (14)	4
Increased alanine aminotransferase level	3 (11)	4
Hypertension	3 (11)	3
Neutropenia	2 (7)	3
Hypokalemia	2 (7)	2
Pain	2 (7)	2
Sepsis	2 (7)	2

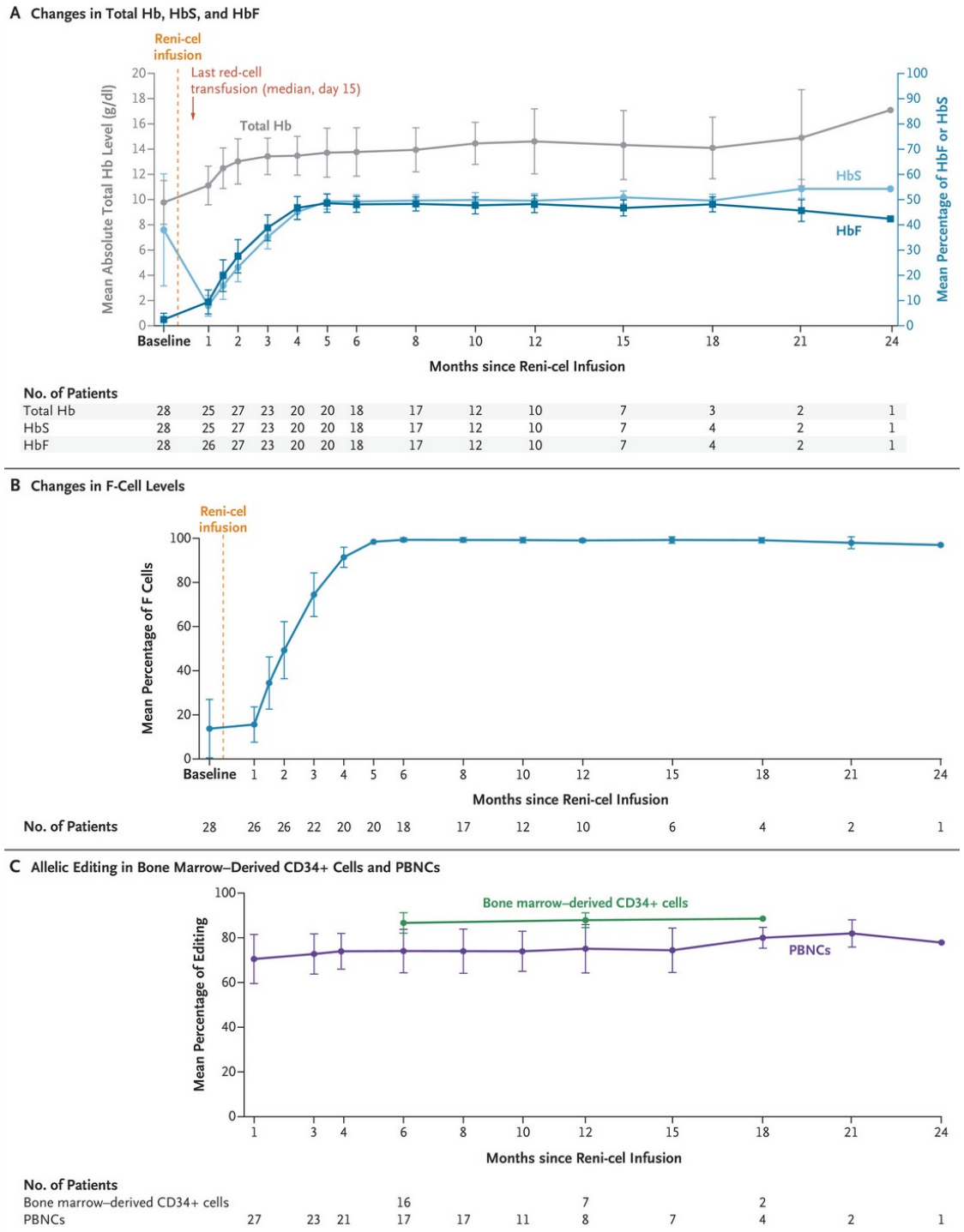

Changes in Hemoglobin Levels, Percentage of F Cells, and Allelic Editing after Reni-cel Infusion.

Panel A shows the changes from baseline in the mean total hemoglobin (Hb) level and the percentage of sickle hemoglobin (HbS) and fetal hemoglobin (HbF) among 13 male patients and 15 female patients. The central laboratory reference range for the total absolute Hb level is 12.0 to 16.0 g per deciliter for females and 13.6 to 18.0 g per deciliter for males. Among the 28 patients, the last red-cell transfusion occurred a median of 15 days (range, 0 to 35) after renizgamglogene autogedtemcel (reni-cel) infusion. Panel B shows the change from baseline in the percentage of F cells (erythrocytes expressing HbF). Panel C shows allelic editing in bone marrow–derived CD34+ cells and peripheral-blood nucleated cells (PBNCs). The corresponding number of patients are shown below each time point. Not all patients had a sample that could be evaluated at each time point. I bars indicate the standard deviation in all three panels.

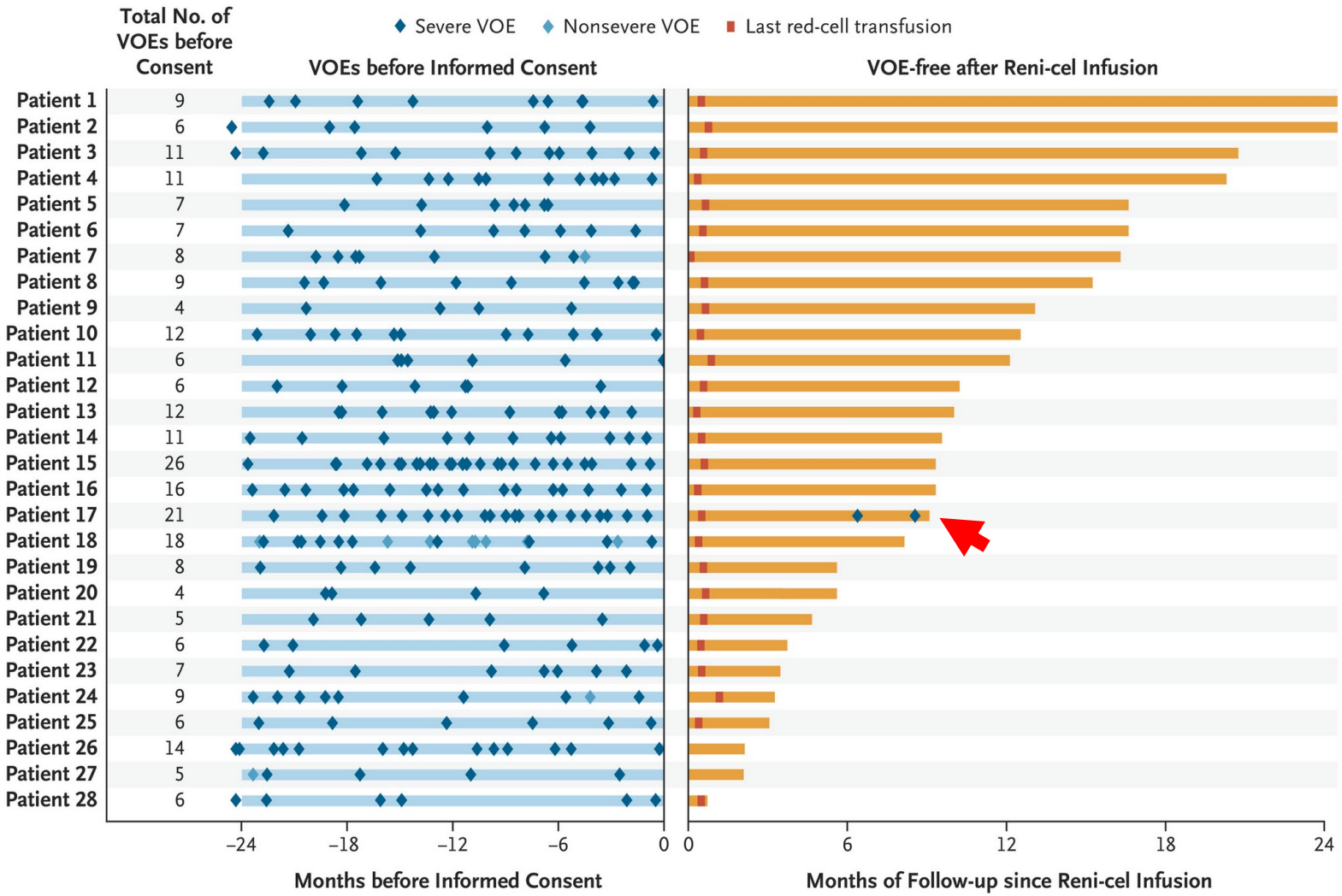

Duration of Freedom from Vaso-occlusive Events after Reni-cel Infusion.

Each row of the swim-lane plot represents an individual patient. The left plot begins 2 years before enrollment and ends at the date that informed consent was provided (0 on the x axis). The right plot starts at the date of reni-cel infusion (0 on the x axis) and represents the duration of follow-up after infusion. All vaso-occlusive events (VOEs) were reported by a study investigator (before consent was obtained and after reni-cel infusion). One post-treatment severe VOE in Patient 17 was adjudicated as not being a VOE. The second post-treatment severe VOE is pending review. In the 2 years before the date of informed consent, this patient had 21 severe VOEs. The increases in the percentage of HbF (to 44.7%) and in the total Hb level (to 14.2 g per deciliter) in this patient at month 6 after reni-cel infusion were in line with the increases observed in the other treated patients.

Discussion

Normalization of the hemoglobin level is a clinically significant improvement in patients with sickle cell disease. Beyond reducing the frequency of vaso-occlusive events, higher hemoglobin levels are associated with a reduced risk of both progressive end-organ damage and death. In this analysis, the mean total hemoglobin level was within the normal range by 6 months after reni-cel treatment.

One patient had two investigator-reported severe vaso-occlusive events. This patient had 21 severe vaso-occlusive events during the 2 years before study enrollment and had a medical history of sickle cell disease–related chronic pain and avascular necrosis of the right hip. Increases in the fetal hemoglobin percentage and total hemoglobin level were in line with those observed for other treated patients. One treated patient had acute respiratory distress syndrome. Acute respiratory distress syndrome occurs in 3 to 5% of HSCT recipients within 1 year after transplantation, with most cases occurring before 100 days.

A safety profile generally consistent with that of myeloablative busulfan-based conditioning and autologous HSCT was observed. All the patients who were followed for more than 1 month after treatment showed successful engraftment and encouraging platelet and neutrophil engraftment kinetics, which are important for limiting infection and the risk of bleeding.

The limitations of this study are that the results are descriptive and longer follow-up is needed. Of the 28 patients treated with reni-cel at the time of this analysis, only 11 had been followed for 1 year or more.

The findings of the RUBY study provide clinical validation of targeting the *HBG1* and *HBG2* promoters to reactivate γ-globin expression and provide insight for the development of in vivo gene editing therapies for sickle cell disease.

Die **Beta-Thalassämie** ist eine erbliche Bluterkrankung, bei der der Körper den roten Blutfarbstoff (Hämoglobin) nicht in ausreichender Menge oder Qualität herstellen kann. Hämoglobin ist für den Sauerstofftransport im Blut verantwortlich; fehlt es, entsteht eine Blutarmut (Anämie).

Krankheitsformen und Schweregrade

Je nachdem, wie stark die Produktion der Beta-Globinketten gestört ist, unterscheidet man drei Hauptformen:

- **Beta-Thalassaemia minor (Anlageträgerschaft):** Die Betroffenen haben meist keine oder nur sehr leichte Symptome einer Blutarmut. Sie können das veränderte Gen jedoch an ihre Kinder weitergeben.
- **Beta-Thalassaemia intermedia:** Diese mittelschwere Form zeigt ein breites Spektrum an Symptomen. Regelmäßige Bluttransfusionen sind oft erst im späteren Verlauf oder in Belastungssituationen (z. B. Schwangerschaft) notwendig.
- **Beta-Thalassaemia major (Cooley-Anämie):** Dies ist die schwerste Form, die bereits im ersten Lebensjahr zu einer massiven Anämie führt. Die Betroffenen benötigen lebenslang alle 2 bis 5 Wochen Bluttransfusionen.

ß Thalassaemia. Deletions in the ß globin gene result in an imbalance in α and ß chain synthesis. As a result, there is excess formation of α chains. These precipitate in erythroid precursors, affecting their maturation and resulting in intramedullary destruction of erythroid precursors. Excess α chains in mature RBCs also have toxic effects on the RBC membrane, resulting in rigid cells with a shortened red cell survival.

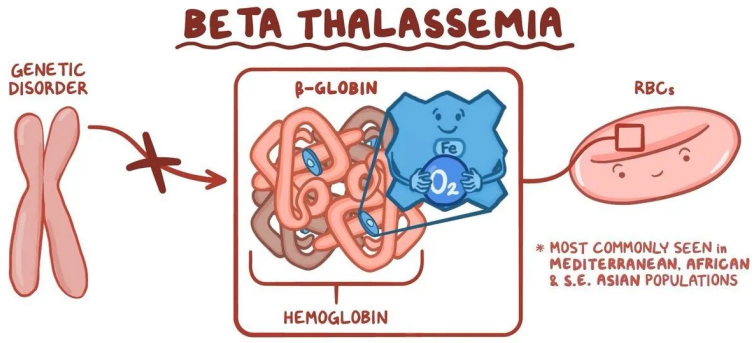

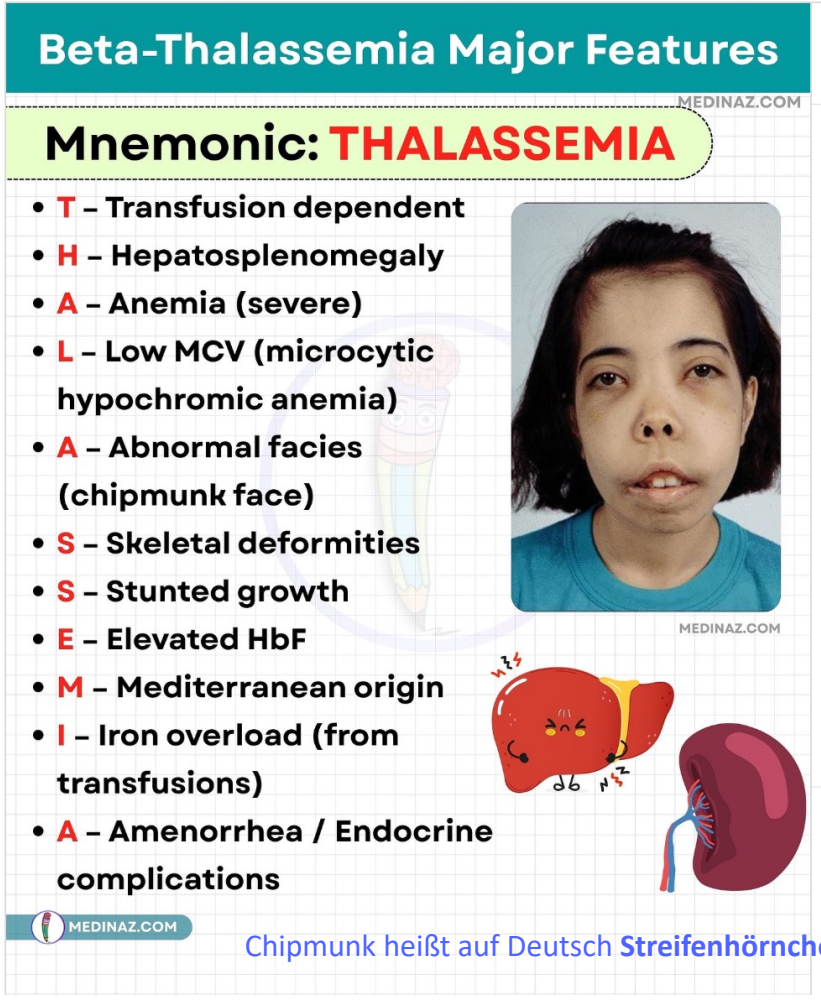

Chipmunk heißt auf Deutsch **Streifenhörnchen**

Patients in the RUBY Trial Receive a Single Infusion of Reni-cel and are Monitored for 24 Months

Ruby

SCREENING → **MOBILIZATION & APHERESIS** → **DRUG PRODUCT MANUFACTURING** → **MYELOABLATION & RENI-CEL INFUSION** → **ENGRAFTMENT & 24 MONTH FOLLOW-UP**

Obtain consent and screen patients

HSPC mobilization and apheresis

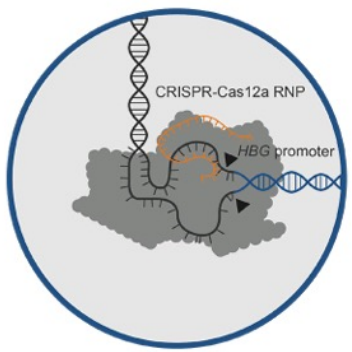

CD34⁺ cells edited at *HBG1* and *HBG2* promoters with CRISPR-AsCas12a

Myeloablative conditioning with busulfan and reni-cel drug product infusion

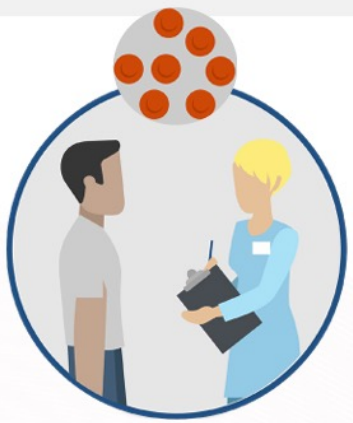

24-month follow-up for primary endpoint

CRISPR-Cas12a Gene Editing of *HBG1* and *HBG2* Promoters to Treat β-Thalassemia

Renizgamglogene autogedtemcel (reni-cel) is an investigational clustered regularly interspaced short palindromic repeats (CRISPR)–Cas12a gene-edited autologous hematopoietic stem-cell therapy. The therapy was designed to disrupt the BCL11A binding sites in the *HBG1* and *HBG2* promoters to reactivate fetal hemoglobin production for the treatment of transfusion-dependent β-thalassemia. We conducted a phase 1–2, multicenter, open-label, single-group study of reni-cel in participants 18 to 35 years of age with transfusion-dependent β-thalassemia. The participants received myeloablative conditioning with busulfan before reni-cel infusion. The primary end points were neutrophil engraftment by 42 days after infusion and frequency and severity of adverse events. Participants were monitored for hemoglobin-related measures and transfusion independence. The study was terminated early on the basis of the sponsor's reassessment of clinical development priorities. Results of an analysis that was not prespecified are reported.

Conclusions

Treatment with reni-cel resulted in rapid neutrophil engraftment, an increase in fetal hemoglobin expression, and transfusion independence. These data support further investigation of Cas12a gene editing of the promoters of *HBG1* and *HBG2* in the treatment of transfusion-dependent β-thalassemia.

Transfusion-dependent β-thalassemia is an inherited blood disorder characterized by a reduced or lack of synthesis of the β-globin chains of hemoglobin leading to chronic anemia. The degree of imbalance between the α-globin and β-globin chains is directly related to the severity of anemia and ineffective erythropoiesis. Patients with transfusion-dependent β-thalassemia typically present in early childhood with profound anemia, growth retardation, and skeletal deformities due to ineffective erythropoiesis and bone marrow expansion. Without intervention, the condition is invariably fatal. The mainstay of treatment for transfusion-dependent β-thalassemia involves regular red-cell transfusions, which alleviate anemia and suppress ineffective erythropoiesis in the bone marrow. However, lifelong transfusion therapy is associated with iron overload warranting long-term chelation therapy, reduced quality of life, and end-organ damage.

Renizgamglogene autogedtemcel (reni-cel) is an investigational nonviral gene-edited autologous hematopoietic stem-cell therapy designed to reactivate γ-globin and induce fetal hemoglobin expression. The therapy comprises CD34+ cells edited within the *HBG1* and *HBG2* promoters at the BCL11A transcriptional repressor binding site by an engineered variant of the acidaminococcus species Cas12a (AsCas12a) gene-editing nuclease. We selected this genomic target on the basis of our preclinical studies that showed a relatively robust induction of fetal hemoglobin expression through editing the BCL11A binding sites in the *HGB1* and *HBG2* promoters (as compared with editing the erythroid enhancer of *BCL11A*). We did not observe a negative effect on erythropoiesis.

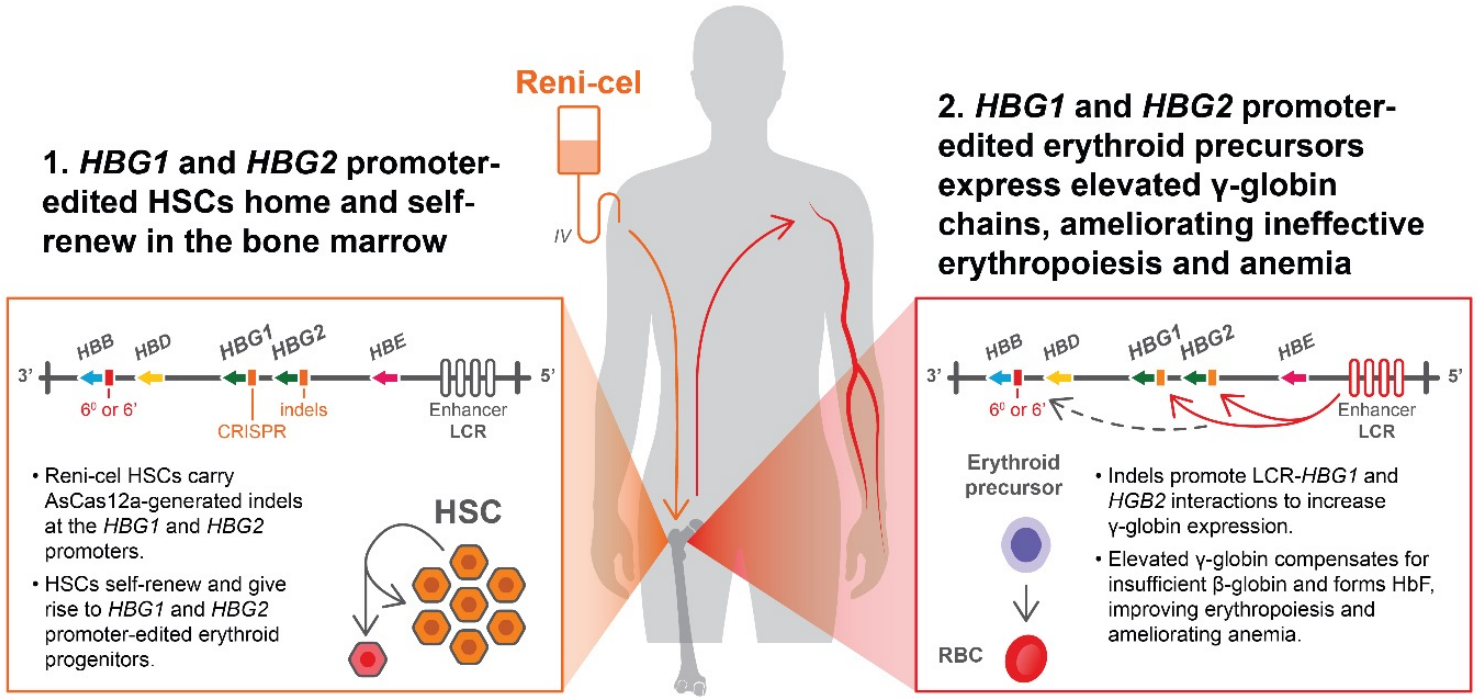

HBB, β-globin gene; *HBD*, hemoglobin D gene; *HBE*, hemoglobin E gene; *HBG*, γ-globin gene; HbF, fetal hemoglobin; HSC, hematopoietic stem cell; indels, insertions and/or deletions; LCR, locus control region; reni-cel, renizgamglogene autogedtemcel; RBC, red blood cell.

Participants

Eligible participants were 18 to 35 years of age who had a confirmed diagnosis of β-thalassemia (including the hemoglobin E genotype) with either homozygous or compound heterozygous mutations and who were transfusion-dependent, defined as having received packed red-cell transfusions of at least 100 ml per kilogram of body weight per year (or 10 units per year) in the 2-year period before providing written informed consent. Full eligibility criteria are described in the study protocol.

Mobilization was performed with a combination of granulocyte colony-stimulating factor and plerixafor. CD34+ HSPCs were collected from each participant by means of leukapheresis over 2 to 3 consecutive days to ensure availability of a sufficient number of cells for manufacturing reni-cel and cryopreservation of rescue cells. Reni-cel was manufactured from each participant's pooled CD34+ HSPCs by gene editing of the BCL11A binding site within the *HBG1* and *HBG2* promoters with the use of an engineered variant of AsCas12a (see the Supplementary Methods). Before reni-cel infusion, participants received myeloablative conditioning with pharmacokinetically adjusted busulfan over 4 consecutive days, followed by a washout period for a minimum of 72 hours. Reni-cel was infused at a single minimum dose of 3×10^6 CD34+ cells per kilogram (post-thaw). All the participants received red-cell transfusions to maintain a hemoglobin level of 11 g per deciliter for at least 30 days before mobilization and before reni-cel infusion. Disease-modifying therapy was discontinued at least 60 days before mobilization. All the participants received antibacterial, antiviral, antifungal, and veno-occlusive disease prophylaxis after reni-cel infusion according to institutional standard of care.

Patients

Characteristic	Participants (N=9)
β-Thalassemia genotypes — no. (%)	
β^0/β^0 and non-β^0/β^0–like mutations	
β^0/β^0	3 (33)
β^+/β^+, homozygous IVS-I-110 G→A mutation	1 (11)
Non–β^0/β^0 and non-β^0/β^0–like mutations	
β^0/β^+	4 (44)
β^E/β^0	1 (11)
Median age (range) — yr	20 (18–29)
Sex — no. (%)	
Male	5 (56)
Female	4 (44)
Race — no. (%)†	
Asian	7 (78)
White	2 (22)
Annualized baseline transfusion volume before study entry — ml/kg/yr	145.7±50.2
Total hemoglobin level at baseline — g/dl‡	11.3±1.6
Fetal hemoglobin level at baseline — g/dl‡	0.8±0.6
Median no. of mobilization and apheresis cycles (range)§	1.0 (1.0–4.0)
Median total reni-cel dose (range) — $\times 10^{-6}$ CD34+ cells/kg	6.1 (3.3–11.9)
Median time to neutrophil engraftment (range) — days¶	23.0 (16.0–30.0)
Median time to platelet engraftment (range) — days‖	37.0 (23.0–49.0)
Median follow-up duration (range) — mo	17.5 (3.8–23.4)
Busulfan dose and exposure**	
Median last-measured AUC value with the once-daily dose regimen (range) — μmol·min/liter	5308 (5001–5615)
Median last-measured AUC value with the every-6-hr dose regimen (range) — μmol·min/liter	1177 (957–1470)

Adverse events

Event	Participants (N=9)	No. of Events
	no. (%)	
Any adverse event	9 (100)	191
Any adverse event related to reni-cel†	1 (11)	2
Any adverse event related to busulfan†	9 (100)	130
Any serious adverse event	4 (44)	6
Any serious adverse event related to reni-cel†	0	0
Any grade 3 or 4 adverse event	9 (100)	69
Any grade 3 or 4 adverse event related to reni-cel†	1 (11)	1
Any adverse event of interest‡	1 (11)	1
Grade 3 or 4 adverse events in ≥2 participants		
Decreased platelet count	5 (56)	13
Decreased neutrophil count	5 (56)	12
Stomatitis	6 (67)	6
Decreased appetite	5 (56)	5
Febrile neutropenia	5 (56)	5
Mucosal inflammation	3 (33)	3

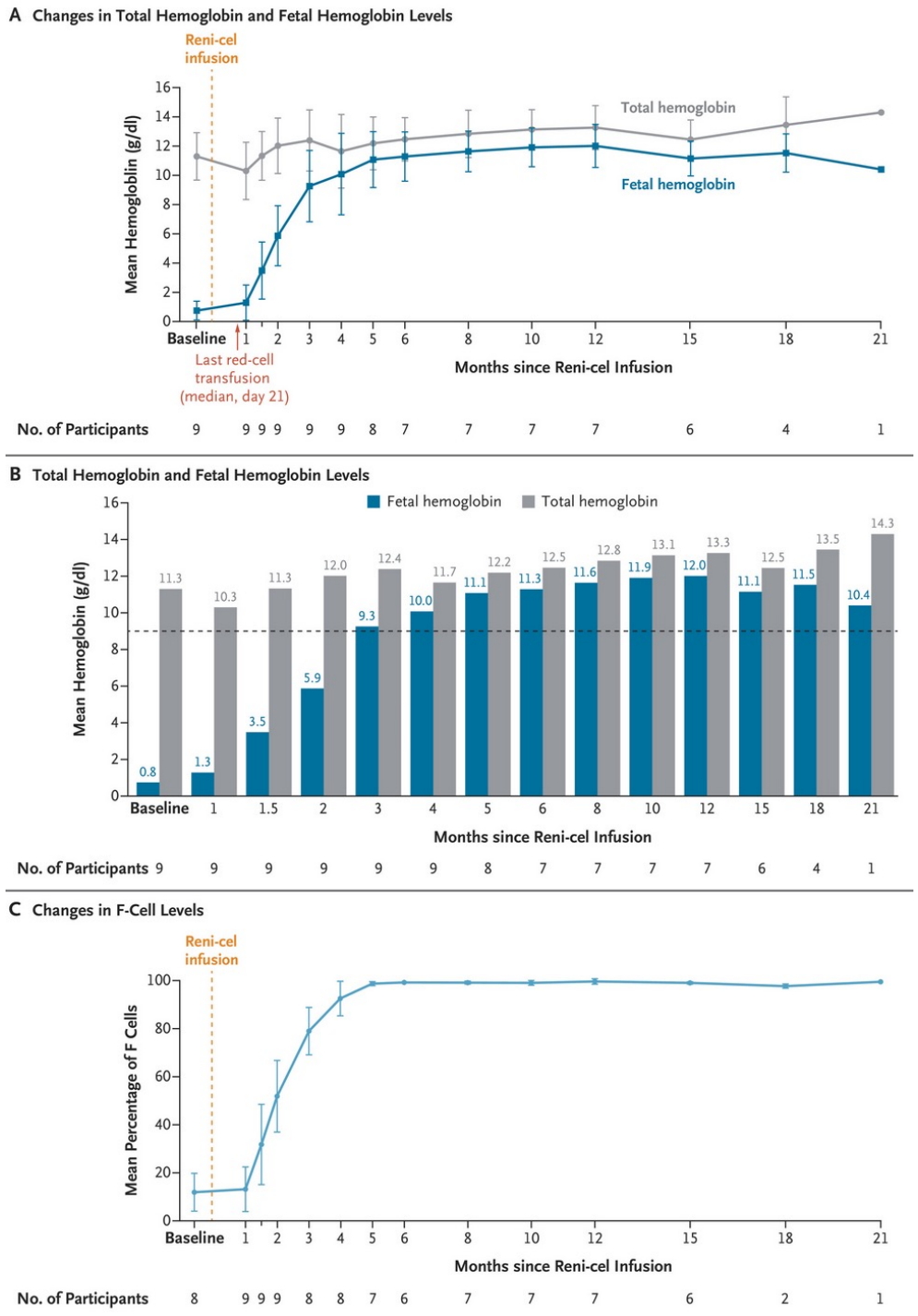

Changes in Hemoglobin Levels and Percentage of F Cells after Reni-cel Infusion.

Panels A and B show the changes in the total and fetal hemoglobin levels, respectively, after renizgamglogene autogedtemcel (reni-cel) infusion. The central laboratory reference range for total absolute hemoglobin level is 12.0 to 16.0 g per deciliter for females and 13.6 to 18.0 g per deciliter for males. The dashed horizontal line in Panel B indicates the threshold at or above which participants were considered to be transfusion independent (total hemoglobin level, 9 g per deciliter). Panel C shows the percentage of red cells expressing fetal hemoglobin. Not all participants had samples that could be evaluated at each time point. At baseline, the fetal hemoglobin level could be evaluated in eight participants. The last red-cell transfusion, which could be evaluated in nine participants, occurred at a median of 21 days (range, 16 to 66) after reni-cel infusion. The I bars in Panels A and C indicate standard deviations.

Transfusion independence was achieved

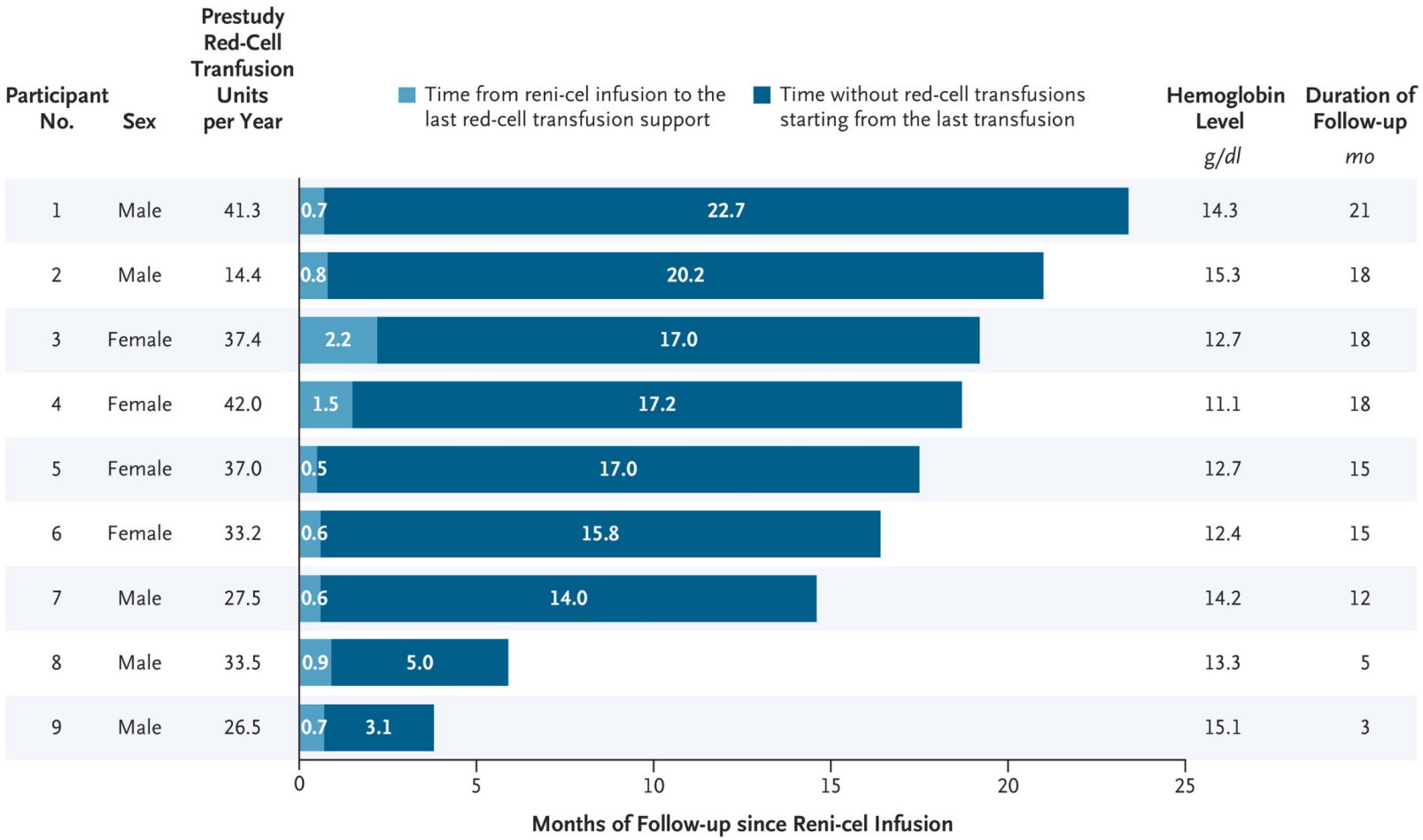

Duration of Freedom from Transfusions after Reni-cel Infusion.

Each row in the swim-lane plot represents an individual participant. The plot starts at the date of reni-cel infusion and represents the duration of postinfusion follow-up. Labels inside the bars indicate the number of months. Labels to the right of the blue bars indicate the hemoglobin levels at the last follow-up visit. The number of red-cell transfusion units received per year before the study was annualized over a 2-year period.

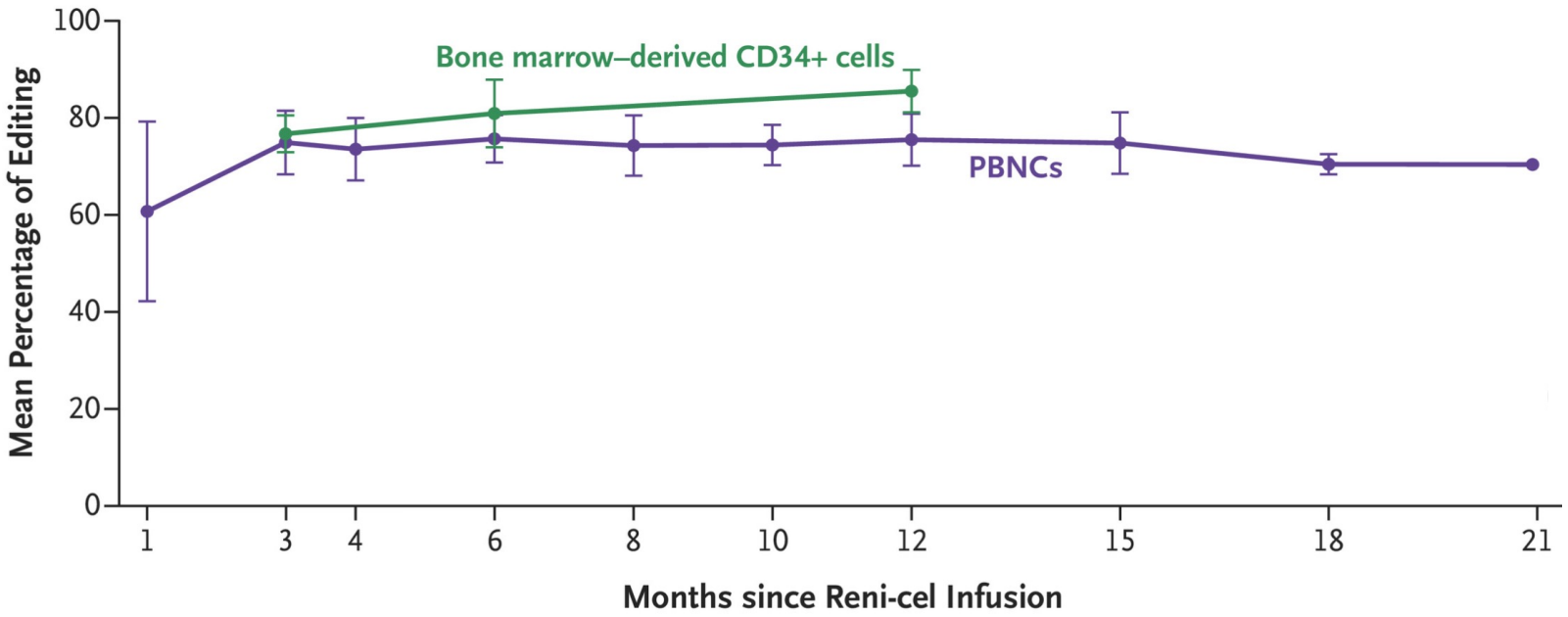

Allelic Editing in Peripheral-Blood Nucleated Cells and Bone Marrow–Derived CD34+ Cells.

Shown is the mean percentage of editing for *HBG1* and *HBG2* alleles in peripheral-blood nucleated cells (PBNCs) and bone marrow–derived CD34+ cells.

The "Lineage-Specific" Strategy: Because systemic or ubiquitous inhibition of BCL11A damages immune cells (as noted above), modern gene therapy (e.g., *exa-cel*) specifically targets the **erythroid enhancer** of BCL11A rather than the whole gene. This approach keeps BCL11A functional in lymphoid cells while silencing it only in red blood cells.

Discussion

We describe an investigational gene-editing approach in nine adult participants with transfusion-dependent β-thalassemia who received treatment with reni-cel. Reactivating γ-globin and increasing fetal hemoglobin levels has clinical benefit in patients with transfusion-dependent β-thalassemia. Reni-cel is composed of CD34+ HSPCs that have been edited within the BCL11A binding site of the *HBG1* and *HBG2* promoters by a highly specific gene-editing nuclease, AsCas12a, to induce fetal hemoglobin expression. This approach is similar to that used to generate ristoglogene autogetemcel (risto-cel), in which the GATA1 binding site of the *HBG1* and *HBG2* promoters is targeted with an adenine base editor. No off-target editing was observed in the analyzed reni-cel product lots, thereby confirming that the ribonucleoprotein complex used to target the *HBG1* and *HBG2* promoter regions is specific, with a low risk of unintended genetic modifications.

In general, adverse events were consistent with those caused by myeloablative conditioning with busulfan and autologous hematopoietic stem-cell transplantation, although we observed grade 2 and grade 3 adverse events (decreased lymphocyte counts) that were attributed to treatment with reni-cel. No serious adverse events related to reni-cel or secondary malignant conditions have been observed, and no deaths occurred in the study.

RCTs in the Reperfusion era

CAPITAL-RCT | ABYSS | REDUCE-AMI

Stopping beta-blockers in patiens with MI without LV dysfunction

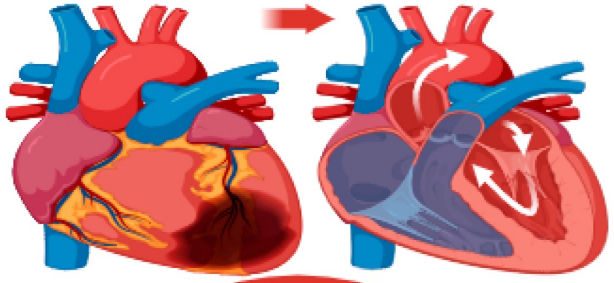

What is known

- No differences in MACE (death, MI, stroke)
- Increase in hospitalizations for angina and angiography
- Increase in heart rate and blood pressure
- No differences in EQ-5D score

Der EQ-5D ist ein standardisierter Fragebogen zur Messung der gesundheitsbezogenen Lebensqualität.

Gaps in Evidence

- Outcomes in MI patients with mrEF (40 - 49%)
- Adverse events related to beta-blockers
- Quality of life assessment considering side-effects of beta-blockers
- Effect of third-generation beta-blockers over second-generation ones

Ongoing RCTs

REBOOT-CNIC | SMART-DECISION | DANBLOCK | BETAMI

Discontinuation of Beta-Blocker Therapy after Myocardial Infarction

The role of long-term beta-blocker therapy after a myocardial infarction in patients without left ventricular systolic dysfunction or heart failure is unclear in the era of contemporary coronary-artery reperfusion and secondary prevention interventions.

We conducted an open-label, randomized, noninferiority trial at 25 centers in South Korea. Patients whose condition remained stable after a myocardial infarction, who had a left ventricular ejection fraction of at least 40% and no heart failure, and who had received beta-blocker therapy for at least 1 year after the myocardial infarction were randomly assigned in a 1:1 ratio to discontinue or to continue beta-blocker therapy. The primary end point was a composite of death from any cause, recurrent myocardial infarction, or hospitalization for heart failure. The prespecified noninferiority margin was an upper limit of the 95% confidence interval for the hazard ratio of 1.4.

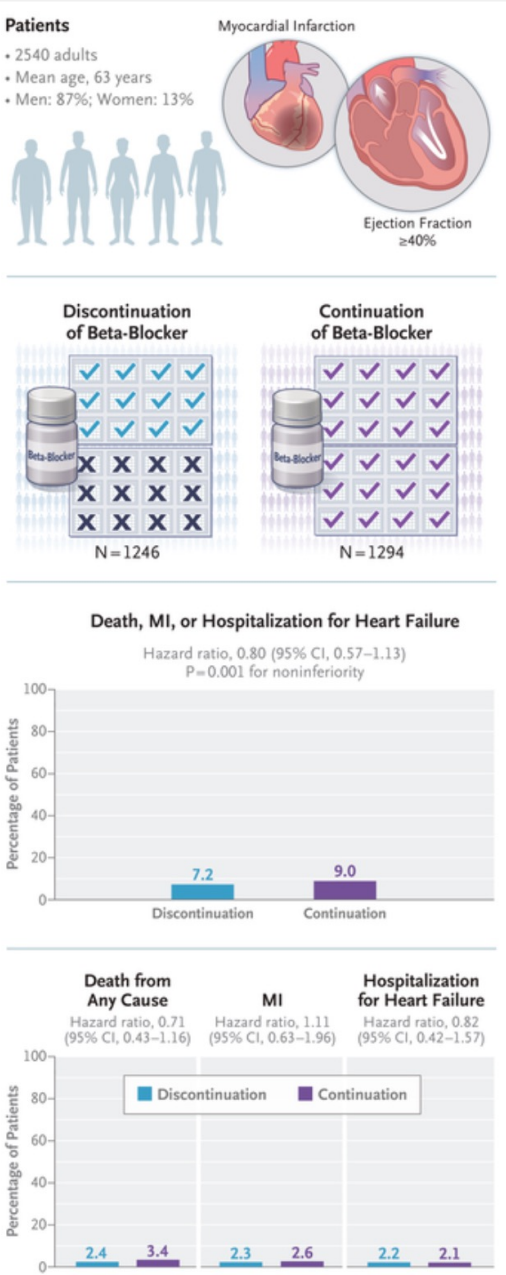

Despite the evolving evidence, the limited support for prolonged beta-blocker therapy in patients without heart failure or left ventricular systolic dysfunction, and the potential adverse effects, many patients continue to receive beta-blockers for years solely because of a previous myocardial infarction. The unresolved clinical question is whether survivors of myocardial infarction who are in stable condition and who have remained event-free should receive beta-blocker treatment over the long term. Observational studies evaluating continuation beyond the first year have shown inconsistent associations and remain susceptible to confounding by indication and treatment-selection bias. The ABYSS trial (Assessment of Beta-Blocker Interruption 1 Year after an Uncomplicated Myocardial Infarction on Safety and Symptomatic Cardiac Events Requiring Hospitalization), which directly compared interruption with continuation of long-term beta-blocker therapy after a myocardial infarction, did not show noninferiority of beta-blocker interruption. However, the ABYSS trial used a composite primary end point that included hospitalization for cardiovascular causes, a component that may be susceptible to clinical decision making in an open-label design. Therefore, the SMART-DECISION trial (Smart Angioplasty Research Team: Decision on Medical Therapy in Patients with Coronary Artery Disease or Structural Heart Disease Undergoing Intervention) was designed to determine whether discontinuation of long-term beta-blocker therapy in patients who were in stable condition after a myocardial infarction and did not have heart failure or left ventricular systolic dysfunction would be noninferior to the continuation of beta-blockers with respect to major clinical outcomes.

Population

Patients in stable condition who had had a myocardial infarction, had been receiving beta-blocker therapy for at least 1 year, and were event-free from the time of the index myocardial infarction to screening were candidates for enrollment. No restrictions on the beta-blocker type or dose were applied, and no upper limit was imposed on the interval from the index myocardial infarction diagnosis to enrollment. Key exclusion criteria were ongoing treatment for heart failure, a reduced ejection fraction (<40%), contraindications to beta-blocker therapy, and atrial fibrillation.

Randomization and Procedures

Patients were randomly assigned in a 1:1 ratio with the use of a Web-based randomization system (Internet-based Clinical Research and Trial Management System, version 2, National Institute of Health, South Korea) to discontinue or to continue beta-blocker therapy. In the discontinuation group, beta-blocker therapy was stopped immediately after randomization, whereas patients in the continuation group continued to receive beta-blocker treatment with the same agent at the same dose. Randomization was stratified according to type of myocardial infarction (ST-segment elevation or non–ST-segment elevation), beta-blocker received (carvedilol, bisoprolol, nebivolol, or other), and participating center. Clinical follow-up was performed at 6, 12, 24, and 30 months and annually thereafter.

End Points

The primary end point was a composite of death from any cause, recurrent myocardial infarction, or hospitalization for heart failure.

Characteristic	Discontinuation of Beta-Blocker (N=1246)	Continuation of Beta-Blocker (N=1294)
Age — yr	63.4±9.9	63.0±10.3
Sex — no. (%)		
Male	1088 (87.3)	1126 (87.0)
Female	158 (12.7)	168 (13.0)
Median body-mass index (IQR)†	25.2 (23.3–27.2)	25.0 (23.3–27.1)
Characteristics of index myocardial infarction		
Type — no. (%)		
STEMI	714 (57.3)	729 (56.3)
NSTEMI	532 (42.7)	565 (43.7)
Multivessel disease — no./total no. (%)	752/1239 (60.7)	758/1293 (58.6)
Revascularization strategy		
Percutaneous coronary intervention — no. (%)	1214 (97.4)	1262 (97.5)
Coronary-artery bypass grafting — no. (%)	2 (0.2)	6 (0.5)
Complete revascularization — no./total no. (%)	879/1203 (73.1)	970/1266 (76.6)
Combined revascularization procedure — no. (%)	1 (0.1)	3 (0.2)
Medical treatment only — no. (%)	29 (2.3)	23 (1.8)
Fibrinolysis — no. (%)	1 (0.1)	2 (0.2)
Median time from index myocardial infarction to randomization (IQR) — yr	4.6 (2.4–8.5)	4.8 (2.3–8.4)
Cardiovascular risk factors — no. (%)		
Hypertension	754 (60.5)	766 (59.2)
Diabetes mellitus	501 (40.2)	468 (36.2)
Dyslipidemia	785 (63.0)	788 (60.9)
Current smoking	366 (29.4)	352 (27.2)
Chronic kidney disease‡	106 (8.5)	122 (9.4)
Previous myocardial infarction before the index myocardial infarction	85 (6.8)	102 (7.9)
Previous stroke	30 (2.4)	37 (2.9)
Peripheral vascular disease	11 (0.9)	12 (0.9)
Health status at randomization		
Left ventricular ejection fraction by echocardiography (IQR) — %§	59.0 (53.7–64.6)	59.0 (53.0–65.0)
Median systolic blood pressure (IQR) — mm Hg	127 (118–136)	126 (117–136)
Median diastolic blood pressure (IQR) — mm Hg	73 (65–79)	73 (66–80)
Median heart rate (IQR) — beats/min	72 (65–80)	72 (65–80)
Beta-blocker received — no. (%)		
Carvedilol	596 (47.8)	614 (47.4)
Bisoprolol	404 (32.4)	417 (32.2)
Nebivolol	245 (19.7)	261 (20.2)
Other	1 (0.1)	2 (0.2)

Primary and Secondary End Points.

End Point	Discontinuation of Beta-Blocker (N=1246)		Continuation of Beta-Blocker (N=1294)		Risk Difference (95% CI)	Hazard Ratio (95% CI)
	no. (%)	*events/100 person-yr*	*no. (%)*	*events/100 person-yr*	*percentage points*	
Primary end point						
Composite of death from any cause, recurrent myocardial infarction, or hospitalization for heart failure†	58 (7.2)	1.57	74 (9.0)	1.95	−1.8 (−5.5 to 1.9)	0.80 (0.57 to 1.13)
Secondary end points						
Death from any cause	27 (2.4)	0.60	39 (3.4)	0.85	−1.0 (−2.4 to 0.5)	0.71 (0.43 to 1.16)
Recurrent myocardial infarction‡	25 (2.3)	0.67	23 (2.6)	0.60	−0.3 (−2.2 to 1.5)	1.11 (0.63 to 1.96)
Hospitalization for heart failure	16 (2.2)	0.43	20 (2.1)	0.52	0.0 (−2.0 to 2.0)	0.82 (0.42 to 1.57)
Death from cardiovascular cause	17 (1.6)	0.38	23 (1.9)	0.50	−0.3 (−1.4 to 0.8)	0.76 (0.40 to 1.42)
Any hospitalization	129 (13.1)	3.65	154 (18.2)	4.25	−5.1 (−10.0 to −0.2)	0.86 (0.68 to 1.09)
Hospitalization for cardiovascular cause	78 (7.8)	2.15	87 (11.0)	2.34	−3.2 (−7.2 to 0.8)	0.92 (0.68 to 1.25)
Hospitalization for acute coronary syndrome	33 (3.8)	0.89	35 (4.8)	0.92	−1.1 (−4.2 to 2.1)	0.96 (0.60 to 1.55)
Death from any cause or recurrent myocardial infarction	50 (5.8)	1.35	59 (7.2)	1.55	−1.4 (−4.7 to 1.8)	0.86 (0.59 to 1.26)
Death from cardiovascular cause or recurrent myocardial infarction	41 (4.8)	1.10	43 (4.5)	1.13	0.3 (−2.3 to 2.8)	0.97 (0.63 to 1.49)
Recurrent myocardial infarction or hospitalization for heart failure	36 (4.0)	0.97	38 (4.3)	1.00	−0.4 (−3.0 to 2.3)	0.97 (0.61 to 1.53)
Any revascularization	38 (4.3)	1.03	45 (6.7)	1.19	−2.4 (−6.1 to 1.3)	0.86 (0.56 to 1.33)
Recurrent myocardial infarction or any revascularization	39 (4.4)	1.06	48 (7.0)	1.27	−2.6 (−6.2 to 1.1)	0.83 (0.54 to 1.26)
Composite of death from cardiovascular cause, recurrent myocardial infarction, or hospitalization for heart failure	49 (6.2)	1.33	58 (6.2)	1.53	−0.0 (−3.2 to 3.1)	0.86 (0.59 to 1.26)
Composite of death from cardiovascular cause, recurrent myocardial infarction, or any revascularization	55 (6.9)	1.49	67 (8.7)	1.78	−1.8 (−5.8 to 2.2)	0.84 (0.58 to 1.19)
Atrial fibrillation occurrence	14 (1.5)	0.37	20 (1.8)	0.53	−0.3 (−1.5 to 0.9)	0.72 (0.36 to 1.43)
Stroke	8 (0.7)	0.21	19 (1.8)	0.50	−1.1 (−2.1 to −0.1)	0.43 (0.19 to 0.99)
Exploratory end point						
Composite of death, nonfatal myocardial infarction, nonfatal stroke, or hospitalization for cardiovascular reasons	100 (11.0)	2.76	116 (14.5)	3.12	−3.5 (−8.1 to 1.1)	0.89 (0.68 to 1.16)

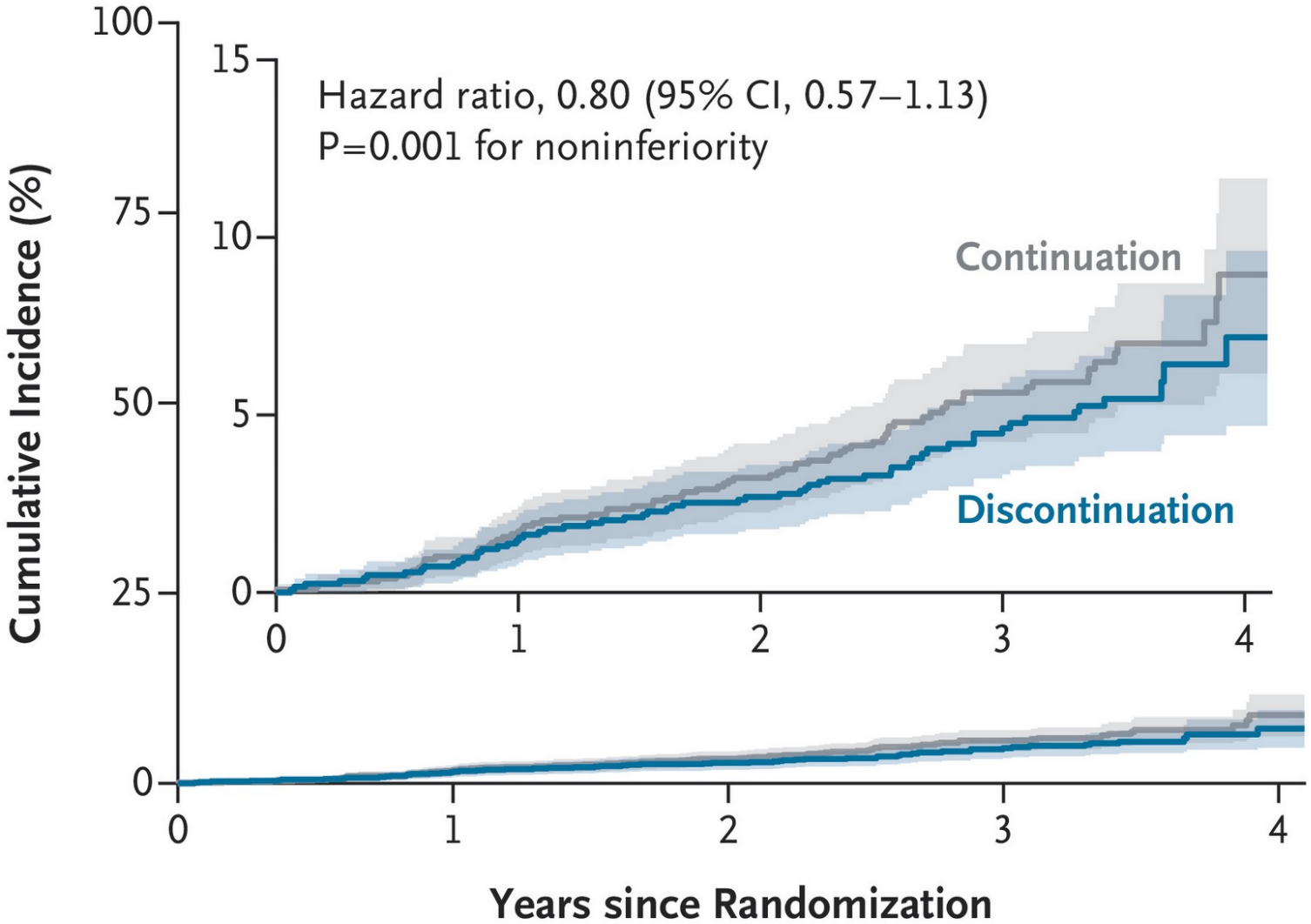

Death from Any Cause, Recurrent Myocardial Infarction, or Hospitalization for Heart Failure.

Shown are the Kaplan–Meier estimates of the cumulative incidence of death from any cause, recurrent myocardial infarction, or hospitalization for heart failure (the primary composite end point), with 95% confidence intervals indicated by the shaded regions. The inset shows the same data on an expanded y axis.

Subgroup	Total No. of Patients	Discontinuation of Beta-Blocker	Continuation of Beta-Blocker	Hazard Ratio (95% CI)
		no. of patients with event/no. of patients (4-year Kaplan–Meier estimate, %)		
All patients	2540	58/1246 (7.2)	74/1294 (9.0)	0.80 (0.57–1.13)
Age				
<65 yr	1416	14/678 (2.4)	21/738 (5.5)	0.72 (0.36–1.41)
≥65 yr	1124	44/568 (13.6)	53/556 (13.9)	0.78 (0.52–1.16)
Sex				
Male	2214	49/1088 (6.3)	69/1126 (9.1)	0.72 (0.50–1.05)
Female	326	9/158 (17.1)	5/168 (10.0)	1.95 (0.65–5.82)
Body-mass index				
<25	1175	31/558 (10.6)	47/617 (12.3)	0.72 (0.46–1.14)
≥25	1254	23/632 (4.4)	25/622 (6.1)	0.89 (0.51–1.57)
Hypertension				
No	1020	26/492 (9.8)	28/528 (8.7)	1.00 (0.59–1.70)
Yes	1520	32/754 (6.0)	46/766 (9.2)	0.68 (0.43–1.07)
Diabetes mellitus				
No	1571	31/745 (6.2)	49/826 (8.6)	0.67 (0.43–1.05)
Yes	969	27/501 (8.7)	25/468 (9.3)	1.02 (0.59–1.76)
Chronic kidney disease				
No	2312	50/1140 (6.9)	57/1172 (7.6)	0.89 (0.61–1.30)
Yes	228	8/106 (11.3)	17/122 (23.2)	0.53 (0.23–1.23)
Left ventricular ejection fraction				
40–50%	2144	51/1063 (7.0)	62/1081 (9.0)	0.82 (0.57–1.19)
>50%	396	7/183 (9.9)	12/213 (7.8)	0.64 (0.25–1.63)
Systolic blood pressure				
<140 mm Hg	2073	49/1021 (7.6)	55/1052 (8.5)	0.91 (0.62–1.33)
≥140 mm Hg	451	9/214 (5.5)	19/237 (10.6)	0.50 (0.22–1.10)
Heart rate				
<60 beats/min	238	6/117 (5.8)	1/121 (0.8)	5.94 (0.71–49.49)
≥60 beats/min	2279	52/1112 (7.4)	73/1167 (9.8)	0.73 (0.51–1.05)
Type of myocardial infarction				
STEMI	1443	31/714 (6.4)	40/729 (9.8)	0.78 (0.49–1.25)
NSTEMI	1097	27/532 (8.3)	34/565 (7.8)	0.81 (0.49–1.35)
Beta-blocker received				
Carvedilol	1210	24/596 (8.5)	33/614 (7.9)	0.74 (0.44–1.26)
Bisoprolol	821	17/404 (5.0)	22/417 (8.2)	0.78 (0.41–1.47)
Nebivolol	506	17/245 (9.8)	19/261 (14.0)	0.91 (0.48–1.76)
Other	3	0/1 (0)	0/2 (0)	—
Time since index myocardial infarction				
<4.7 yr	1275	24/636 (5.6)	35/639 (8.0)	0.67 (0.40–1.13)
≥4.7 yr	1265	34/610 (8.8)	39/655 (9.8)	0.93 (0.58–1.47)
Complete revascularization				
No	620	18/324 (9.5)	22/296 (11.1)	0.75 (0.40–1.41)
Yes	1849	39/879 (6.5)	52/970 (8.5)	0.80 (0.53–1.21)

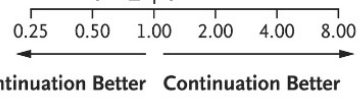

Analysis of the Primary End Point in Prespecified Subgroups (Intention-to-Treat Population).

The body-mass index is the weight in kilograms divided by the square of the height in meters. Chronic kidney disease was defined as kidney damage (pathologic abnormalities or markers of damage, including abnormalities on blood or urine testing or imaging) or an estimated glomerular filtration rate of less than 60 ml per minute per 1.73 m^2 of body-surface area. The median time since the index myocardial infarction was 4.7 years. NSTEMI denotes non–ST-segment elevation myocardial infarction, and STEMI ST-segment elevation myocardial infarction.

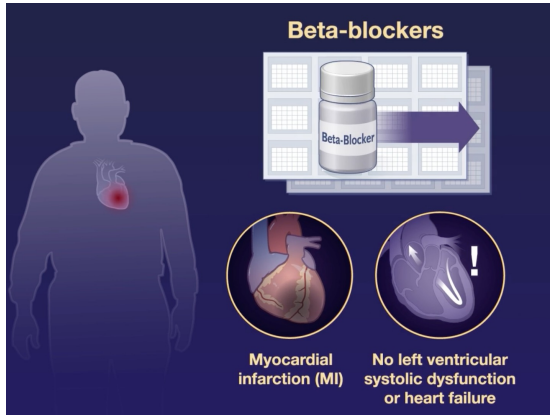
Beta-blockers
Beta-Blocker
Myocardial infarction (MI)
No left ventricular systolic dysfunction or heart failure

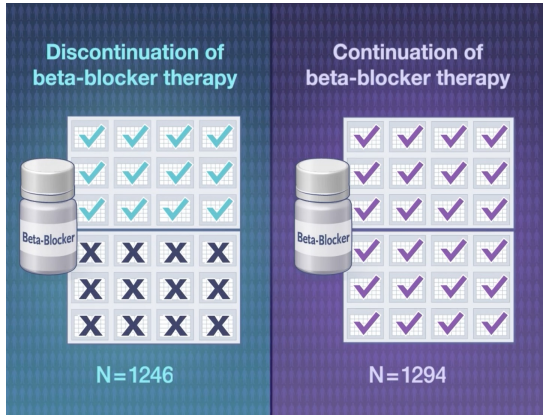
Discontinuation of beta-blocker therapy
Continuation of beta-blocker therapy
Beta-Blocker
N=1246
N=1294

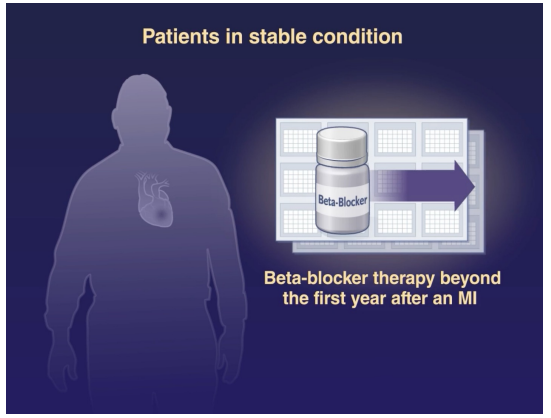
Patients in stable condition
Beta-Blocker
Beta-blocker therapy beyond the first year after an MI

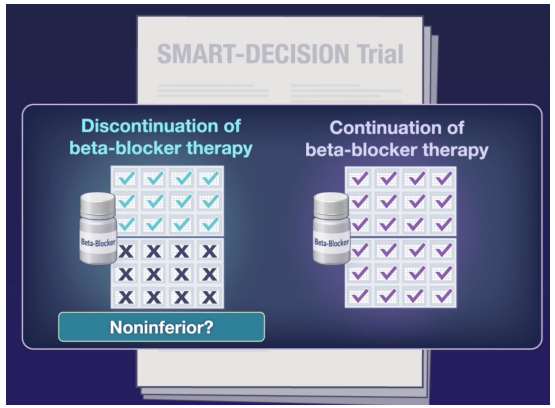
SMART-DECISION Trial
Discontinuation of beta-blocker therapy
Continuation of beta-blocker therapy
Noninferior?

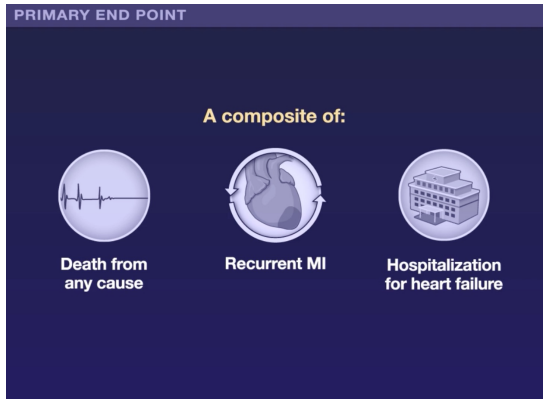
PRIMARY END POINT
A composite of:
Death from any cause
Recurrent MI
Hospitalization for heart failure

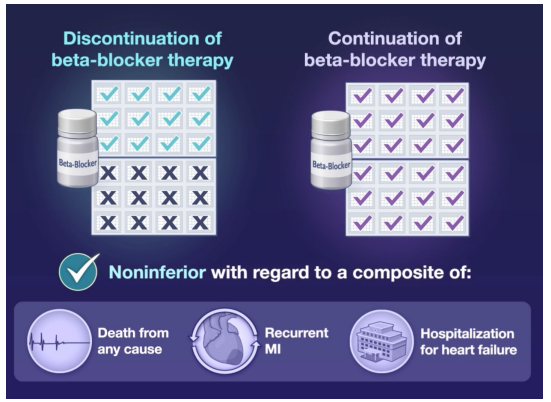
Discontinuation of beta-blocker therapy
Continuation of beta-blocker therapy
Noninferior with regard to a composite of:
Death from any cause
Recurrent MI
Hospitalization for heart failure

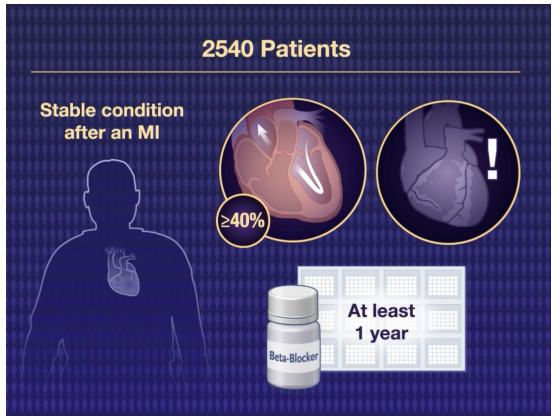
2540 Patients
Stable condition after an MI
≥40%
At least 1 year
Beta-Blocker

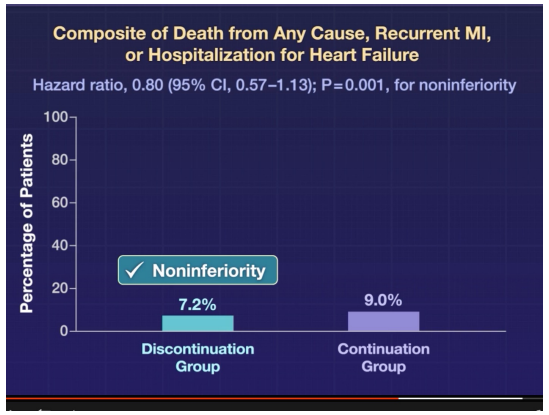
Composite of Death from Any Cause, Recurrent MI, or Hospitalization for Heart Failure
Hazard ratio, 0.80 (95% CI, 0.57–1.13); P=0.001, for noninferiority
Percentage of Patients
100
80
60
40
20
0
Noninferiority
7.2%
9.0%
Discontinuation Group
Continuation Group

GLP-1 Receptor Agonists

Summary

Glucagon-like peptide-1 (GLP-1) receptor agonists are incretin analogues that promote glucose-mediated insulin release and are used to treat type 2 diabetes mellitus and obesity. GLP-1 receptor agonists and GLP-1 and glucose-dependent insulinotropic peptide agonists have several mechanisms of action, including reduction of gastric emptying, inhibition of glucagon secretion, beneficial changes in the intestinal microbiome, and direct effects on hypothalamic nuclei to enhance satiety (which promotes weight loss). Beyond the impressive effects of GLP-1 receptor agonists on blood glucose levels and body weight, large-scale randomized, controlled trials have shown that GLP-1 receptor agonists reduce cardiovascular risk and slow progression to renal failure in persons at high risk and those with type 2 diabetes. Adverse side effects from GLP-1 receptor agonists are mostly gastrointestinal but may also include loss of muscle and bone mass. Questions remain about long-term adherence, weight regain after discontinuation of treatment, and the functional implications of the loss of muscle and bone mass. Recent and ongoing targeted studies suggest the possibility of additional uses for GLP-1 receptor agonists.

GLP-1 Receptor Agonists

- Glucagon-like peptide-1 (GLP-1) receptor agonists work through enhanced glucose-mediated insulin secretion, augmented by double or triple GLP-1 receptor agonists and glucose-dependent insulinotropic peptide (GIP) receptor agonists.
- GLP-1 receptor agonists indirectly lower blood glucose levels by reducing gastric emptying, inhibiting glucagon secretion, and contributing to a beneficial intestinal microbiome.
- GLP-1 receptor agonists and GIP receptor agonists have direct effects on hypothalamic nuclei that enhance satiety and promote weight loss.
- Large-scale randomized, controlled trials have shown that GLP-1 receptor agonists reduce cardiovascular risk and progression to renal failure in persons at high risk and those with type 2 diabetes.
- Adverse events and side effects associated with GLP-1 receptor agonists are predominantly gastrointestinal but also include loss of muscle and bone mass.

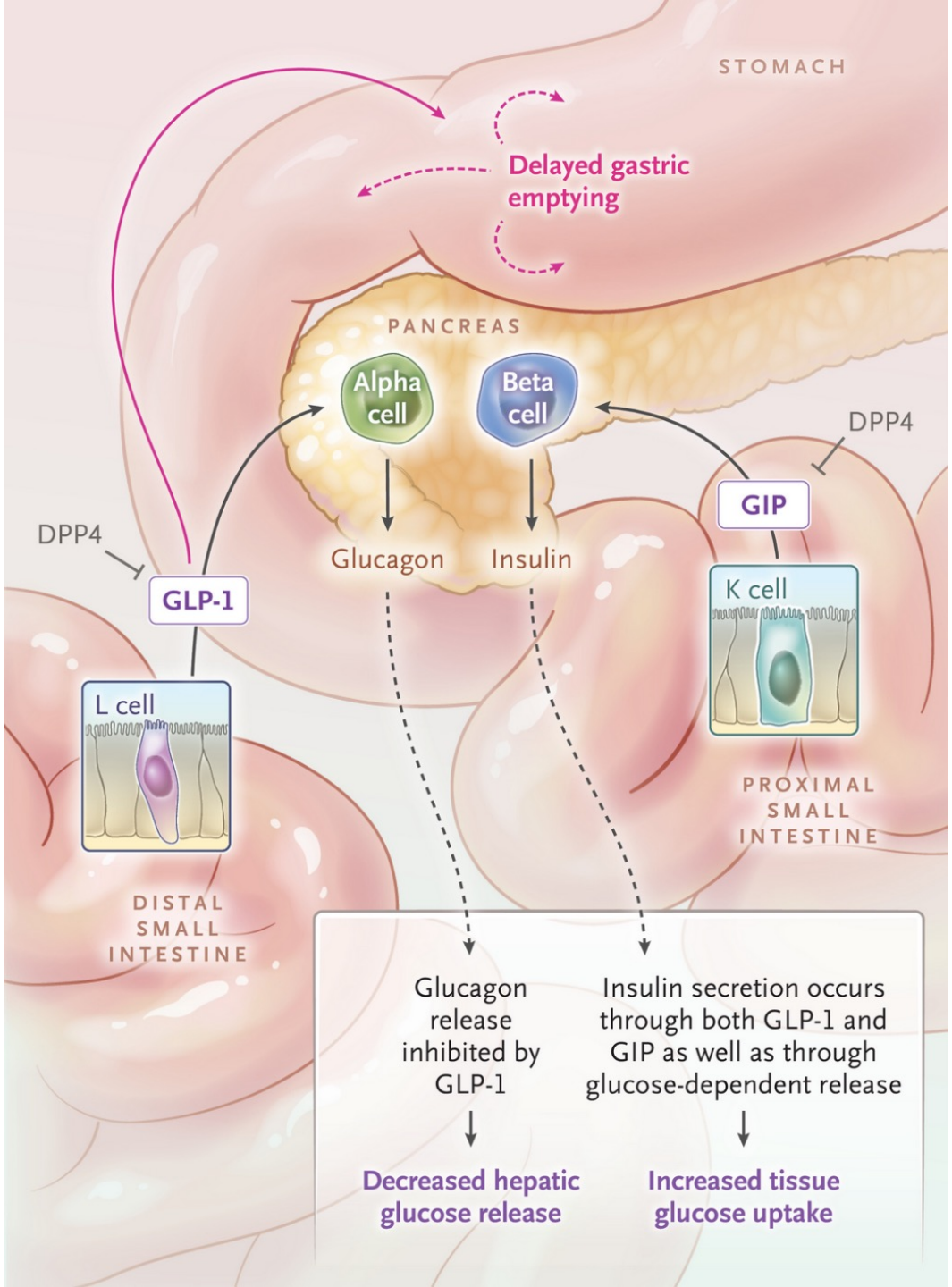

Physiologic Effects of the Incretin Family of Drugs.

The three major insulinotropic peptides (glucagon-like peptide 1 [GLP-1], glucose-dependent insulinotropic peptide [GIP], and glucagon) are synthesized by several tissues, although the pancreas and the small intestine are major sources of the circulating forms. Synthesis begins with the 160–amino acid glucagon precursor, proglucagon (PG), which is differentially processed in the pancreas but not in the gut and brain. Proglucagon is cleaved to glucagon in the pancreas, and in the gut, four fragments having important functions are produced.

Adverse events

- Adverse events
  - Gastrointestinal — nausea, vomiting, abdominal pain, diarrhea, constipation, bloating, belching, flatulence
  - Glycemic — hypoglycemia in persons with diabetes mellitus
  - General well-being — fatigue, dizziness
  - Central nervous system — headache, mood changes
  - Drug interactions
- Serious adverse events
  - Allergy — anaphylaxis
  - Pancreatic — acute pancreatitis
  - Gallbladder — acute cholelithiasis
  - Kidney — acute kidney injury
  - Mood — mood changes, suicidality
  - Tumorigenesis — risk of thyroid C-cell tumors (only in animal models to date)
  - Ophthalmologic — risk of worsening diabetic retinopathy

Agents

Agent	Description
Approved to date	
Dulaglutide (Trulicity)	Long-acting agent
Exenatide (Byetta)	Short-acting agent; first such agent approved in the United States
Exenatide extended release (Bydureon)	
Liraglutide (Victoza, Saxenda)	Intermediate-acting agent
Lixisenatide (Adlyxin)	Once-daily dose
Semaglutide injection (Ozempic)	
Semaglutide tablets (Rybelsus)	For treatment of diabetes
Tirzepatide	Dual-receptor agonist; approved in 2022 for type 2 diabetes and in 2023 for weight loss
Under development	
Retatrutide	GIP, GLP-1, and GLP-1 receptor agonist
Orforglipron	Oral capsule of a chemical GLP-1 receptor agonist; phase 3 study of orforglipron will end in 2027
Danuglipron	Oral medication, a chemical GLP-1 receptor agonist, entering phase 2 studies
APHD-012	Once-daily oral medication; manufacturer describes it as a distal jejunal-release dextrose bead; phase 2 study nearing completion
ARD-101	Oral medication that works at intestinal bitter-taste receptors, where it activates appetite-suppressing hormones such as GLP-1, GLP-2, and cholecystokinin; phase 2 studies are ongoing
Amycretin	Oral medication that is a dual GLP-1 receptor and amylin agonist; once-daily dose, with subcutaneous injection being developed; phase 2 study stage in progress
Monlunabant	Oral medication, cannabinoid receptor-1 inverse agonist; once-daily dose; phase 2 study stage in progress
GSBR-1290	Oral GLP-1 medication; phase 2 study stage in progress
Cagrilintide–semaglutide (Cagri-Sema)	Once-weekly injection that combines cagrilintide (amylin mimic) with semaglutide GLP-1 receptor agonist
Ecnoglutide (XW003)	GLP-1 receptor agonist; injectable, once weekly
Mazdutide (IBI362)	GLP-1 receptor agonist that also mimics glucagon; being studied for weight loss and type 2 diabetes in adults; phase 3 studies in China nearing completion
Survodutide	Once-weekly injection; activates GLP-1 and glucagon receptors; action similar to that of mazdutide
VK2735	Once-weekly injection; dual GLP-1 receptor agonist and GIP receptor agonist, similar to tirzepatide; oral version in development
Maridebart cafraglutide (MariTide)	Injectable monthly; mimics GLP-1 receptor agonist but blocks GIP receptor agonists
Bimagrumab	Monoclonal antibody against activin receptors; administered intravenously monthly

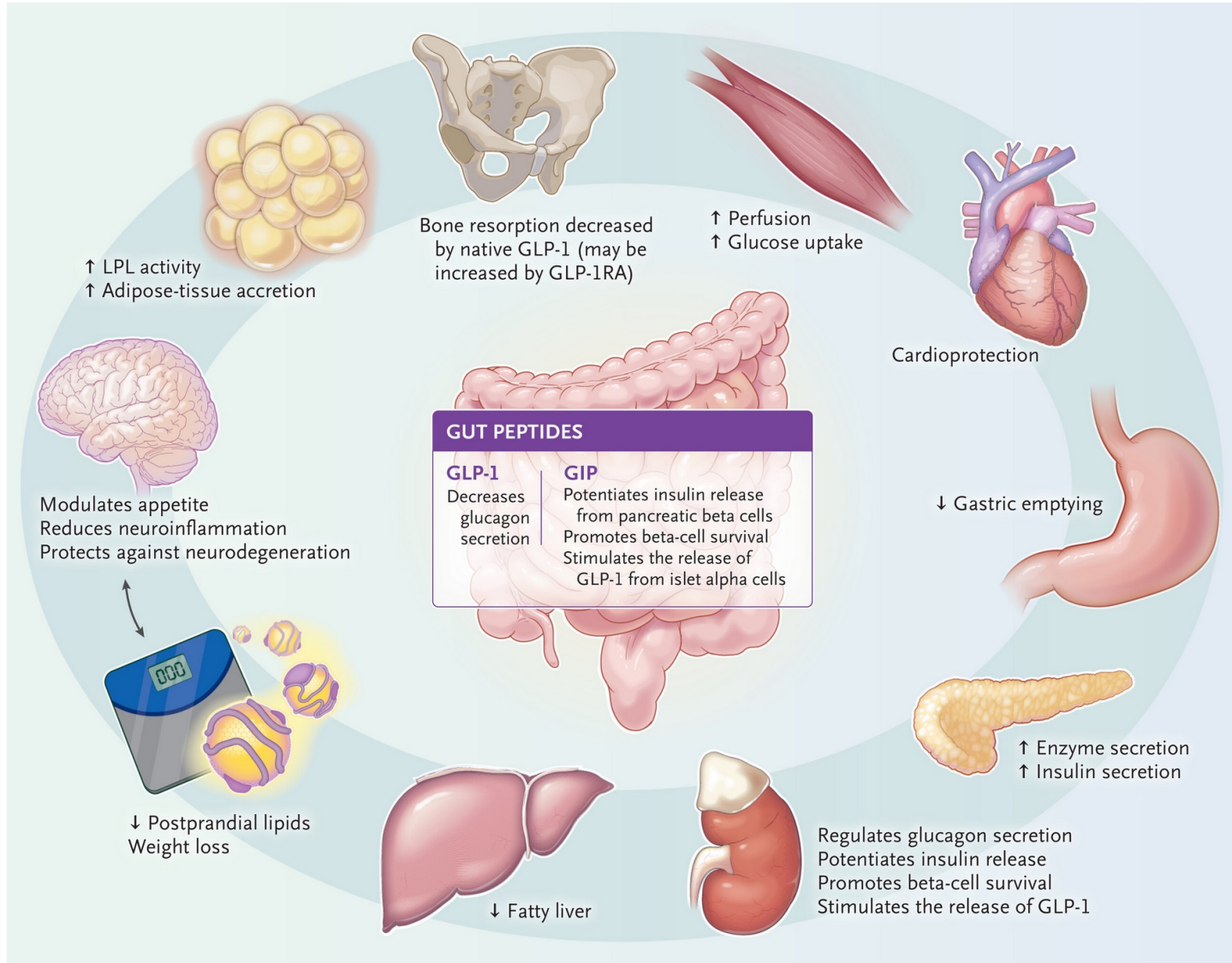

Effects of Combined GLP-1 and GIP Receptor Agonists.

GLP-1 Receptor Agonists and Health Equity

Underrepresented populations are often excluded from clinical trials for multiple reasons; thus, generalizations about the effectiveness of virtually any drug or intervention of necessity must be qualified. Such exclusion is particularly relevant for persons with type 2 diabetes and obesity, because Hispanic and Black persons make up a large proportion of the population with these diseases. Of importance, although the recruitment of members of minority groups into large trials has improved somewhat over the past decade, trial populations often do not reflect the truly affected populations. One substudy from the SURPASS-1 trial, which enrolled patients with type 2 diabetes, showed that Hispanic participants had responses similar to those of non-Hispanic White participants with regard to weight loss and lowering of glucose levels. However, few other studies have analyzed the effectiveness of the GLP-1 receptor agonists in minority populations or have included enough Black or Hispanic participants in large trials to draw clinically relevant conclusions about efficacy. Complicating this concern is the cost of the newer GLP-1 receptor agonist agents. As more evidence accumulates regarding the safety and efficacy of long-term treatments, there should be price adjustments and plans for greater distribution of these drugs to underrepresented populations.

Conclusions

Taken together, clinical data on incretin-based agents now place them at the top of the therapeutic armamentarium for persons with type 2 diabetes or obesity (or both). The development of new dual and triple GLP-1 receptor agonists forecasts that other effective drugs may be approved after rigorous phase 2 and phase 3 trials. Strong evidence from large phase 3 clinical trials and numerous meta-analyses support the role of GLP-1 receptor agonists in stabilizing blood glucose levels in patients with type 2 diabetes as well as in effecting clinically important weight loss. Similarly, longer-term protective effects on cardiovascular and renal outcomes are impressive. Although reported safety signals are relatively reassuring, longer-term studies are needed, with a particular focus on weight regain and changes in muscle and bone mass. Health equity in trials and the marketplace is required to more broadly include persons who need these drugs. Furthermore, GLP-1 receptor agonists also show promise in the targeting of other disorders, including neurodegenerative disorders, metabolic liver disease, heart failure, and cancer. The future looks promising as these GLP-1 receptor agonists enter a second half-century of study.

Too Much of a Good Thing

(An otherwise „ok“ obese man lapses into NH4-coma after „all-you-can-eat“)

A 57-year-old man with a 3-day history of vomiting and progressive confusion was brought to the emergency department by his wife. He had been in his usual state of health until 3 days earlier, when he had become disoriented to the day of the week. By the morning of his arrival at the emergency department, he was unable to remember the names of his medications. He reported generalized weakness and difficulty speaking and swallowing but no headache, numbness, visual disturbance, fever, recent weight loss, or other systemic symptoms. Aside from vomiting, he had no gastrointestinal symptoms.

The patient’s medical history included hypertension, type 2 diabetes, primary hypothyroidism, asthma, and obesity with obstructive sleep apnea. He had had a myocardial infarction 16 years earlier and a laparoscopic cholecystectomy 14 years earlier. He was followed by his primary care physician. His medications included amlodipine, metformin, levothyroxine, a formoterol–budesonide inhaler, as-needed salbutamol, clopidogrel, pantoprazole, metoprolol, and rosuvastatin (the latter four were prescribed after the myocardial infarction). He had quit smoking 4 years earlier after a 20-pack-year history, and he had never used alcohol or illicit drugs. His family history was negative for neurocognitive disorders.

His blood pressure was 164/116 mm Hg, heart rate 95 beats per minute, respiratory rate 16 breaths per minute, oxygen saturation 100% while he was breathing ambient air, temperature (tympanic) 35.8°C, and body-mass index (BMI; the weight in kilograms divided by the square of the height in meters) 31.9. He opened his eyes to speech and obeyed commands but was confused, findings consistent with a Glasgow Coma Scale (GCS) score of 13 (on a scale from 3 to 15, with lower scores indicating less responsiveness). Neurologic examination revealed slowed cognitive processing and dysarthria. Cranial-nerve function was intact. Proximal and distal muscle strength was 4/5 in both legs, 4+/5 in the left arm, and 5/5 in other muscle groups. Sensory examination was normal. Deep tendon reflexes were intact, with flexor plantar responses. There was no nuchal rigidity. Abdominal examination revealed normal bowel sounds, tympanic percussion, no tenderness, and no palpable masses or hepatosplenomegaly. The rest of the examination was unremarkable.

The white-cell count was 7400 per microliter. The hemoglobin level and platelet count were normal. The glucose level was 221 mg per deciliter (reference range, 74 to 106); the rest of his basic metabolic panel was normal, as were the prothrombin time and levels of total bilirubin, alanine aminotransferase, aspartate aminotransferase, γ-glutamyltransferase, alkaline phosphatase, and C-reactive protein (CRP). A venous blood gas analysis yielded normal results. The albumin level was 2.7 g per deciliter (reference range, 3.5 to 5.0). The thyroid-stimulating hormone (TSH) level was 0.1 mIU per liter (reference range, 0.5 to 4.3). Urinalysis was positive for glucose but negative for white cells, nitrite, and ketones.

What about BUN and creatinine?

The patient was admitted to the neurology service. Computed tomography (CT) and magnetic resonance imaging (MRI) of the head showed no evidence of ischemia, hemorrhage, cerebral venous sinus thrombosis, neoplasm, or encephalitis. Blood and urine cultures were obtained. A lumbar puncture revealed a cerebrospinal fluid (CSF) leukocyte count of less than 5 cells per microliter (reference value, <5), protein level of 0.36 g per liter (reference range, 0.18 to 0.58), and glucose level of 133 mg per deciliter (reference range, 45 to 80).

That afternoon, the patient became unresponsive (GCS score of 3), prompting intubation and transfer to the intensive care unit. Plasma ammonia was measured and was 344 µmol per liter (reference value, <45). Hepatic ultrasonography was performed and showed no evidence of cirrhosis or portosystemic shunting.

Because of the diagnosis of noncirrhotic hyperammonemia, our specialized inherited metabolic diseases expert center was consulted and provided guidance. Blood samples were collected for plasma amino acids and acylcarnitines and urine samples for organic acids, including orotic acid, and treatment was initiated immediately. To reduce ammonia production, protein intake was stopped, and continuous infusion of 2 liters of 10% dextrose daily was started. Several medications were started to further reduce ammonia levels, including sodium benzoate, arginine, and carnitine; these were locally unavailable but were delivered in less than 2 hours from our center by express courier. Isotonic saline was coadministered to promote diuresis and the effectiveness of sodium benzoate. Meanwhile, lactulose and rifaximin were administered by nasogastric tube, and preparations were made to initiate venovenous hemofiltration.

Plasma ammonia, glucose, sodium, and potassium were monitored every 3 hours, as were venous blood gases. Three hours after treatment initiation, the plasma ammonia level had decreased to 265 µmol per liter; at 6 hours, it had declined to 160 µmol per liter; and by the following morning — 12 hours after treatment initiation — it had reached 110 µmol per liter.

After consultation with dietary services, protein intake was increased by 0.3 g per kilogram of body weight per day, to a maximum of 1.2 g per kilogram per day over a period of 4 days. Caloric requirements were met by carbohydrates and fats. By hospital day 5 (3 days after treatment initiation), the plasma ammonia level had decreased to 29 µmol per liter. The patient regained full consciousness and was extubated and transferred to the internal medicine ward. There, intravenous medications were transitioned to oral formulations. Sodium benzoate was gradually tapered and discontinued after 6 days, together with carnitine. Rifaximin and lactulose were discontinued 2 days later. Arginine was replaced with citrulline, which was continued pending the results regarding metabolic analytes obtained during hyperammonemia.

The patient was questioned regarding dietary changes before symptom onset; he reported no such changes and no use of protein supplements. An abdominal MRI did not reveal an intrahepatic shunt. Blood, urine, and CSF cultures that were obtained early in the admission yielded negative results. On hospital day 7, results of plasma amino acids and acylcarnitines became available. The level of glutamine was 1137 µmol per liter (reference range, 462 to 762), glutamic acid 172 µmol per liter (reference range, 0 to 48), citrulline 10 µmol per liter (reference range, 16 to 56), and arginine 22 µmol per liter (reference range, 32 to 108).

Additional history taking revealed that 3 days before admission, he had consumed a large protein-rich meal at an all-you-can-eat restaurant.

Family history was notable for the death of his brother at 12 years of age, reportedly due to meningitis. DNA sequencing of the proximal urea-cycle genes identified a pathogenic variant in *OTC*: NM_000531.6(OTC):c.119G→A, p.(Arg40His), resulting in a diagnosis of OTC deficiency.

The patient was advised not to exceed a protein intake of 1.2 g per kilogram per day, and citrulline was continued. He received a personalized plan for management during acute illness and was referred to clinical genetics services for family counseling. He reported fatigue and short-term memory loss since the hyperammonemic episode, for which he was referred for neurocognitive rehabilitation. At a 3-month follow-up, he had not had further episodes of hyperammonemia, although his fatigue and short-term memory loss persisted.

In Ornithine Transcarbamylase (OTC) deficiency, **blood urea nitrogen (BUN) levels are typically low** or within the low-normal range, often below 10 mg/dL, despite the presence of severe hyperammonemia. This indicates a failure to convert nitrogen waste into urea, resulting in high levels of ammonia, high glutamine, and low citrulline.

Key Findings in OTC Deficiency:

- **Urea/BUN:** Low or low-normal, reflecting decreased production.
- **Ammonia:** Critically high (Hyperammonemia).
- **Citrulline:** Low or absent.
- **Orotic Acid:** Highly elevated in urine.
- **Glutamine:** High.

Noncirrhotic hyperammonemia is an underrecognized medical emergency requiring immediate treatment

Agent	Mechanism of Action	Route of Administration	Dose
Nitrogen scavengers that bypass the urea cycle†			
Sodium benzoate	Conjugates glycine to form hippurate, which is excreted renally	IV in 10% dextrose	5.5 g/m² bolus over 90–120 min, then 5.5 g/m²/day continuous (maximum daily dose, 12 g)‡
Sodium phenylacetate§	Conjugates glutamine to form phenylacetylglutamine, which is excreted renally	IV in 10% dextrose	Same dose as sodium benzoate (maximum daily dose, 12 g)‡
Sodium phenylbutyrate	Same mechanism as sodium phenylacetate	IV in 10% dextrose and enteral	IV: same dose as sodium benzoate; oral: 5 g/m²/day in four divided doses (maximum daily dose, 12 g)‡
Glycerol phenylbutyrate	Prodrug of sodium phenylbutyrate; same mechanism	Enteral	5 g/m²/day in three divided doses (maximum daily dose, 12 g)‡
Agents that enhance the urea cycle			
Arginine	Replenishes arginine, which is essential for urea-cycle activity	IV in 10% dextrose	250 mg/kg bolus over 90–120 min, then 250 mg/kg/day continuous (maximum daily dose, 12 g)
Carnitine	Activates CPS1, neutralizes toxic metabolites, and corrects secondary carnitine deficiency	IV	100 mg/kg/day in three divided doses
N-carbamylglutamate¶	Allosterically activates CPS1	Enteral	100 mg/kg bolus, then 25–62.5 mg/kg every 6 hr
Agents that reduce intestinal ammonia production and absorption			
Lactulose	Lowers colonic pH, thereby reducing bacterial ammonia production; traps ammonia as nonabsorbable ammonium	Enteral	10 ml one to three times daily, adjusted to two or three loose stools/day
Rifaximin	Reduces ammonia-producing gut flora	Enteral	550 mg twice daily

Ornithine transcarbamylase (OTC) deficiency — the most common urea-cycle disorder.

Urea comes from here

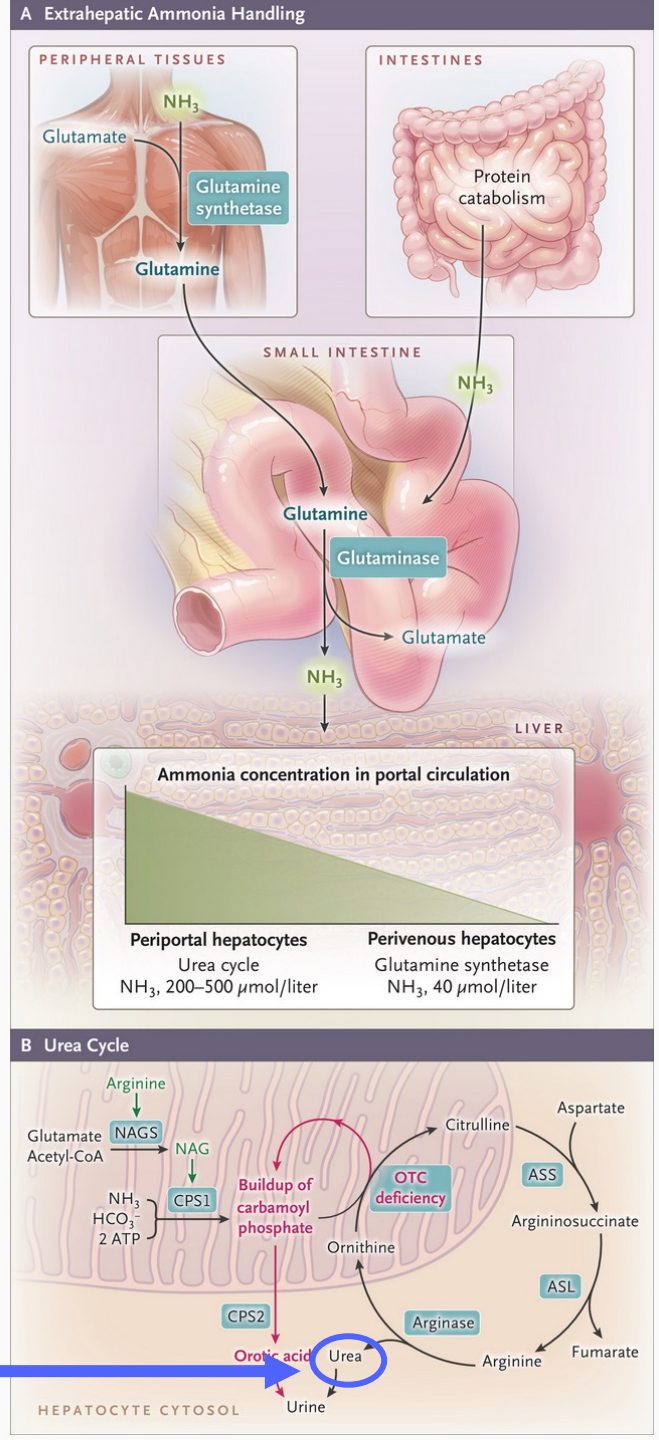

Extrahepatic Ammonia Handling and the Urea Cycle.

As shown in Panel A, ammonia (NH_3) is produced during protein catabolism and in the intestines. In peripheral tissues, ammonia is incorporated with glutamate into glutamine by glutamine synthetase. In the small intestine, glutaminase releases ammonia and glutamate from glutamine. Ammonia enters the liver through the portal circulation, where periportal hepatocytes convert ammonia into urea through the urea cycle. Residual ammonia is taken up by perivenous hepatocytes and incorporated into glutamine again. As shown in Panel B, the urea cycle consists of five catalytic enzymes and one cofactor-producing enzyme. It incorporates two nitrogen atoms (one from ammonia and one from aspartate) into a single urea molecule. Deficiency of ornithine transcarbamylase (OTC), the second enzyme of the cycle, is the most common urea-cycle disorder. OTC deficiency results in accumulation of carbamoyl phosphate and overflow into the cytosol, where carbamoyl phosphate synthetase 2 (CPS2) converts it into orotic acid, which is detectable in the urine. ASL denotes argininosuccinate lyase, ASS argininosuccinate synthase, CoA coenzyme A, CPS1 carbamoyl phosphate synthetase 1, HCO_3^- bicarbonate, NAG *N*-acetylglutamate, and NAGS *N*-acetylglutamate synthase.

THE LANCET

Childhood Cancer Awareness

A Future of Hope

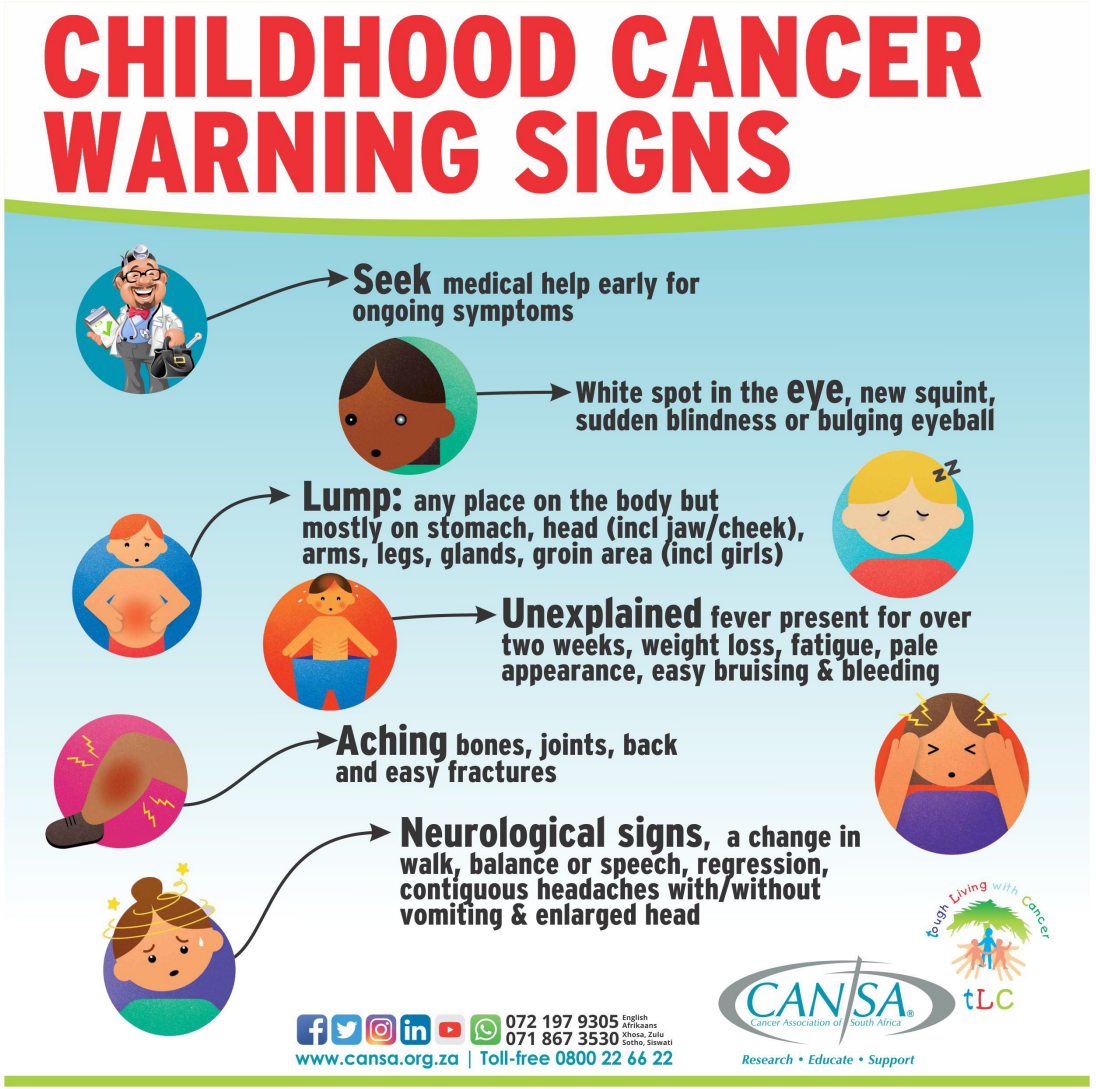

The cancer survival index is a summary measure, usually expressed as a percentage, indicating the proportion of people alive a specific time (often one, five, or 10 years) after a cancer diagnosis. It acts as a statistical tool to track population-level trends, such as improvements in early detection and treatment.

Key Aspects of the Cancer Survival Index:

- **Measurement:** It estimates net survival, which compares the survival of cancer patients against the expected survival of the general population of the same age and sex, effectively isolating mortality directly caused by cancer.
- **Population Focus:** It is designed to monitor trends over time, such as in the UK's NHS outcomes, rather than predict an individual's personal prognosis.
- **Data Included:** The index often combines data from multiple major cancers (such as breast, colorectal, and lung) to provide a single, comprehensive overview.
- **Trends:** As of 2026, 5-year survival rates for all cancers combined have reached roughly 70% in some regions, a significant increase from 50% in the 1970s, due to improved treatments like immunotherapy.

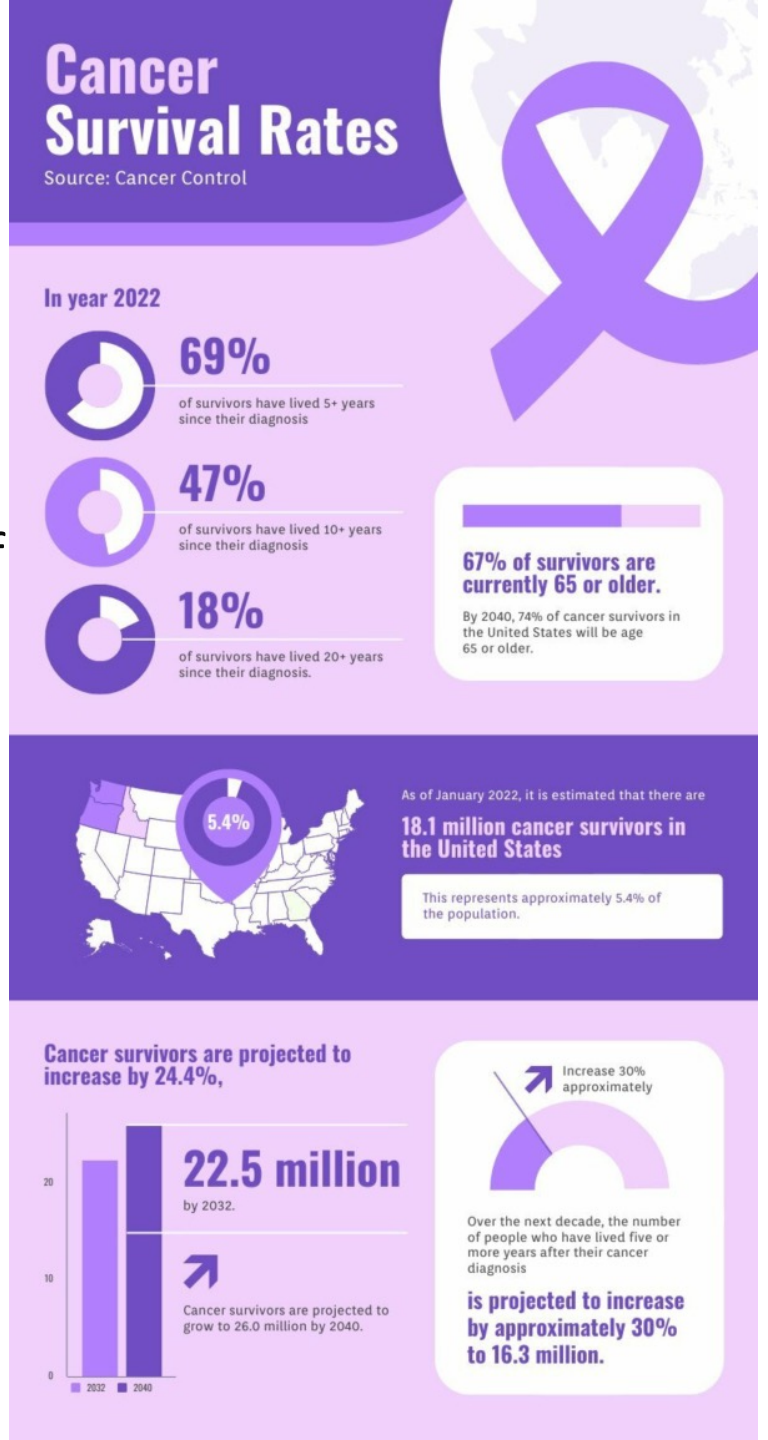

Progress towards the WHO Global Initiative for Childhood Cancer target of 60% 5-year survival for all childhood cancers combined, 1990–2019 (CONCORD-4): a Cancer Survival Index derived for 68 countries by analysis of individual records for 613 021 children from 307 population-based cancer registries

(Development of a CSI for children)

Summary

Background CONCORD is a global public health programme for long-term surveillance of population-based cancer survival. The first three cycles of this programme focused primarily on adults. In CONCORD-4, for the first time, we also included all cancers in children. The WHO Global Initiative for Childhood Cancer (GICC), published in 2018, set a target for 5-year survival for all childhood cancers combined, worldwide, to reach 60% by 2030. We designed the protocol for CONCORD-4 to assess progress towards this target in as many countries as possible.

Methods We identified population-based cancer registries from the members of the International Association of Cancer Registries and other sources. We invited 513 registries in 101 countries to submit anonymised individual records for all children (aged 0–14 years) living in their territory who were diagnosed with any form of cancer during the 30-year period 1990–2019, or later years. The data included demographic variables, the morphological type and anatomical location of the tumour, and the follow-up for the vital status of each child. We used the data for 2010–19 to construct a set of weights that reflect the global frequency distribution of childhood cancers, by age, sex, and subtype, both for the 12 major groups in the third edition of the International Classification of Childhood Cancer (ICCC-3) and for the six WHO tracer cancers prioritised in the GICC. We estimated 5-year net survival for children diagnosed during 1990–2019 by age, sex, and type of cancer, using the Pohar Perme estimator. We then used the weights to construct a Cancer Survival Index (CSI) as a weighted average of these survival estimates, for each country and each 5-year period during 1990–2019 for the 12 ICCC-3 groups and separately for the six WHO tracer cancers.

Findings We received 679 776 individual records for children diagnosed with cancer during 1990–2022 from 307 population-based cancer registries in 68 countries and territories, 52 with 100% national coverage. We produced two sets of weights, by age, sex, and type of cancer, reflecting the global distribution of cancer in children, both for all childhood cancers and for the six WHO tracer cancers. We restricted survival analyses to 613 021 children diagnosed during 1990–2019. The 5-year CSI for all childhood cancers combined increased in most countries between 1990 and 2019. For children diagnosed during 2015–19, the CSI was more than 80% in most high-income countries, in the range 60–80% in most upper-middle-income countries, and in the range 50–60% in the five participating lower-middle-income countries.

Interpretation The new CSI enables quantitative international comparison of trends in survival for all childhood cancers combined and for the six WHO tracer cancers, through a simple three-way standardisation by age, sex and subtype. The CSI should be a useful tool to monitor future trends. In most high-income, upper-middle-income, and lower-middle-income countries participating in CONCORD-4, the all-cancers CSI was either close to or had already passed the GICC target to reach 60% 5-year survival for all childhood cancers combined, worldwide, by 2030. The GICC target therefore may not be ambitious enough.

Funding Cancer Research UK, Institut National du Cancer (France), St Jude Children's Research Hospital (USA), US National Cancer Institute, and Dell Technologies.

Introduction

The target of the WHO Global Initiative for Childhood Cancer (GICC), published in 2018, is to reach 60% survival for all childhood cancers combined, worldwide, by 2030.[1] The duration of survival was not explicitly stated, but was presumed to be 5 years.

In 2021, WHO prioritised six "tracer" cancers, to help monitor overall progress: acute lymphoblastic leukaemia, Burkitt lymphoma, Hodgkin lymphoma, retinoblastoma, Wilms tumour, and low-grade glioma.[2] The tracer cancers were not chosen to imply greater importance than other cancers, but "to help inform a broader response relevant to all childhood cancers".[2] The six tracer cancers were described as representing 50–60% of all childhood cancers, as being highly curable with proven therapies, and with potential 5-year survival of 85% or higher.

Methods

Study design

On Dec 13, 2022, we invited 513 population-based cancer registries from the members of the International Association of Cancer Registries and other sources in 101 countries to submit anonymised individual records in a single file for all children (aged 0–14 years) living in their territory who were diagnosed with any form of cancer during the 20-year period 2000–19 or later years. Older registries were also invited to submit data for children diagnosed during the 1990s. We also invited submission of data for adults (aged 15–99 years) diagnosed with one of 22 cancers or groups of cancers: we will report on those data separately. A further invitation was issued jointly with the Organisation for Economic Co-operation and Development (OECD) in May, 2023.

Of the 513 registries, 18 were in Africa (11 countries), 58 were in central and South America, including the Caribbean (19 countries), 71 were in North America (two countries), 143 were in Asia (25 countries), 212 were in Europe (40 countries), and 11 were in Oceania (four countries).

Countries and territories were defined by their UN name and continent as of 2025.[20] The names of jurisdictions used in the text, tables, graphics, maps, and appendix are based on those used for statistical purposes by the Statistics Division of the UN Secretariat; similarly, we use the term "national coverage" to contrast with "regional coverage" for statistical purposes. These designations and the presentation of data do not imply any assumption regarding the political affiliation of countries or territories, or the expression of any opinion whatsoever on the part of the CONCORD programme concerning the legal status of any country, territory, city, or area, or of its authorities, or concerning the delimitation of its frontiers or boundaries. Cyprus is a member state of the European Union but it is part of Asia. Barbados, Costa Rica, Cuba, El Salvador, French Guiana, Guadeloupe, Guatemala, Martinique, Mexico, Puerto Rico, and Trinidad and Tobago (Caribbean and central America) were grouped with South America as central and South America.

	1990–94	1995–99	2000–04	2005–09	2010–14	2015–19	2020–22	All records	All classified records, 1990–2022
ICCC-3 group									
I: Leukaemias	6216 (30·4%)	7494 (29·8%)	39 664 (31·4%)	44 058 (30·3%)	50 551 (30·0%)	50 207 (29·7%)	7749 (31·5%)	205 939 (30·3%)	205 939 (30·4%)
II: Lymphomas	2500 (12·2%)	3040 (12·1%)	15 025 (11·9%)	16 597 (11·4%)	20 320 (12·0%)	20 877 (12·4%)	3108 (12·6%)	81 467 (12·0%)	81 467 (12·0%)
III: CNS	4086 (20·0%)	5036 (20·0%)	26 074 (20·6%)	31 993 (22·0%)	37 312 (22·1%)	37 260 (22·1%)	5116 (20·8%)	146 877 (21·6%)	146 877 (21·7%)
IV: Neuroblastoma	1286 (6·3%)	1489 (5·9%)	8064 (6·4%)	9007 (6·2%)	9953 (5·9%)	9558 (5·7%)	1317 (5·4%)	40 674 (6·0%)	40 674 (6·0%)
V: Retinoblastoma	536 (2·6%)	598 (2·4%)	3195 (2·5%)	3696 (2·5%)	4096 (2·4%)	4000 (2·4%)	599 (2·4%)	16 720 (2·5%)	16 720 (2·5%)
VI: Renal tumours	1004 (4·9%)	1344 (5·3%)	6434 (5·1%)	6926 (4·8%)	7665 (4·5%)	7347 (4·4%)	1078 (4·4%)	31 798 (4·7%)	31 798 (4·7%)
VII: Hepatic tumours	225 (1·1%)	285 (1·1%)	1878 (1·5%)	2191 (1·5%)	2785 (1·7%)	2833 (1·7%)	484 (2·0%)	10 681 (1·6%)	10 681 (1·6%)
VIII: Bone tumours	866 (4·2%)	1122 (4·5%)	5721 (4·5%)	6097 (4·2%)	7050 (4·2%)	7026 (4·2%)	1026 (4·2%)	28 908 (4·3%)	28 908 (4·3%)
IX: Soft tissue sarcomas	1375 (6·7%)	1741 (6·9%)	7943 (6·3%)	10 153 (7·0%)	11 655 (6·9%)	11 548 (6·8%)	1570 (6·4%)	45 985 (6·8%)	45 985 (6·8%)
X: Germ-cell tumours	732 (3·6%)	988 (3·9%)	4880 (3·9%)	5873 (4·0%)	6596 (3·9%)	6692 (4·0%)	932 (3·8%)	26 693 (3·9%)	26 693 (3·9%)
XI: Other epithelial neoplasms	1239 (6·1%)	1644 (6·5%)	5864 (4·6%)	6609 (4·5%)	8177 (4·8%)	8862 (5·2%)	1207 (4·9%)	33 602 (4·9%)	33 602 (5·0%)
XII: Other and unspecified neoplasms	244 (1·2%)	312 (1·2%)	1250 (1·0%)	1623 (1·1%)	1831 (1·1%)	2058 (1·2%)	301 (1·2%)	7619 (1·1%)	7619 (1·1%)
Unclear	32 (0·2%)	39 (0·2%)	155 (0·1%)	189 (0·1%)	209 (0·1%)	204 (0·1%)	32 (0·1%)	860 (0·1%)	..
Unknown	111 (0·5%)	54 (0·2%)	253 (0·2%)	271 (0·2%)	440 (0·3%)	383 (0·2%)	76 (0·3%)	1588 (0·2%)	..
Other	..	..	..	..	..	..	..	365 (0·1%)	..
All childhood malignancies	20 452 (100·0%)	25 186 (100·0%)	126 400 (100·0%)	145 283 (100·0%)	168 640 (100·0%)	168 855 (100·0%)	24 595 (100·0%)	679 776 (100·0%)	676 963 (100·0%)
WHO tracer cancer									
1: Acute lymphoblastic leukaemia	4664 (22·8%)	5582 (22·2%)	29 185 (23·1%)	32 446 (22·3%)	37 953 (22·5%)	37 354 (22·1%)	6007 (24·4%)	153 191 (22·5%)	153 191 (22·6%)
2: Hodgkin lymphoma	1021 (5·0%)	1209 (4·8%)	5668 (4·5%)	5954 (4·1%)	6326 (3·8%)	6341 (3·8%)	924 (3·8%)	27 443 (4·0%)	27 443 (4·1%)
3: Burkitt lymphoma	293 (1·4%)	425 (1·7%)	2521 (2·0%)	2829 (1·9%)	3103 (1·8%)	2899 (1·7%)	541 (2·2%)	12 611 (1·9%)	12 611 (1·9%)
4: Retinoblastoma	536 (2·6%)	598 (2·4%)	3195 (2·5%)	3696 (2·5%)	4096 (2·4%)	4000 (2·4%)	599 (2·4%)	16 720 (2·5%)	16 720 (2·5%)
5: Wilms tumour	919 (4·5%)	1213 (4·8%)	5764 (4·6%)	6161 (4·2%)	6863 (4·1%)	6419 (3·8%)	948 (3·9%)	28 287 (4·2%)	28 287 (4·2%)
6: Low-grade glioma	1105 (5·4%)	1793 (7·1%)	10 692 (8·5%)	12 855 (8·8%)	15 249 (9·0%)	15 029 (8·9%)	2059 (8·4%)	58 782 (8·6%)	58 782 (8·7%)
All WHO tracer cancers	8538 (41·7%)	10 820 (43·0%)	57 025 (45·1%)	63 941 (44·0%)	73 590 (43·6%)	72 042 (42·7%)	11 078 (45·0%)	297 034 (43·7%)	297 034 (43·9%)
All other cancers	11 771 (57·6%)	14 273 (56·7%)	68 967 (54·6%)	80 882 (55·7%)	94 401 (56·0%)	96 226 (57·0%)	13 409 (54·5%)	379 929 (55·9%)	379 929 (56·1%)
Unclear	32 (0·2%)	39 (0·2%)	155 (0·1%)	189 (0·1%)	209 (0·1%)	204 (0·1%)	32 (0·1%)	860 (0·1%)	..
Unknown	111 (0·5%)	54 (0·2%)	253 (0·2%)	271 (0·2%)	440 (0·3%)	383 (0·2%)	76 (0·3%)	1588 (0·2%)	..
Other	..	..	...	..	..	..	..	365 (0·1%)	..
All childhood malignancies	20 452 (100·0%)	25 186 (100·0%)	126 400 (100·0%)	145 283 (100·0%)	168 640 (100·0%)	168 855 (100·0%)	24 595 (100·0%)	679 776 (100·0%)	676 963 (100·0%)

Data are n (%). ICCC-3=International Classification of Childhood Cancer (3rd edition).[21] Unclear=site–morphology combination does not match any ICCC-3 group or WHO tracer cancer.[2] Unknown=no morphology code. Other=year of diagnosis later than 2022 or unknown.

Table 1: **Number of records received for children diagnosed with cancer during 1990–2022 (CONCORD-4) for 12 major ICCC-3 groups and six WHO tracer cancers, by calendar period of diagnosis**

	Boys				Girls			
	<1 year	1–4 years	5–9 years	10–14 years	<1 year	1–4 years	5–9 years	10–14 years
ICCC-3 group								
I: Leukaemias	0·010255	0·083534	0·060463	0·049568	0·008039	0·066805	0·047372	0·035999
II: Lymphomas	0·002604	0·019281	0·030680	0·030350	0·002291	0·009559	0·012599	0·017613
III: CNS	0·005559	0·028776	0·032381	0·027685	0·004635	0·024453	0·027790	0·023620
IV: Neuroblastoma	0·007529	0·012922	0·003282	0·000396	0·006908	0·011060	0·003084	0·000563
V: Retinoblastoma	0·004588	0·013330	0·000539	0·000001	0·004627	0·012116	0·000426	0·000013
VI: Renal tumours	0·003219	0·013092	0·004446	0·001173	0·002648	0·015070	0·005456	0·001577
VII: Hepatic tumours	0·003092	0·005492	0·000822	0·001323	0·002076	0·003168	0·000770	0·000630
VIII: Bone tumours	0·000169	0·001200	0·006436	0·015110	0·000131	0·001017	0·005989	0·013460
IX: Soft tissue sarcomas	0·003044	0·009055	0·008509	0·009033	0·002361	0·006973	0·006411	0·009275
X: Germ-cell tumours	0·002963	0·007154	0·001836	0·005765	0·002493	0·002748	0·004239	0·009074
XI: Other epithelial neoplasms	0·000255	0·000881	0·003589	0·009951	0·000391	0·001059	0·003802	0·014567
XII: Other and unspecified neoplasms	0·001722	0·004228	0·002906	0·003716	0·001448	0·003821	0·002165	0·003704
WHO tracer cancer								
1: Acute lymphoblastic leukaemia	0·009380	0·142430	0·101124	0·072144	0·007941	0·113308	0·078514	0·050842
2: Hodgkin lymphoma	0·000024	0·008548	0·024779	0·028036	0·000024	0·001667	0·007803	0·019528
3: Burkitt lymphoma	0·000016	0·009155	0·012782	0·009222	0·000053	0·002979	0·004525	0·003799
4: Retinoblastoma	0·009919	0·028817	0·001165	0·000002	0·010002	0·026192	0·000920	0·000029
5: Wilms tumour	0·006236	0·025887	0·008646	0·001600	0·004950	0·030042	0·011039	0·002284
6: Low-grade glioma	0·002807	0·020406	0·021785	0·019778	0·002012	0·020577	0·020399	0·015883

The sum of the weights is unity (1·000000), both for the 12 ICCC-3 groups and for the six WHO tracer cancers. ICCC-3=International Classification of Childhood Cancer (3rd edition).

Table 2: **Weights by age (years), sex, and type of cancer, used to create the Cancer Survival Index for all childhood cancers combined (12 ICCC-3 groups), and for the six WHO tracer cancers combined**

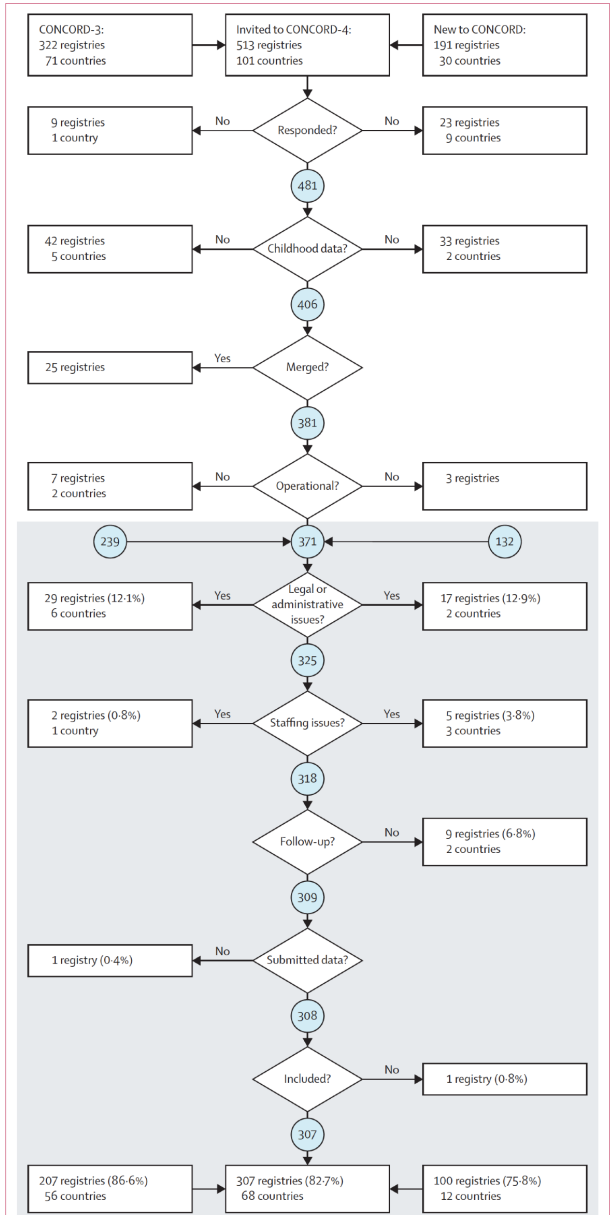

Figure 1: **Recruitment of cancer registries**
The numbers of countries excluded refer to countries for which the only cancer registry or all registries had to be excluded. The percentages refer to the number of operational registries (shaded area).

	1990–94	1995–99	2000–04	2005–09	2010–14	2015–19
Africa						
Algeria*†	52·4% (48·0–57·1)	39·6% (38·2–41·0)	35·7% (31·1–41·1)	62·3% (57·6–67·5)	43·5% (39·4–48·1)	47·7% (43·3–52·6)
La Réunion‡	..	..	..	..	55·1% (51·7–58·9)	..
Nigeria†§	..	..	40·1% (35·7–45·1)	64·5% (57·5–72·3)	70·8% (67·1–74·8)	58·8% (52·7–65·5)
South Africa*†	..	..	73·9% (71·7–76·2)	74·5% (73·6–75·4)	66·6% (59·8–74·3)	77·7% (75·3–80·2)
Central and South America						
Argentina*‡	..	..	60·5% (59·4–61·7)	66·2% (65·0–67·3)	71·1% (70·0–72·1)	72·0% (71·0–73·0)
Brazil*	..	55·8% (50·1–62·2)	62·8% (60·1–65·6)	66·0% (63·5–68·6)	67·2% (64·9–69·5)	67·7% (65·2–70·2)
Chile‡	..	..	61·5% (55·9–67·7)	71·7% (69·6–73·8)	71·3% (69·7–73·0)	77·1% (75·6–78·7)
Colombia*	..	..	57·7% (54·0–61·6)	60·5% (57·4–63·7)	67·0% (63·8–70·4)	72·7% (69·9–75·7)
Costa Rica*‡	..	..	91·4% (89·1–93·8)	83·5% (81·2–85·9)	79·3% (76·7–82·1)	78·1% (74·8–81·5)
Cuba*‡	..	..	58·3% (55·8–60·9)	65·5% (63·0–68·0)	67·9% (65·4–70·5)	65·4% (62·7–68·2)
Ecuador*	57·9% (52·9–63·3)	53·6% (49·4–58·1)	53·9% (50·5–57·5)	59·8% (57·3–62·5)	58·0% (55·6–60·4)	64·0% (61·7–66·3)
El Salvador‡§	..	..	..	..	48·0% (43·7–52·6)	55·3% (52·3–58·5)
French Guiana‡	..	..	..	..	66·0% (62·2–69·9)	61·4% (58·3–64·8)
Guadeloupe†‡	..	..	..	..	66·4% (59·0–74·8)	60·2% (59·7–60·8)
Guatemala‡§	..	..	..	..	61·3% (58·1–64·6)	59·3% (56·9–61·8)
Martinique†‡	..	..	..	..	49·5% (44·5–55·0)	57·3% (55·7–58·9)
Mexico*	..	..	..	..	58·8% (51·7–66·8)	68·2% (64·2–72·4)
Peru*	..	..	..	..	56·5% (54·6–58·5)	61·0% (58·3–63·9)
Puerto Rico‡	..	..	76·4% (73·1–79·8)	78·1% (74·6–81·8)	81·0% (78·1–84·1)	88·2% (85·8–90·8)
Trinidad and Tobago‡	..	..	60·8% (55·2–66·8)	46·0% (40·1–52·9)	51·2% (45·4–57·8)	69·9% (66·5–73·4)
Uruguay‡	..	..	..	..	69·3% (64·9–74·1)	77·9% (74·4–81·6)
North America						
Canada	74·9% (72·8–77·1)	76·4% (74·4–78·5)	81·9% (80·6–83·2)	83·2% (82·0–84·5)	83·5% (82·2–84·8)	84·2% (83·0–85·4)
USA‡	..	..	81·0% (80·7–81·4)	84·2% (83·9–84·6)	86·3% (85·9–86·6)	87·1% (86·6–87·5)
Asia						
Cyprus‡	..	..	..	73·5% (68·4–78·9)	71·4% (64·3–79·1)	73·8% (70·0–77·7)
Georgia*‡	..	..	..	..	..	75·8% (72·4–79·4)
Indonesia§	..	..	..	..	53·7% (49·6–58·1)	54·1% (50·0–58·6)
Israel‡	..	..	81·2% (79·2–83·3)	80·8% (79·0–82·6)	83·2% (81·6–84·9)	87·0% (85·4–88·5)
Japan‡	66·2% (63·6–68·8)	74·2% (71·6–76·8)	74·2% (72·6–75·8)	76·7% (75·3–78·2)	83·3% (82·2–84·3)	85·9% (85·1–86·6)
Kuwait‡	..	..	65·2% (61·1–69·6)	57·9% (54·3–61·8)	68·6% (64·3–73·2)	75·5% (71·8–79·4)
Mongolia‡§	..	..	..	..	32·3% (29·3–35·6)	58·7% (54·0–63·7)
Qatar‡	..	..	57·3% (49·7–66·2)	61·1% (50·0–74·7)	57·0% (50·9–63·7)	75·8% (70·1–82·0)
Saudi Arabia‡	..	..	..	..	75·8% (74·1–77·6)	80·5% (78·9–82·2)
Singapore‡	..	..	72·5% (69·1–76·0)	74·8% (71·6–78·2)	83·1% (80·3–85·9)	83·2% (80·5–86·0)
South Korea‡	..	..	67·6% (66·1–69·1)	71·8% (70·4–73·1)	72·9% (71·6–74·2)	75·2% (74·0–76·5)
Taiwan‡	..	..	69·8% (68·2–71·5)	72·6% (70·9–74·3)	73·1% (71·4–74·9)	77·4% (75·7–79·2)
Thailand*	..	..	..	55·7% (52·2–59·4)	64·5% (61·1–68·1)	66·0% (62·8–69·4)
Türkiye*	..	49·7% (44·2–55·9)	65·6% (63·0–68·4)	72·1% (70·3–73·9)	75·9% (74·6–77·3)	80·2% (78·9–81·5)

(Table 3 continues on next page)

	1990–94	1995–99	2000–04	2005–09	2010–14	2015–19
(Continued from previous page)						
Europe						
Austria‡	77·0% (74·6–79·5)	81·3% (79·0–83·6)	81·1% (78·8–83·5)	84·3% (82·2–86·3)	85·0% (82·9–87·1)	85·1% (83·1–87·1)
Belarus*‡	..	..	73·2% (70·9–75·6)	75·9% (73·6–78·4)	82·3% (80·3–84·2)	84·2% (82·5–86·0)
Belgium‡	..	..	80·6% (77·3–84·0)	84·4% (82·8–86·1)	85·4% (83·8–87·0)	84·9% (83·4–86·5)
Bulgaria*‡	48·1% (44·1–52·4)	53·7% (50·4–57·2)	53·6% (50·4–57·0)	66·9% (63·9–70·0)	72·1% (69·3–75·1)	73·7% (70·6–77·0)
Croatia‡	..	..	74·0% (71·2–77·0)	79·1% (75·7–82·5)	79·0% (76·2–82·0)	81·1% (78·5–83·8)
Czech Republic‡	..	..	81·9% (79·8–84·1)	83·3% (81·5–85·3)	87·2% (85·2–89·3)	86·9% (85·3–88·6)
Denmark‡	..	..	77·6% (74·9–80·4)	81·6% (78·8–84·4)	82·1% (79·3–85·0)	83·1% (80·8–85·4)
Estonia‡	..	..	66·5% (61·6–71·8)	70·9% (66·7–75·3)	74·3% (69·8–79·0)	85·7% (82·8–88·7)
France‡	..	..	81·4% (80·6–82·3)	84·1% (83·4–84·9)	85·5% (84·8–86·2)	86·3% (85·4–87·1)
Germany	65·3% (61·2–69·6)	63·2% (58·6–68·3)	71·2% (66·9–75·7)	83·9% (82·2–85·6)	86·8% (85·6–88·0)	85·2% (84·0–86·5)
Hungary‡	..	..	70·2% (67·9–72·6)	78·1% (75·9–80·5)	77·9% (75·8–80·1)	80·7% (78·6–82·9)
Ireland‡	73·6% (68·1–79·6)	78·7% (75·6–82·0)	80·4% (77·9–83·0)	81·1% (78·5–83·8)	84·9% (82·9–87·0)	87·7% (85·7–89·7)
Italy	71·5% (68·7–74·3)	79·1% (77·1–81·3)	81·6% (80·0–83·1)	84·2% (83·1–85·3)	86·4% (85·5–87·3)	86·9% (86·0–87·8)
Latvia‡	..	..	69·7% (65·1–74·6)	72·2% (66·8–78·1)	74·0% (67·0–81·7)	80·8% (77·1–84·8)
Lithuania‡	46·9% (43·3–50·8)	52·8% (48·8–57·0)	60·1% (56·5–64·0)	69·0% (64·7–73·4)	81·2% (77·5–85·0)	85·6% (82·8–88·4)
Malta‡	..	..	66·7% (60·6–73·6)	71·8% (67·4–76·5)	66·7% (64·0–69·6)	82·7% (79·7–85·8)
Netherlands‡	..	..	79·0% (77·5–80·5)	81·5% (80·0–83·0)	85·7% (84·4–87·0)	..
Norway‡	78·2% (75·4–81·2)	77·2% (74·4–80·1)	84·5% (82·2–86·8)	81·7% (79·2–84·1)	84·7% (82·0–87·6)	89·0% (87·1–90·9)
Poland‡	..	..	74·3% (72·9–75·7)	78·6% (77·3–79·8)	82·5% (81·3–83·8)	84·0% (82·8–85·2)
Portugal‡	..	69·7% (65·4–74·4)	76·8% (74·8–78·9)	81·0% (79·1–82·9)	83·2% (81·3–85·2)	85·5% (83·7–87·4)
Romania*‡	..	..	..	..	68·7% (66·4–71·1)	73·2% (71·1–75·3)
Russia*	..	70·2% (65·1–75·8)	63·8% (59·9–68·0)	70·0% (66·7–73·5)	76·4% (73·5–79·3)	81·5% (78·9–84·3)
Slovenia‡	62·8% (58·4–67·6)	71·2% (66·8–75·8)	78·2 (74·2–82·5)	79·0% (74·9–83·5)	81·6% (77·9–85·6)	87·8% (84·7–91·0)
Spain	62·9% (50·0–79·1)	71·6% (65·3–78·6)	76·4% (74·9–77·9)	78·6% (77·3–79·9)	82·4% (81·2–83·6)	85·4% (84·3–86·5)
Switzerland‡	74·2% (71·7–76·7)	77·7% (75·2–80·2)	80·6% (78·3–82·9)	83·0% (80·9–85·1)	85·8% (83·9–87·7)	88·5% (86·8–90·2)
UK‡	72·1% (70·9–73·2)	74·8% (73·8–75·8)	79·1% (78·1–80·0)	83·3% (82·5–84·1)	84·6% (83·8–85·3)	85·8% (85·1–86·5)
Oceania						
Australia‡	..	75·7% (73·9–77·5)	80·9% (79·5–82·2)	82·7% (81·4–83·9)	85·8% (84·6–87·1)	86·1% (85·1–87·2)
New Zealand‡	..	..	76·7% (73·9–79·7)	78·6% (75·8–81·6)	79·9% (77·4–82·4)	82·8% (80·4–85·4)

Data are CSI (95% CI). CSI=Cancer Survival Index. *Upper-middle-income country. †Less reliable estimates (see text). ‡Data with 100% coverage of the national population; for Chile from 2007 and for Japan from 2016. §Lower-middle-income country (World Bank national income group; 2015).

Table 3: **5-year Cancer Survival Index for all childhood cancers combined, by continent, country, and calendar period of diagnosis**

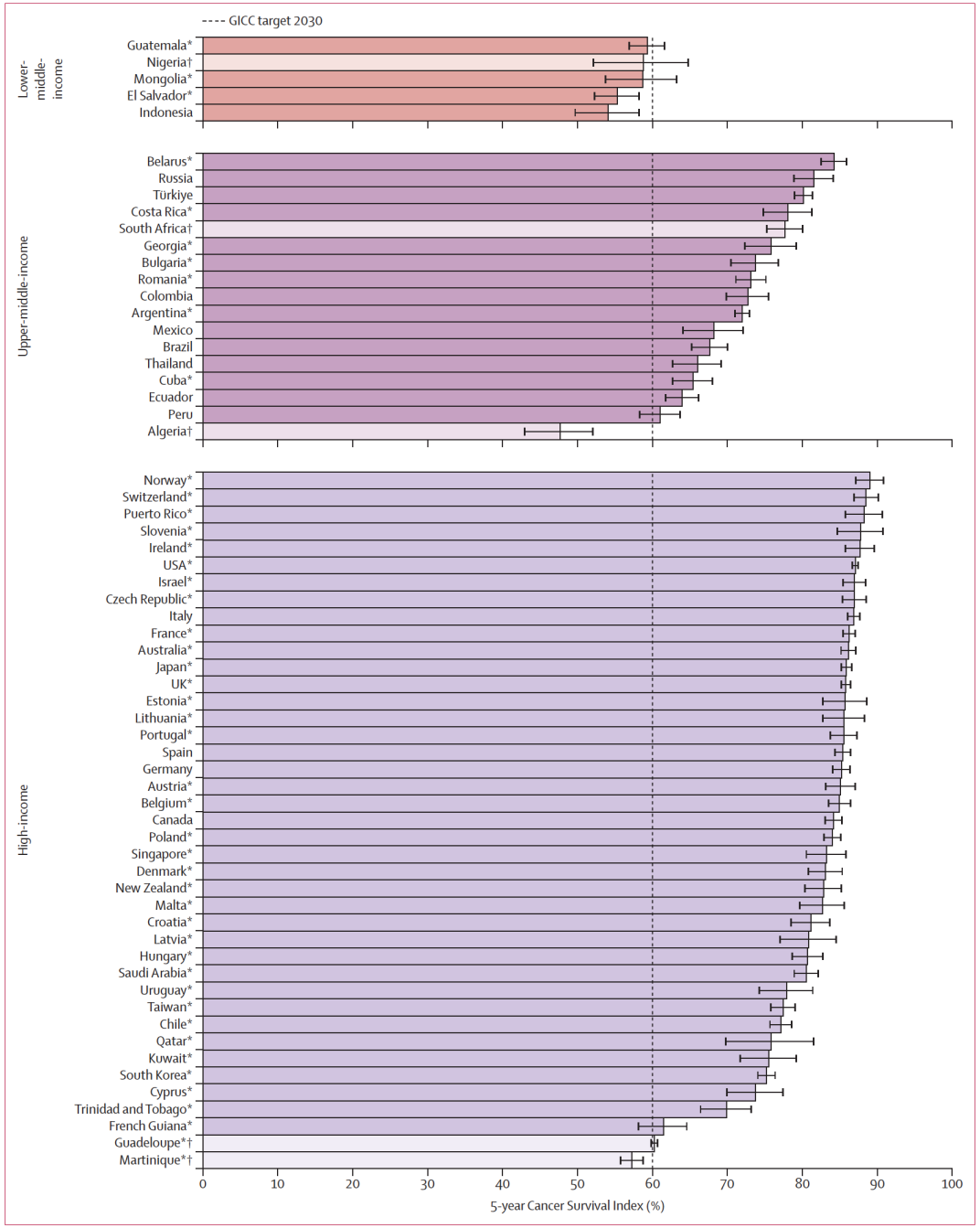

Figure 2: **5-year Cancer Survival Index for all childhood cancers combined, 2015–19, by country, and World Bank national income group in 2015**
La Réunion and the Netherlands did not submit data for children diagnosed during 2015–19 (see table 3). GICC=Global Initiative for Childhood Cancer. Error bars represent 95% CIs. *Data with 100% coverage of national population; Japan from 2016. †Less reliable estimates (see text) are shown in paler colours.

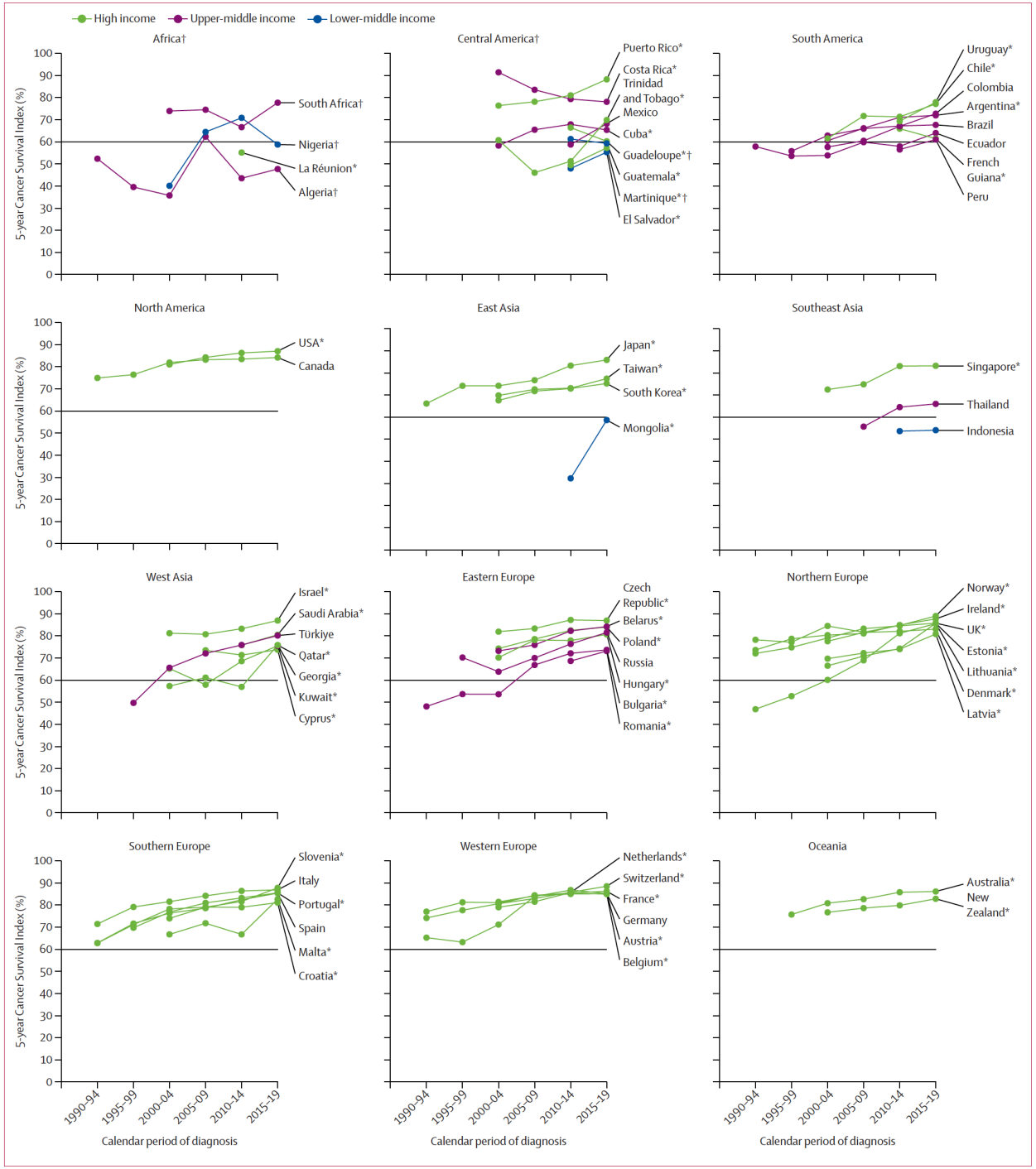

	1990–94	1995–99	2000–04	2005–09	2010–14	2015–19
(Continued from previous page)						
Europe						
Austria‡	85·3% (81·2–89·5)	88·0% (84·4–91·8)	87·7% (84·8–90·7)	91·7% (89·0–94·4)	91·5% (88·4–94·6)	93·4% (91·1–95·7)
Belarus‡*	..	..	82·7% (79·5–86·0)	87·6% (84·8–90·6)	91·3% (89·0–93·7)	93·8% (91·9–95·8)
Belgium‡	..	..	86·8% (82·4–91·5)	92·6% (90·6–94·6)	91·8% (89·8–93·8)	93·4% (91·7–95·2)
Bulgaria‡*	57·4% (51·5–64·0)	65·9% (58·2–74·7)	65·2% (60·0–70·9)	77·5% (73·2–81·9)	81·0% (77·2–84·9)	84·5% (80·6–88·7)
Croatia‡	..	..	81·7% (77·5–86·1)	88·9% (85·2–92·7)	89·2% (85·7–93·0)	91·8% (88·7–95·1)
Czech Republic‡	..	..	90·8% (88·2–93·5)	91·0% (88·8–93·2)	92·1% (89·8–94·6)	91·0% (88·7–93·4)
Denmark‡	..	..	88·1% (84·0–92·4)	91·5% (88·9–94·0)	89·6% (87·2–92·1)	89·5% (86·3–92·9)
Estonia‡	..	..	63·5% (55·9–72·1)	84·6% (78·5–91·2)	89·6% (83·3–96·3)	94·7% (91·2–98·3)
France‡	..	..	89·7% (88·8–90·7)	91·7% (90·9–92·5)	91·1% (90·2–91·9)	91·9% (90·8–92·9)
Germany	82·6% (79·2–86·2)	69·3% (62·1–77·3)	72·2% (65·4–79·6)	91·1% (88·9–93·4)	92·8% (91·2–94·5)	91·8% (90·1–93·5)
Hungary‡	..	..	83·7% (80·6–87·0)	86·7% (83·8–89·7)	85·6% (82·9–88·4)	86·7% (84·0–89·6)
Ireland‡	70·6% (63·1–78·9)	84·9% (81·3–88·8)	85·9% (82·6–89·2)	88·3% (85·0–91·6)	93·4% (90·8–96·0)	93·9% (91·7–96·1)
Italy	67·2% (63·4–71·1)	86·3% (83·8–88·9)	86·9% (85·0–88·9)	90·3% (89·0–91·7)	90·1% (89·0–91·4)	91·2% (90·0–92·3)
Latvia‡¶	..	..	74·6% (69·2–80·4)	66·6% (59·3–74·8)	83·5% (76·5–91·1)	38·9%
Lithuania‡	52·8% (47·8–58·2)	56·4% (50·3–63·3)	77·6% (72·2–83·4)	76·9% (71·1–83·2)	84·0% (79·7–88·5)	93·9% (90·1–97·8)
Malta‡¶	..	..	77·8% (69·9–86·7)	81·1% (75·8–86·9)	80·4% (67·3–96·1)	92·6%
Netherlands‡	..	..	87·9% (86·2–89·7)	90·0% (88·3–91·8)	92·2% (90·8–93·7)	..
Norway‡	88·1% (85·0–91·3)	85·3% (81·7–89·1)	89·7% (86·6–92·9)	88·8% (85·4–92·3)	90·4% (87·5–93·3)	94·3% (92·1–96·5)
Poland‡	..	..	83·1% (81·1–85·1)	85·5% (83·7–87·3)	89·1% (87·3–90·9)	87·4% (85·6–89·3)
Portugal‡	..	79·1% (72·1–86·8)	82·9% (80·1–85·8)	88·7% (86·0–91·4)	89·5% (87·1–91·9)	90·9% (88·5–93·5)
Romania‡*	..	..	..	..	77·7% (74·6–80·9)	82·9% (80·3–85·6)
Russia*	..	18·1% (18·1–18·1)	32·9% (28·5–37·8)	76·0% (69·5–83·1)	83·0% (78·0–88·2)	88·0% (84·5–91·8)
Slovenia‡	70·2% (64·2–76·8)	81·7% (76·2–87·6)	83·5% (78·0–89·4)	85·6% (81·4–90·0)	85·5% (80·3–91·2)	96·2% (92·9–99·6)
Spain	67·1% (47·7–94·5)	84·7% (80·6–89·0)	85·4% (83·5–87·4)	86·2% (84·4–88·0)	88·2% (86·6–89·7)	90·9% (89·5–92·3)
Switzerland‡	81·3% (78·1–84·8)	88·5% (85·3–91·9)	89·0% (86·2–91·9)	89·8% (87·1–92·7)	91·1% (89·1–93·1)	94·1% (92·3–96·0)
UK‡	79·8% (78·2–81·4)	83·1% (81·8–84·4)	87·5% (86·5–88·6)	91·0% (90·1–91·9)	92·0% (91·2–92·8)	92·3% (91·5–93·1)
Oceania						
Australia‡	..	83·2% (80·9–85·6)	87·9% (86·2–89·5)	89·8% (88·3–91·2)	92·0% (90·7–93·4)	93·9% (92·8–95·0)
New Zealand‡	..	..	86·2% (83·1–89·5)	86·4% (82·8–90·1)	87·1% (84·5–89·8)	88·6% (86·2–91·0)

Data are CSI (95% CI). CSI=Cancer Survival Index. *Upper-middle-income country. †Less reliable estimates (see text). ‡Data with 100% coverage of the national population; for Chile from 2007 and for Japan from 2016. §Lower-middle-income country (World Bank national income group; 2015). ¶Less reliable estimate, based on small numbers of children; a confidence interval for the CSI cannot be produced for 2015–19. Latvia: no data on acute lymphoblastic leukaemia for 2015–19.

Table 4: **5-year Cancer Survival Index for the six WHO tracer cancers combined, by continent, country and calendar period of diagnosis**

Implications of all the available evidence

The CSI will facilitate monitoring of real-world progress towards the GICC target for childhood cancer survival. The CSI that includes all childhood cancers is a better indicator than the CSI based on the six WHO tracer cancers, especially for lower-middle-income countries, where diagnostic facilities are often inadequate, and the need to improve survival is even more urgent. WHO should devote even greater efforts to increase the coverage of population-based cancer registries worldwide and to facilitate data sharing for international research. In most high-income and upper-middle-income countries, impressive trends in survival for all childhood cancers combined since 1990 have already exceeded the GICC target for 2030, suggesting that a more ambitious target could be set. In low-income countries and lower-middle-income countries, where 60% of the world's children live, late presentation, abandonment of treatment, and suboptimal health-care systems are major contributors to poor survival.

THE LANCET

PROJECTED FOR 2020

DIAGNOSIS RATES OF CHILDREN WITH CANCER (AGE 0-14)

BASED ON INCOME LEVEL OF HOME COUNTRY

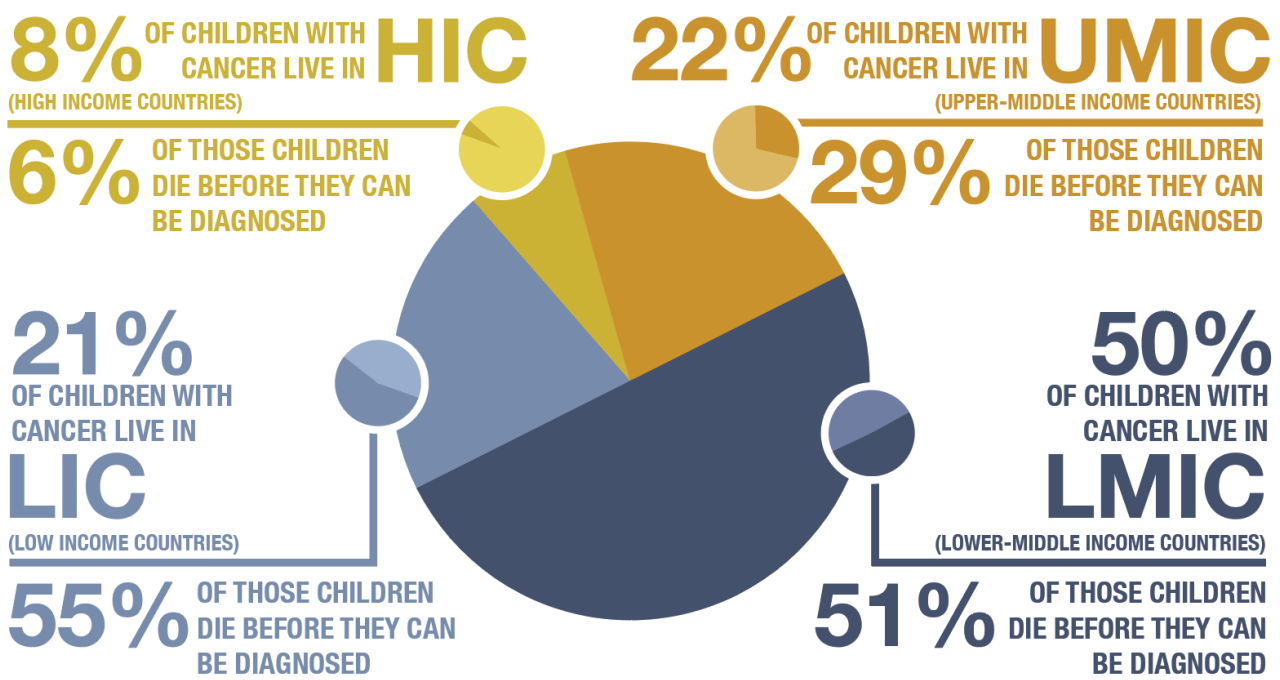

GLOBALLY

44% OF CHILDREN WITH CANCER DIE BEFORE THEY CAN BE DIAGNOSED

Global burden of cancer in children and adolescents aged 0–19 years, 1990–2023: a systematic analysis for the Global Burden of Disease Study 2023

Summary

Background Information on childhood cancer burden is crucial for effective cancer policy planning. Unfortunately, observed paediatric cancer data are not available in every country, and previous global burden estimates have not discretely reported several common cancers of childhood. We aimed to inform efforts to address childhood cancer burden globally by analysing results from the Global Burden of Diseases, Injuries, and Risk Factors Study (GBD) 2023, which now include nine additional cancer causes compared with previous GBD analyses.

Methods GBD 2023 data sources for cancer estimation included population-based cancer registries, vital registration systems, and verbal autopsies. For childhood cancers (defined as those occurring at ages 0–19 years), mortality was estimated using cancer-specific ensemble models and incidence was estimated using mortality estimates and modelled mortality-to-incidence ratios (MIRs). Years of life lost (YLLs) were estimated by multiplying age-specific cancer deaths by the standard life expectancy at the age of death. Prevalence was estimated using survival estimates modelled from MIRs and multiplied by sequelae-specific disability weights to estimate years lived with disability (YLDs). Disability-adjusted life-years (DALYs) were estimated as the sum of YLLs and YLDs. Estimates are presented globally and by geographical and resource groupings, and all estimates are presented with 95% uncertainty intervals (UIs).

Findings Globally, in 2023, there were an estimated 377 000 incident childhood cancer cases (95% UI 288 000–489 000), 144 000 deaths (131 000–162 000), and 11·7 million (10·7–13·2) DALYs due to childhood cancer. Deaths due to childhood cancer decreased by 27·0% (15·5–36·1) globally, from 197 000 (173 000–218 000) in 1990, but increased in the WHO African region by 55·6% (25·5–92·4), from 31 500 (24 900–38 500) to 49 000 (42 600–58 200) between 1990 and 2023. In 2023, age-standardised YLLs due to childhood cancer were inversely correlated with country-level Socio-demographic Index. Childhood cancer was the eighth-leading cause of childhood deaths and the ninth-leading cause of DALYs among all cancers in 2023. The percentage of DALYs due to uncategorised childhood cancers was reduced from 26·5% (26·5–26·5) in GBD 2017 to 10·5% (8·1–13·1) with the addition of the nine new cancer causes. Target cancers for the WHO Global Initiative for Childhood Cancer (GICC) comprised 47·3% (42·2–52·0) of global childhood cancer deaths in 2023.

Interpretation Global childhood cancer burden remains a substantial contributor to global childhood disease and cancer burden and is disproportionately weighted towards resource-limited settings. The estimation of additional cancer types relevant in childhood provides a step towards alignment with WHO GICC targets. Efforts to decrease global childhood cancer burden should focus on addressing the inequities in burden worldwide and support comprehensive improvements along the childhood cancer diagnosis and care continuum.

	Incident cases, thousands	Age-standardised incidence rate per 100 000 person-years	Percentage of global cases	Deaths, thousands	Age-standardised mortality rate per 100 000 person-years	Percentage of global deaths	DALYs, millions	Age-standardised DALY rate per 100 000 person-years	Percentage of global DALYs
Global	377 (288–489)	14·3 (10·9–18·6)	100·0% (100·0–100·0)	144 (131–162)	5·4 (4·9–6·1)	100·0% (100·0–100·0)	11·7 (10·7–13·2)	443·6 (404·0–498·0)	100·0% (100·0–100·0)
WHO regions									
African region	91·3 (74·6–112)	14·3 (11·7–17·6)	24·4% (21·2–27·8)	49·0 (42·6–58·2)	7·7 (6·7–9·1)	34·1% (31·8–36·6)	4·01 (3·50–4·77)	628·6 (546·9–747·0)	34·2% (31·8–36·9)
Eastern Mediterranean region	52·4 (40·1–68·0)	16·1 (12·3–20·9)	13·9% (12·7–14·8)	21·9 (18·5–25·0)	6·7 (5·7–7·7)	15·2% (13·9–16·3)	1·79 (1·51–2·04)	548·1 (463·0–626·1)	15·2% (13·9–16·3)
European region	40·0 (27·6–55·6)	18·6 (12·7–25·9)	10·6% (9·0–11·9)	8·02 (7·64–8·38)	3·7 (3·5–3·8)	5·6% (5·0–6·1)	0·660 (0·627–0·690)	303·6 (288·3–318·2)	5·6% (5·0–6·2)
Region of the Americas	49·5 (37·5–67·5)	17·1 (12·9–23·4)	13·1% (11·8–14·4)	14·3 (13·6–14·8)	4·9 (4·6–5·1)	10·0% (8·9–10·9)	1·16 (1·11–1·20)	397·9 (379·4–413·2)	9·9% (8·8–10·8)
South-East Asia region	49·2 (38·6–63·1)	7·9 (6·2–10·2)	13·1% (11·3–14·6)	23·3 (19·8–27·6)	3·7 (3·2–4·4)	16·2% (14·4–17·9)	1·88 (1·59–2·22)	303·7 (257·3–356·0)	16·0% (14·2–17·7)
Western Pacific region	93·0 (65·1–135)	17·3 (12·1–25·0)	24·5% (21·7–27·8)	26·9 (24·2–31·1)	4·8 (4·3–5·5)	18·7% (17·1–20·3)	2·19 (1·99–2·53)	396·7 (358·7–453·9)	18·7% (17·1–20·3)
SDI quintiles									
High	102 (69·0–149)	18·6 (12·5–27·4)	26·8% (23·4–30·6)	19·5 (18·3–20·9)	3·4 (3·2–3·7)	13·6% (12·3–14·7)	1·60 (1·50–1·71)	284·0 (266·1–305·8)	13·6% (12·3–14·9)
High-middle	73·6 (54·1–102)	16·4 (12·0–22·7)	19·5% (18·2–21·1)	23·7 (21·9–26·0)	5·1 (4·8–5·6)	16·5% (15·5–17·3)	1·92 (1·78–2·10)	421·4 (391·4–460·8)	16·4% (15·4–17·3)
Middle	46·3 (35·2–61·4)	14·0 (10·6–18·6)	12·3% (11·7–12·8)	18·5 (16·9–20·8)	5·6 (5·1–6·2)	12·9% (12·3–13·5)	1·51 (1·37–1·69)	453·8 (412·8–508·4)	12·9% (12·2–13·5)
Low-middle	47·2 (38·2–57·5)	10·4 (8·4–12·7)	12·6% (11·1–13·7)	23·1 (20·1–26·7)	5·1 (4·4–5·9)	16·1% (15·1–17·0)	1·87 (1·62–2·15)	414·3 (358·8–478·7)	16·0% (15·0–16·9)
Low	108 (90·3–133)	12·7 (10·6–15·6)	28·8% (24·9–32·3)	58·8 (51·7–68·7)	6·9 (6·1–8·1)	40·9% (39·0–43·3)	4·81 (4·22–5·61)	566·1 (496·8–660·9)	41·0% (39·0–43·4)

Values in parentheses are 95% uncertainty intervals. Estimates are presented to three significant figures for counts, or to one decimal place for rates and percentages. DALYs=disability-adjusted life-years. SDI=Socio-demographic Index.

Table: **Global burden of childhood cancer in 2023, globally and by WHO region and SDI quintile, for all sexes combined**

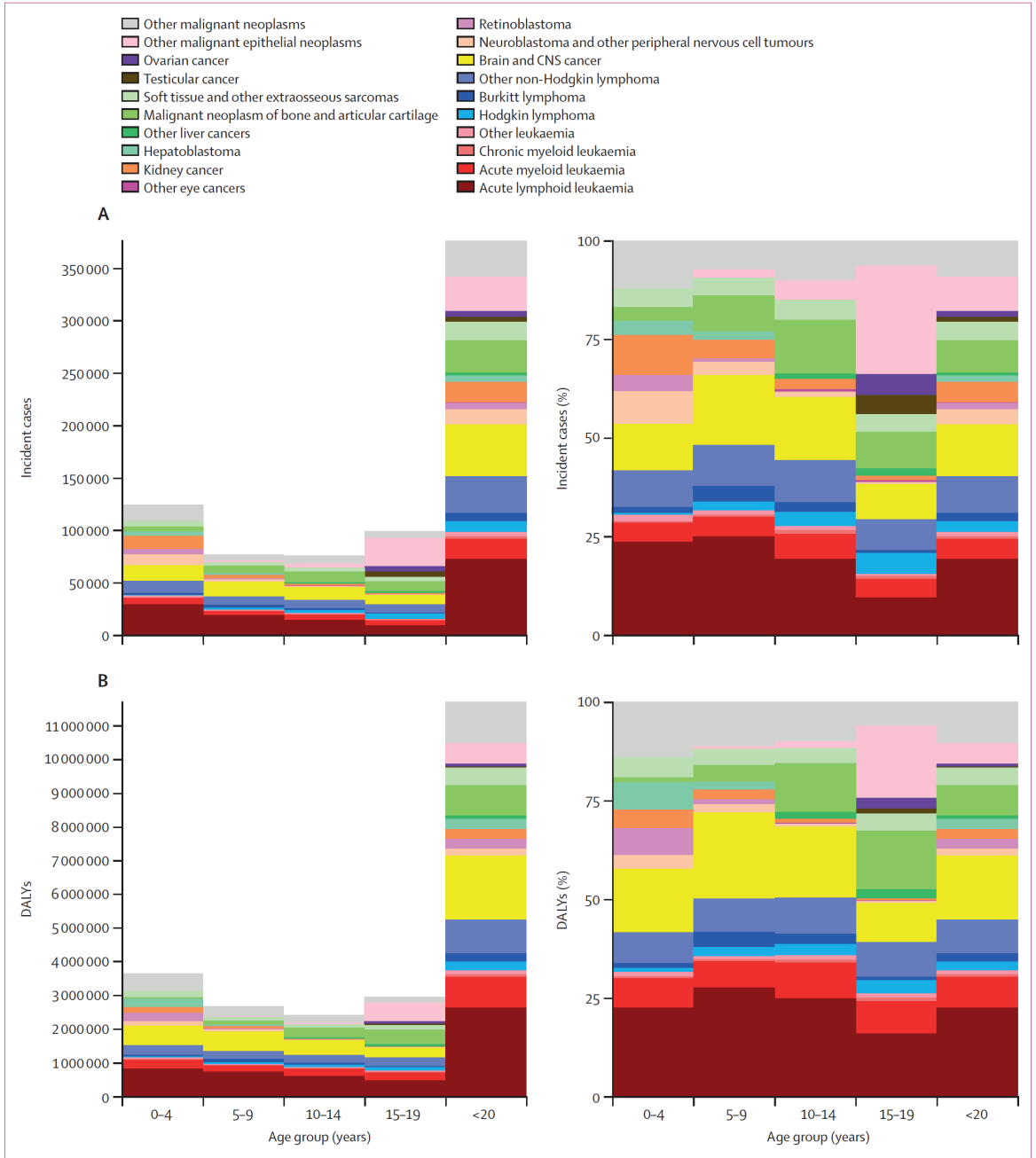

Figure 1: **Global childhood cancer incidence and DALY burden in 2023, by 5-year age group and overall for age 0–19 years, for all sexes combined**
(A) Number of incident cases (left) and proportion of incident cases among all cases of childhood cancer (right), by cancer type. (B) Number of DALYs (left) and proportion of DALYs among all childhood cancer DALYs (right), by cancer type. The <20 years age group represents the total of the age-specific categories. DALYs=disability-adjusted life-years.

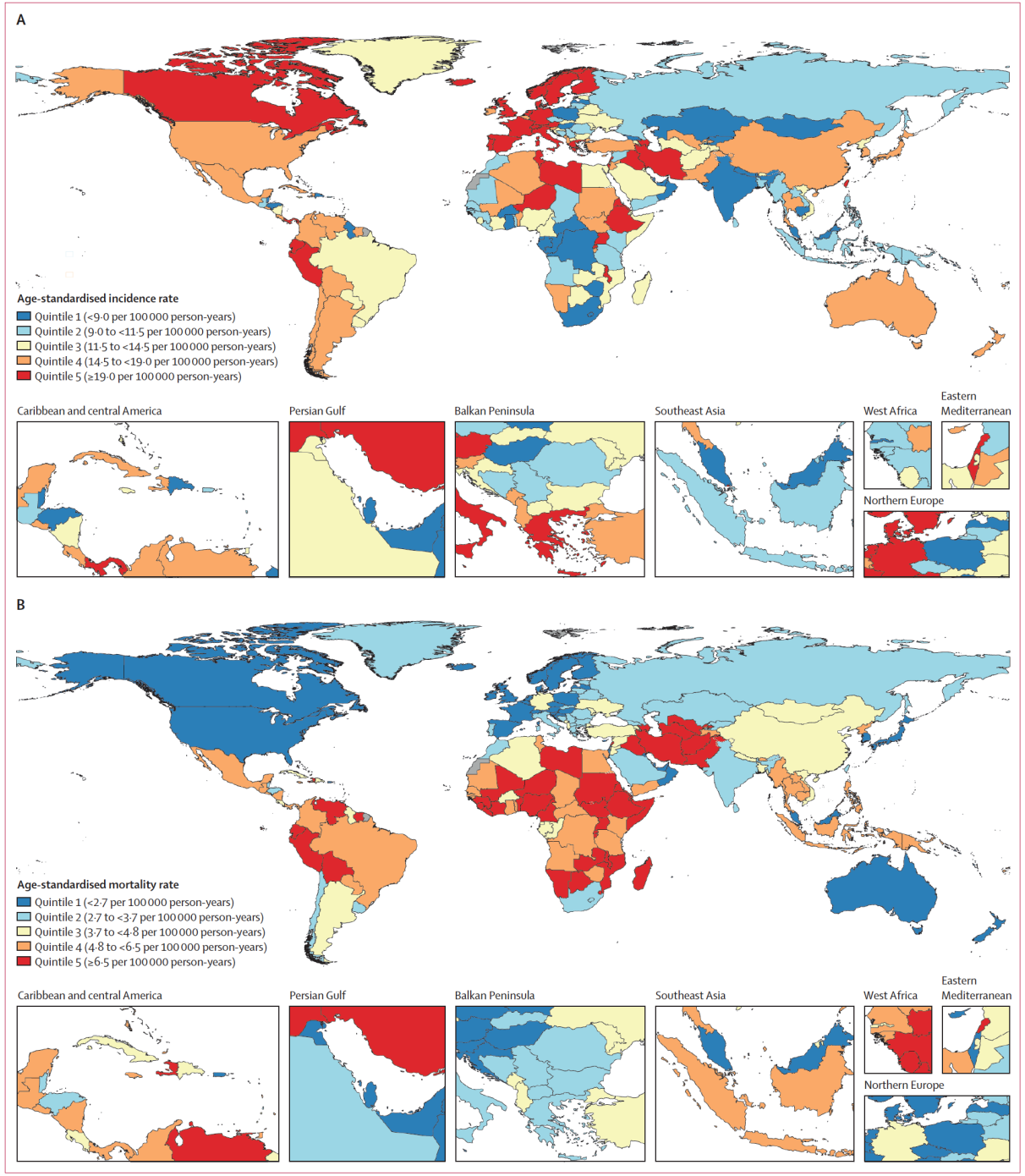

Figure 2: Global map of age-standardised childhood cancer incidence rates (A) and mortality rates (B) in 2023, for all sexes combined

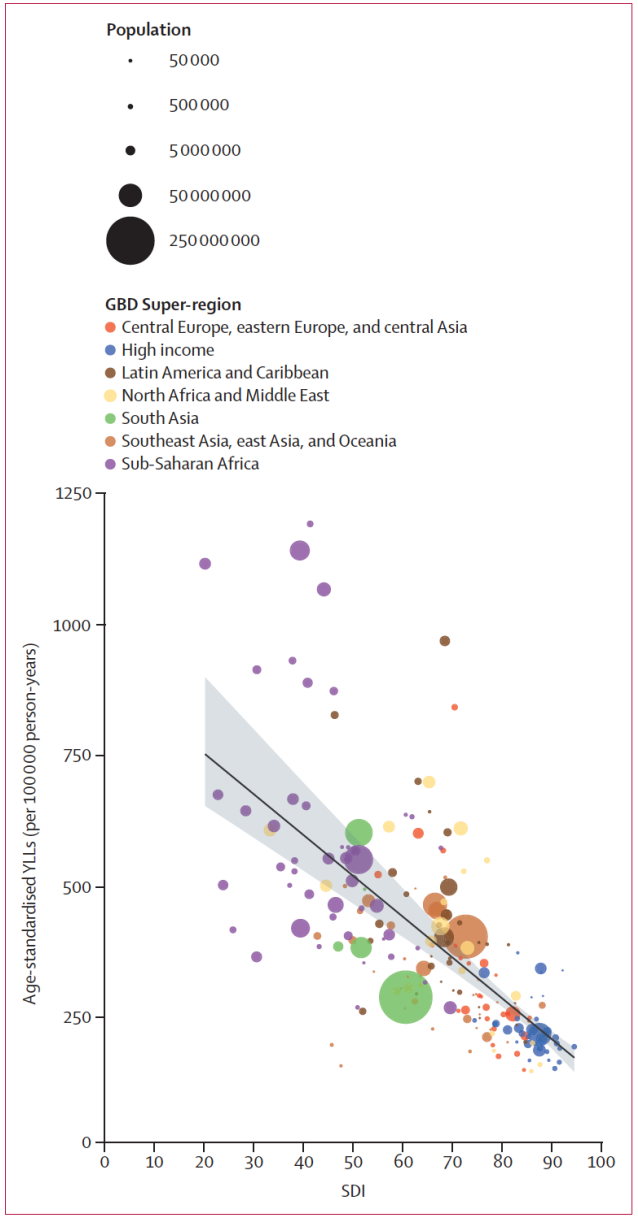

***Figure 3:* The association between SDI and age-standardised rates of childhood cancer YLLs in 2023, for all sexes combined**

Results are presented at the country level. Each circle represents one country, with size relative to the contry's total population aged 0–19 years. The grey line and shading represent the mean and 95% UI, respectively, for a linear regression between SDI and the age-standardised YLL rate (Pearson correlation coefficient −0·675 [95% UI −0·723 to −0·618]). SDI=Socio-demographic Index. UI=uncertainty interval. YLLs=years of life lost.

A

	Deaths (95% UIs)	Rank					
		Global	High SDI	High-middle SDI	Middle SDI	Low-middle SDI	Low SDI
Neonatal disorders	1630000 (1510000–1750000)	1	1	1	1	1	1
Lower respiratory infections	712000 (588000–855000)	2	6	3	3	2	2
Congenital birth defects	510000 (396000–647000)	3	2	2	2	3	5
Malaria	473000 (180000–876000)	4	92	17	5	5	3
Diarrhoeal diseases	380000 (279000–525000)	5	19	6	6	4	4
Road injuries	220000 (170000–282000)	6	4	4	4	6	7
Meningitis	148000 (112000–208000)	7	21	18	10	8	8
Childhood cancer	**144000 (131000–162000)**	**8**	**3**	**5**	**7**	**7**	**13**
Measles	142000 (57700–252000)	9	52	36	26	20	6
Drowning	127000 (95300–166000)	10	9	7	8	9	11
Pertussis	113000 (65000–185000)	11	32	14	12	12	10
Protein-energy malnutrition	105000 (75500–142000)	12	45	13	24	16	9
Tuberculosis	87800 (59400–124000)	13	47	22	16	14	12
Sexually transmitted infections excluding HIV	74100 (27100–143000)	14	35	16	15	17	15
HIV/AIDS	72000 (61900–84700)	15	38	11	29	21	14
Interpersonal violence	68900 (57200–87000)	16	10	8	13	15	19
Self-harm	63400 (53500–76300)	17	7	9	20	11	26
Typhoid and paratyphoid	60500 (31900–101000)	18	48	20	23	10	17
Invasive non-typhoidal salmonella	59300 (43000–80500)	19	77	53	44	28	16
COVID-19	52900 (48300–57800)	20	15	15	9	30	23

B

	DALYs (95% UIs)	Rank					
		Global	High SDI	High-middle SDI	Middle SDI	Low-middle SDI	Low SDI
Tracheal, bronchus, and lung cancer	46600000 (42400000–50700000)	1	1	1	1	2	7
Colon and rectum cancer	26100000 (23700000–28500000)	2	2	3	3	7	6
Breast cancer	24500000 (21600000–28000000)	3	4	4	2	1	3
Stomach cancer	22500000 (19200000–25900000)	4	3	2	4	5	4
Oesophageal cancer	14000000 (12600000–15800000)	5	6	5	10	4	8
Liver cancer	13500000 (11800000–15500000)	6	7	6	5	9	5
Cervical cancer	13100000 (10000000–17100000)	7	15	7	7	3	1
Pancreatic cancer	12300000 (11400000–13100000)	8	5	8	8	17	16
Childhood cancer	**11700000 (10700000–13200000)**	**9**	**20**	**9**	**6**	**6**	**2**
Prostate cancer	8910000 (7870000–10000000)	10	8	12	12	11	10
Brain and CNS cancer	7260000 (6340000–8670000)	11	9	10	9	16	17
Non-Hodgkin lymphoma	7080000 (6160000–8080000)	12	10	13	13	13	11
Lip and oral cavity cancer	6420000 (5540000–7570000)	13	18	11	15	8	9
Ovarian cancer	6400000 (5400000–7540000)	14	12	14	11	10	12
Other malignant neoplasms	5460000 (4720000–6110000)	15	14	15	14	14	13
Bladder cancer	4620000 (4220000–5120000)	16	11	18	18	21	20
Gallbladder and biliary tract cancer	4000000 (3460000–4800000)	17	16	16	21	18	18
Kidney cancer	3780000 (3390000–4200000)	18	13	20	24	28	30
Larynx cancer	3560000 (2990000–4290000)	19	23	17	19	15	15
Other pharynx cancer	3330000 (2680000–4160000)	20	24	19	23	12	14
Acute myeloid leukaemia	3310000 (2800000–3920000)	21	17	21	17	22	23
Uterine cancer	2900000 (2470000–3390000)	22	21	25	22	23	26
Multiple myeloma	2810000 (2540000–3130000)	23	19	24	28	24	28
Nasopharynx cancer	2500000 (2080000–2950000)	24	25	22	16	19	19
Malignant neoplasm of bone and articular cartilage	2120000 (1680000–2690000)	25	28	23	20	20	21
Malignant skin melanoma	1810000 (1600000–2130000)	26	22	30	32	32	31
Acute lymphoid leukaemia	1740000 (1150000–2350000)	27	30	26	25	29	25
Soft tissue and other extraosseous sarcomas	1700000 (1380000–2150000)	28	26	29	29	25	22
Other leukaemia	1690000 (1300000–2190000)	29	29	27	26	26	29
Thyroid cancer	1500000 (1260000–1780000)	30	31	28	27	27	24
Chronic lymphoid leukaemia	983000 (866000–1180000)	31	27	31	34	34	35
Hodgkin lymphoma	922000 (700000–1200000)	32	34	32	31	30	27
Chronic myeloid leukaemia	720000 (562000–922000)	33	33	34	30	31	32
Mesothelioma	624000 (553000–695000)	34	32	35	35	35	36
Testicular cancer	552000 (443000–686000)	35	35	33	33	33	33
Eye cancer	196000 (150000–261000)	36	36	37	36	36	34
Neuroblastoma and other peripheral nervous cell tumours	121000 (104000–147000)	37	37	36	37	37	37

Figure 4: **Contribution of childhood cancer to global child deaths and all-age cancer DALYs in 2023, for all sexes combined**

(A) Rankings by cause comparing the absolute number of global deaths among the top 20 Level 3 categories of disease in GBD in ages 0–19 years. (B) Rankings by cause comparing the absolute number of global DALYs in GBD for childhood cancer (all cancers for ages 0–19 years) with individual cancer causes for ages 20 years to ≥95 years (these cancer-specific rows exclude DALYs for ages 0–19 years). For both sets of rankings, causes are ordered in descending absolute value of the global estimates, with childhood cancer in bold. Cells are coloured according to rank, ranging from highest rank (red) to lowest rank (green). The final five columns provide the rankings of these top global causes within each SDI quintile. DALYs=disability-adjusted life-years. GBD=Global Burden of Diseases, Injuries, and Risk Factors Study. SDI=Socio-demographic Index. UI=uncertainty interval.

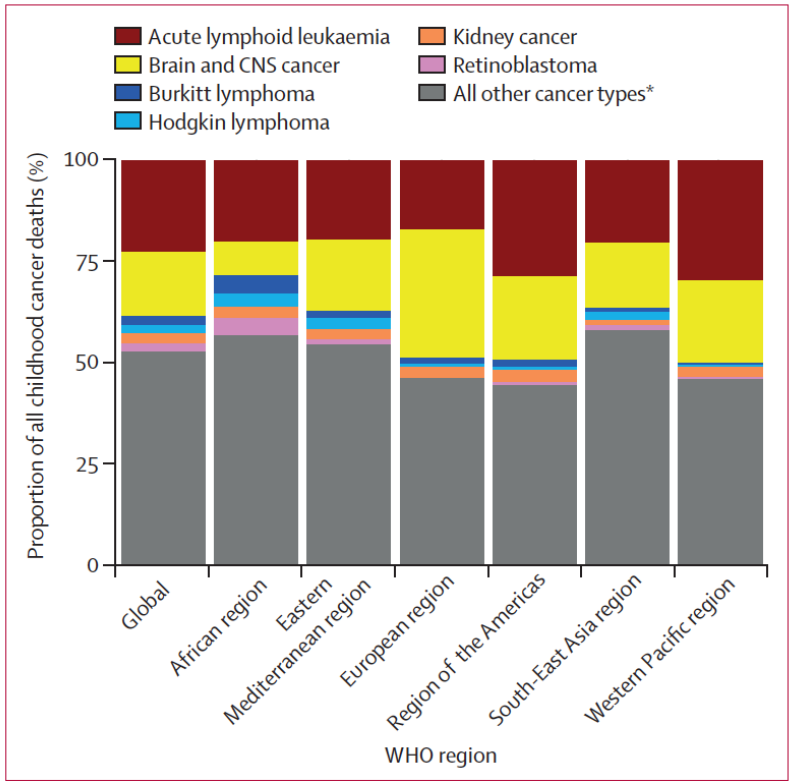

Figure 5: **Proportion of total childhood cancer deaths due to index cancers for the WHO GICC in 2023, globally and by WHO region, for all sexes combined**

Childhood cancer is defined as that occurring at ages 0–19 years. GICC=Global Initiative for Childhood Cancer. *All other cancer types includes all those not reported separately as WHO GICC index cancers.

Implications of all the available evidence

Childhood cancers contribute substantial burden within global child health and global oncology. In countries with the least resources, children with cancer still suffer the greatest premature mortality, highlighting that while progress has been made in outcomes globally over the past several decades, disparities remain. The WHO GICC is a crucial collaborative capacity building and implementation strategy that has fundamentally changed the landscape of childhood cancer since it was established in 2018. The target cancers identified for monitoring of progress in the WHO GICC comprise a sizeable portion of childhood cancer burden globally, but a considerable portion of childhood cancer burden is not part of the identified targets, and this is greater in some world regions than others. These findings reflect the need for WHO GICC efforts to address strengthening of health systems and childhood cancer needs and priorities as a whole in order to implement equitable and sustainable improvements in childhood cancer outcomes.

THE LANCET

Left Main Coronary Artery

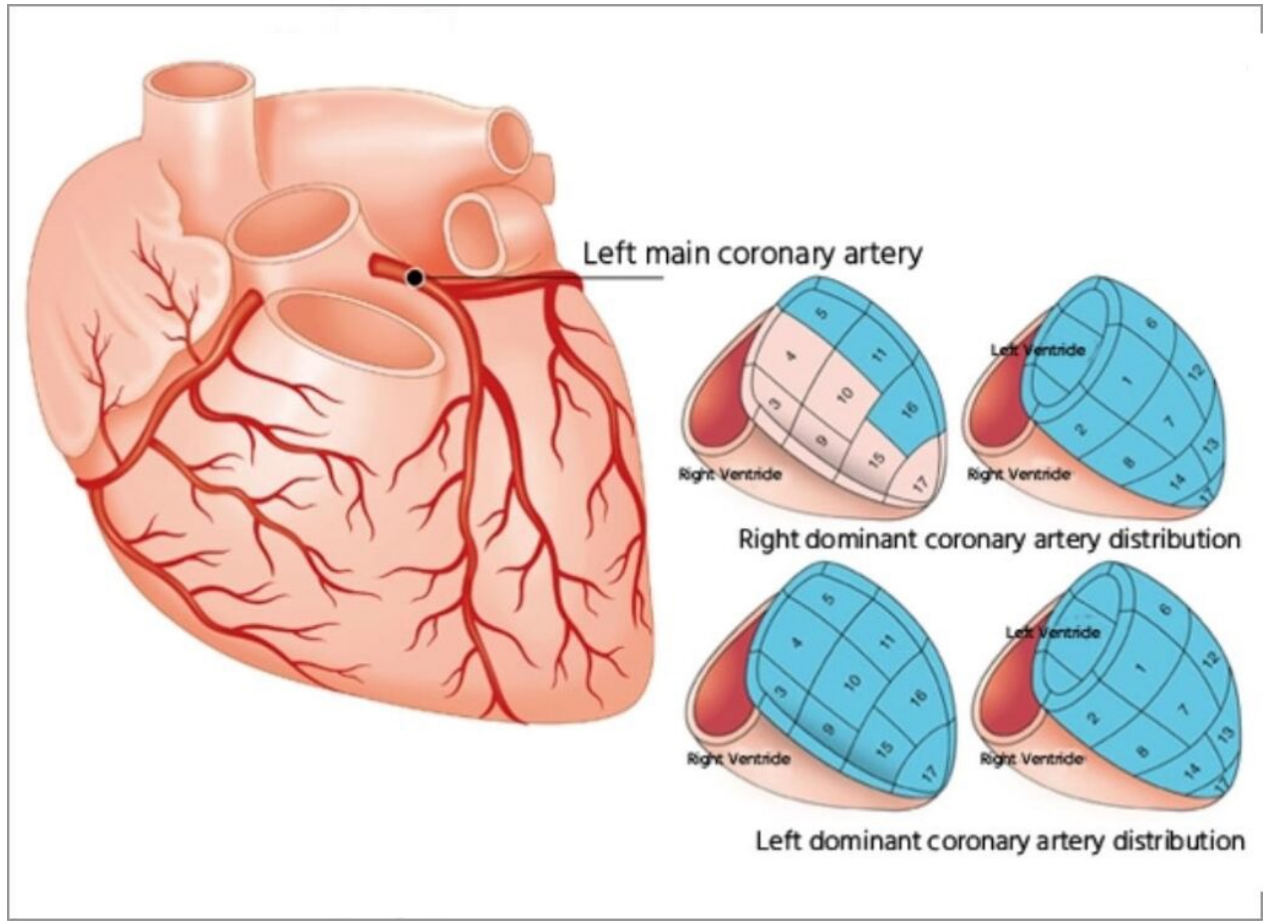

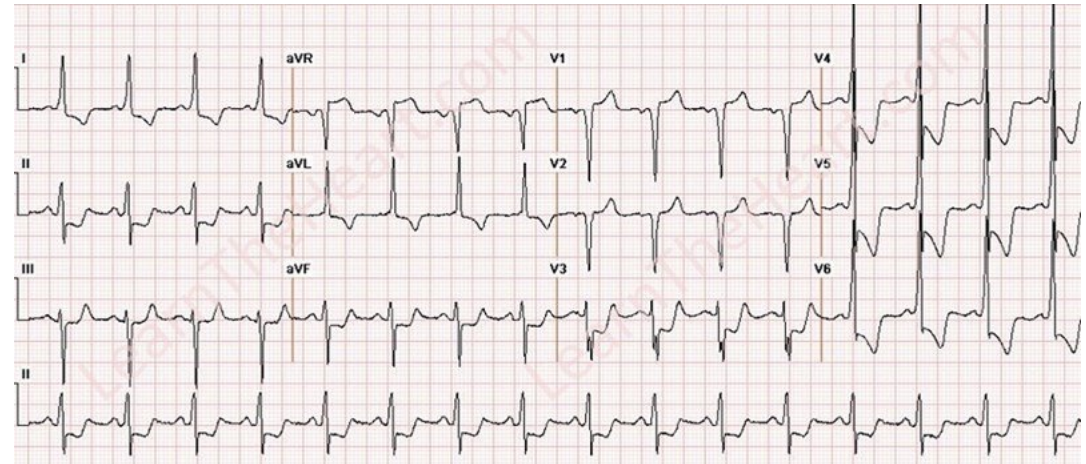

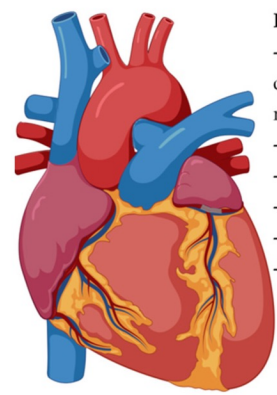

Favours PCI:
- Advanced age, comorbidities, high surgical risk, frailty
- Reduced life expectancy
- Restricted mobility
- Ostial/shaft lesion
- SYNTAX score <23
- Urgent revascularization

Favours CABG:
- Low LVEF
- Doubtful DAPT adherence or contraindications
- Diabetes and multivessel disease
- Bifurcation lesion
- SYNTAX score ≥23
- Concomitant cardiac surgery

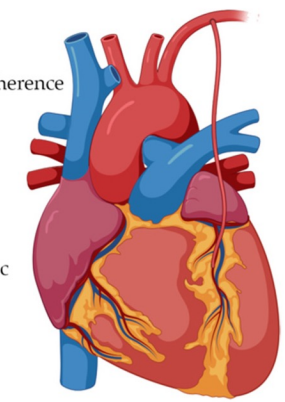

Percutaneous coronary intervention versus coronary artery bypass grafting for unprotected left main stenosis: 10-year final results from the randomised, open-label, non-

Summary

Background Coronary artery bypass grafting (CABG) is recommended over percutaneous coronary intervention (PCI) for patients with significant unprotected left main coronary artery disease. We aim to provide long-term outcome data comparing PCI with newer generation drug-eluting stents and CABG, which are scarce.

Methods This previously published, prospective, randomised, open-label, non-inferiority trial enrolled patients with unprotected left main coronary artery stenosis at 36 hospitals in Denmark, Estonia, Finland, Germany, Latvia, Lithuania, Norway, Sweden, and the UK. Eligibility was determined by a multidisciplinary heart team and defined by clinical criteria (chronic or acute coronary syndrome and a life expectancy of >1 year) and angiographic criteria (left main coronary artery diameter stenosis ≥50% or fractional flow reserve ≤0·80 in the left main ostium, mid-shaft, or bifurcation). Patients with ST elevation myocardial infarction within 24 h or considered at too high risk for CABG or PCI were excluded. Patients with angiographically confirmed significant left main coronary artery disease were randomly assigned (1:1) to PCI or CABG using an online system and stratified by site, sex, distal left main coronary artery bifurcation lesions, and diabetes. The primary outcome was the difference in 10-year all-cause mortality in the intention-to-treat (ITT) population, which was analysed using Kaplan–Meier estimates and unadjusted Cox regression. Patients were censored at the date of death, emigration, withdrawal, or loss to follow-up. Variation in all-cause mortality was assessed in prespecified subgroups. The trial is registered with ClinicalTrials.gov, NCT01496651 (active, not recruiting).

Findings From Dec 9, 2008, to Jan 21, 2015, 1201 patients were randomly assigned to PCI (n=598) or CABG (n=603). 17 patients were lost to follow-up before 1 year. 592 patients in each group were included in the ITT population. Mean age was 66·2 years (SD 9·9) in the PCI group and 66·2 years (9·4) in the CABG group. 256 (22%) of 1184 participants were female and 928 (78%) were male. There was no difference in all-cause mortality at 10 years (136 [23%] of 592 in the PCI group and 145 [25%] of 592 in the CABG group; hazard ratio 0·93 [95% CI 0·74–1·18]; p=0·56). No significant difference in all-cause mortality with SYNTAX score was identified.

Interpretation There was no significant difference in all-cause mortality at 10 years between PCI and CABG for patients with unprotected left main coronary artery disease and no additional complex lesions, indicating that PCI is equally as safe as CABG in patients eligible for both treatments. These results will aid heart teams in developing an individualised patient-centred strategy.

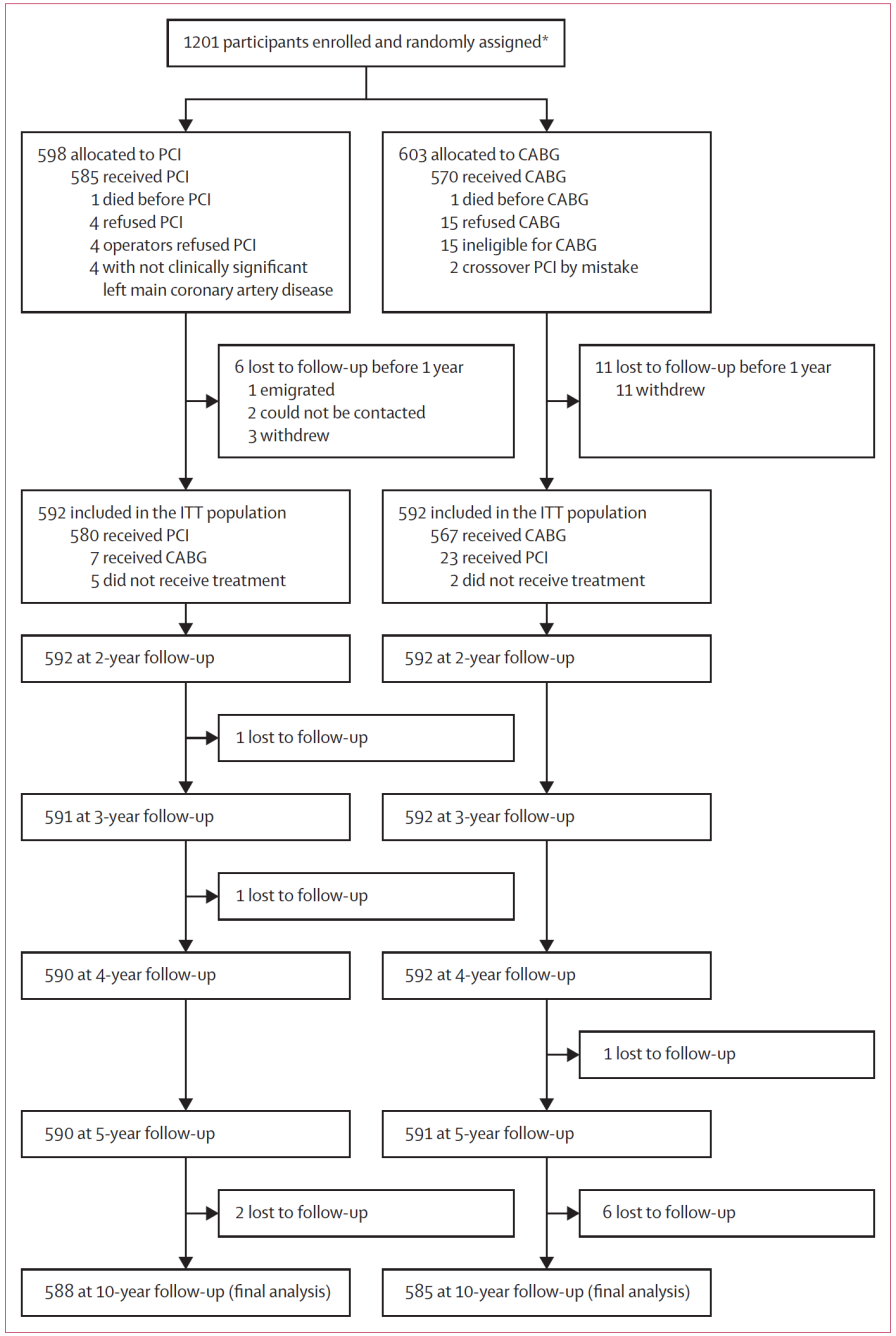

Figure 1: **Trial profile**
CABG=coronary artery bypass grafting. ITT=intention-to-treat. PCI=percutaneous coronary intervention.
*Adapted from Holm et al.[3]

	PCI group (n=592)	CABG group (n=592)	p value
Age, years	66·2 (9·9)	66·2 (9·4)	0·91
Sex			
Female	116 (20%)	140 (24%)	0·09*
Male	476 (80%)	452 (76%)	..
BMI, kg/m²	27·9 (4·5)	28·1 (4·4)	0·53
Type 1 or type 2 diabetes	86 (15%)	90 (15%)	0·94
Family history of ischaemic heart disease	321 (58%)	307 (56%)	0·45
Statin treatment	482 (82%)	464 (78%)	0·17
Hypertension	386 (65%)	489 (66%)	0·91
Active smoking	108 (19%)	127 (22%)	0·18
Previous PCI	116 (20%)	118 (20%)	0·90
Previous CABG	4 (1%)	2 (<1%)	0·41
Ejection fraction	60 (55–65)	60 (52–64)	0·27
New York Heart Association Functional Classification			
I	244 (53%)	195 (43%)	..
II	135 (29·6%)	150 (33%)	..
III	57 (13%)	77 (17%)	..
IV	23 (5%)	33 (7%)	0·012
European System for Cardiac Operative Risk Evaluation	2 (2–4)	2 (2–4)	0·18
SYNTAX score	22·4 (7·8)	22·3 (7·4)	0·74
Indication			
Stable angina pectoris	486 (82%)	491 (83%)	0·66
Acute coronary syndrome	106 (18%)	100 (17%)	0·66
Number of lesions requiring treatment	2 (1–3)	2 (2–3)	<0·0001
Distal left main coronary artery lesion	477 (81%)	482 (81%)	0·77

Data are mean (SD), n (%), median (IQR), or n (IQR). CABG=coronary artery bypass grafting. PCI=percutaneous coronary intervention. *p value shows the overall difference between female and male patients.

Table: **Baseline characteristics**

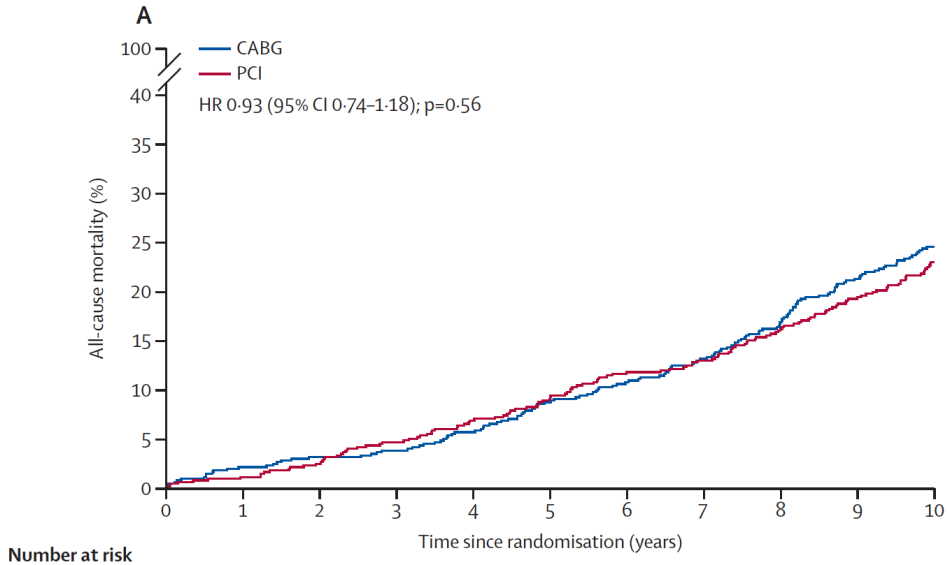

Figure 2: **Primary endpoint and time-dependent landmark analysis**
(A) Cumulative incidence of all-cause mortality. (B) Landmark analysis at 0–5 years and 5–10 years for all-cause mortality. CABG=coronary artery bypass grafting. HR=hazard ratio. PCI=percutaneous coronary intervention.

	PCI group (n=592)		CABG group (n=592)		HR (95% CI)	$p_{interaction}$
	Events/N	Event rate	Events/N	Event rate		
Age						0·64
<67 years	28/282	10%	27/280	10%	1·04 (0·61–1·76)	
≥67 years	108/310	35%	118/312	38%	0·90 (0·69–1·17)	
Sex						0·39
Female	28/116	24%	30/140	21%	1·14 (0·68–1·90)	
Male	108/476	23%	115/452	26%	0·88 (0·68–1·15)	
BMI, kg/m²						0·78
<30	98/413	24%	100/406	25%	0·95 (0·72–1·26)	
≥30	36/166	22%	42/170	25%	0·88 (0·56–1·38)	
Diabetes						0·23
Yes	24/90	27%	34/94	36%	0·71 (0·42–1·20)	
No	112/502	22%	111/498	22%	1·00 (0·77–1·30)	
Lesions requiring treatment						0·14
1	53/214	25%	26/135	19%	1·33 (0·83–2·13)	
2	46/215	21%	46/188	25%	0·86 (0·57–1·30)	
3	32/127	25%	49/198	25%	1·00 (0·64–1·56)	
4	4/28	15%	23/60	38%	0·35 (0·12–1·02)	
Acute coronary syndrome						0·049
Yes	20/106	19%	31/100	31%	0·57 (0·32–0·99)	
No	116/486	24%	114/491	23%	1·04 (0·80–1·34)	
Distal left main coronary artery lesion						0·48
Yes	114/477	24%	118/482	25%	0·97 (0·75–1·25)	
No	22/115	19%	27/110	25%	0·78 (0·44–1·36)	
SYNTAX score						0·27
≤22	63/297	21%	61/316	19%	1·13 (0·79–1·60)	
23–32	59/249	24%	66/220	30%	0·75 (0·53–1·06)	
≥33	14/46	30%	18/56	32%	0·94 (0·47–1·90)	
Overall	**136/592**	**23%**	**145/592**	**25%**	**0·93 (0·74–1·18)**	

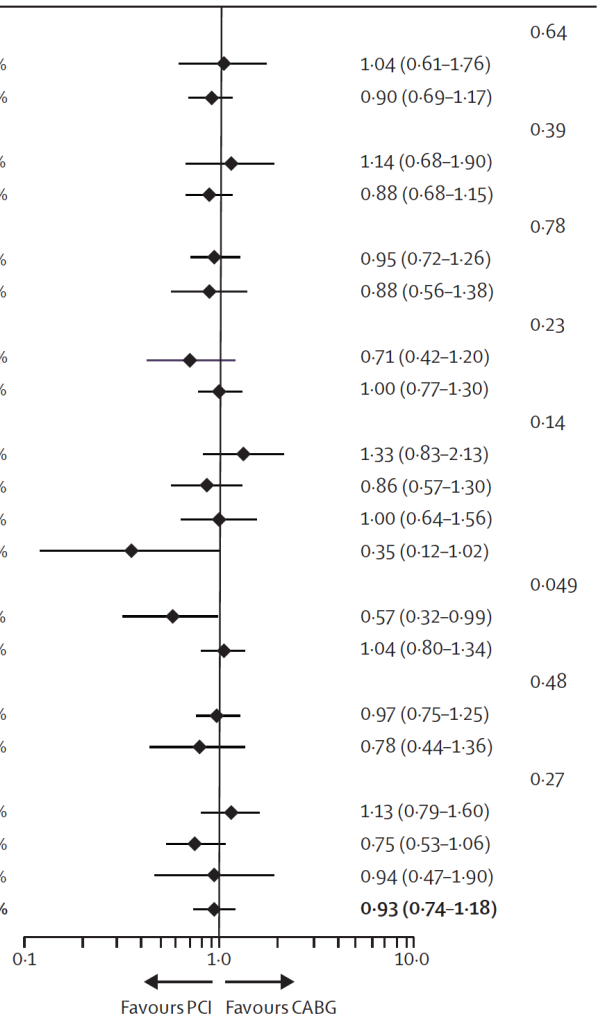

Figure 3: **Forest plot of prespecified subgroups**
CABG=coronary artery bypass grafting. HR=hazard ratio. PCI=percutaneous coronary intervention.

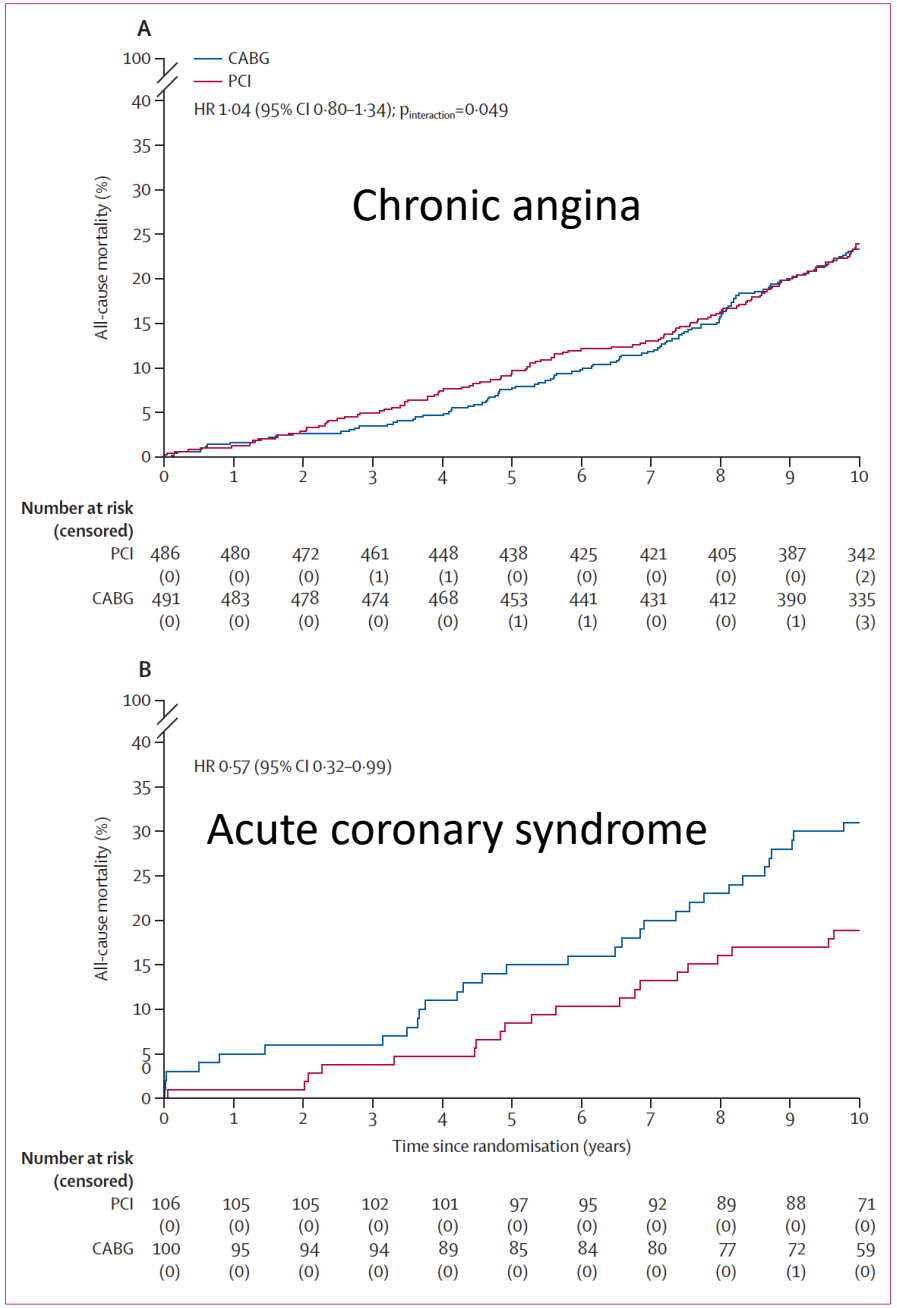

Figure 4: **All-cause mortality stratified by treatment indication**
Cumulative incidence of all-cause mortality in patients with chronic coronary syndrome (A) and acute coronary syndrome (B). CABG=coronary artery bypass grafting. HR=hazard ratio. PCI=percutaneous coronary intervention.

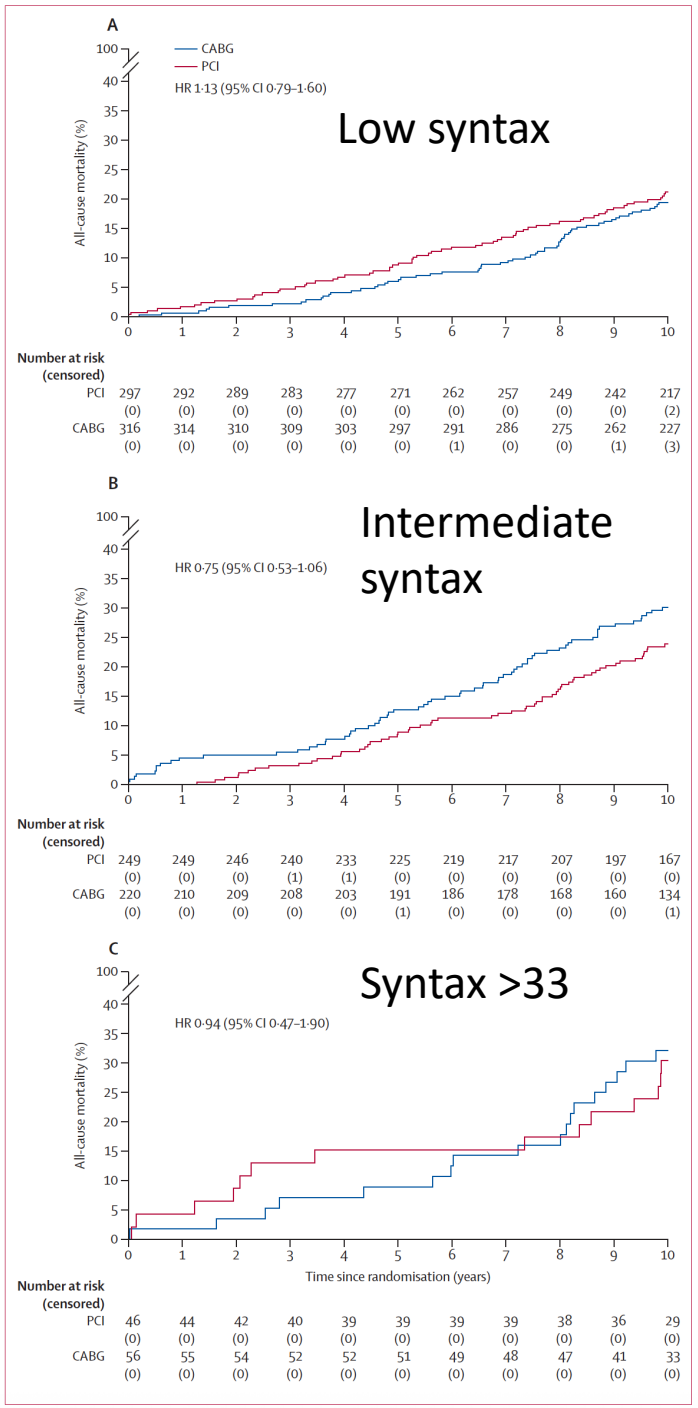

Figure 5: **All-cause mortality stratified by SYNTAX score**
Cumulative incidence of all-cause mortality in patients with a low SYNTAX score of 1–22 (A), intermediate SYNTAX score of 23–32 (B), and a high SYNTAX score of at least 33 (C). CABG=coronary artery bypass grafting. HR=hazard ratio. PCI=percutaneous coronary intervention.

Research in context

Evidence before this study

We searched PubMed from Sept 1, 2021, to Oct 1, 2025, using the search terms "left main", "percutaneous coronary intervention" OR "stent", and "coronary artery bypass grafting" to identify randomised controlled trials comparing percutaneous coronary intervention (PCI) using drug-eluting stents (DES) with coronary artery bypass grafting (CABG) in the left main coronary artery. Studies should report at least 5 years of follow-up because long-term follow-up is mandated when comparing CABG and PCI. We found a systematic review and meta-analysis of the NOBLE, SYNTAX Extended Survival, EXCEL, and PRECOMBAT trials. In a meta-analysis of 4394 patients, spontaneous myocardial infarction and repeat revascularisation was higher in patients who received PCI than those who received CABG 5 years after random assignment, whereas procedural myocardial infarction and stroke was higher in those who received CABG. No difference was observed in all-cause mortality, but the 1–5-year landmark analysis was non-significantly in favour of CABG (odds ratio 1·24 [95% CI 0·99–1·56]; p=0·063) driven by the EXCEL trial. A subgroup analysis of 1305 patients in the PRECOMBAT and SYNTAX Extended Survival trial with 10-year follow-up did not reveal an increased risk of all-cause mortality in patients who received first generation DES compared with CABG.

Added value of this study

In this randomised trial, second generation DES did not show a higher mortality than CABG at 10 years in patients with unprotected left main coronary artery disease who were eligible for both treatments. Landmark analysis between 0–5 years and 5–10 years did not show increased mortality at any timepoint. In a subgroup analysis, a possible differential treatment effect was observed in patients with acute coronary syndrome as PCI was associated with a lower risk of all-cause mortality than CABG. No heterogeneous treatment effect with SYNTAX score was found.

Implications of all the available evidence

The 10-year follow-up in this trial supports the extended findings from the SYNTAX Extended Survival and PRECOMBAT trials using first generation DES. Based on all-cause mortality, PCI with second generation DES is as safe as CABG. Consequently, the higher rate of spontaneous myocardial infarction and repeat revascularisations with PCI does not translate into higher mortality, which supports CABG as the preferred revascularisation option to improve major adverse cardiac events, but equipoise is evident for all-cause mortality. Caution is warranted for the treatment of patients with unprotected left main coronary artery disease and acute coronary syndrome as they might benefit more from PCI than CABG. Since both PCI and CABG are feasible, current evidence supports nuanced shared decision making with clear communication of risks and benefits.

Pyruvat (Anion der Brenztraubensäure), ist ein zentrales Stoffwechselzwischenprodukt, das als Endprodukt der Glykolyse entsteht. Es verbindet den anaeroben (Laktatbildung) und aeroben Stoffwechsel (Citratzyklus). Bei Sauerstoffmangel wird es zu Laktat umgesetzt, unter aeroben Bedingungen zu Acetyl-CoA für die Energiegewinnung.

Hier sind die wichtigsten Aspekte:

- **Stoffwechsel:** Es ist das Endprodukt der Glykolyse und Ausgangspunkt für den Citratzyklus (aerob) sowie die Gluconeogenese.
- **Anaerobe Bedingungen:** Pyruvat wird zu Laktat reduziert, um die Glykolyse aufrechtzuerhalten.
- **Chemische Struktur:**
  Es ist das Salz oder der Ester der Brenztraubensäure.
- **Verzweigungspunkt:** Pyruvat kann zu Alanin transaminiert oder in Acetyl-CoA umgewandelt werden.
- **Ernährung:** Pyruvat (oft als Calciumpyruvat) wird als Nahrungsergänzungsmittel zur Unterstützung des Stoffwechsels vermarktet.

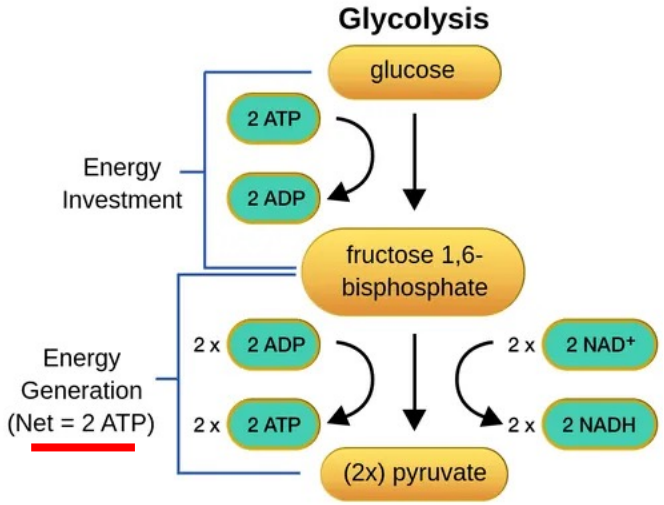

In erythrozyten ist dies Endstation

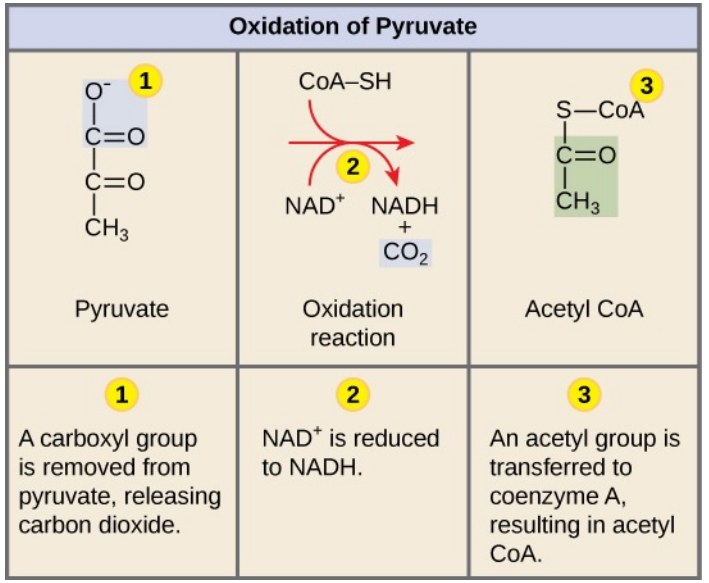

Die **Pyruvatkinase (PK)** ist ein zentrales Enzym des Kohlenhydratstoffwechsels. Sie katalysiert den letzten und **geschwindigkeitsbestimmenden Schritt** der Glykolyse. Dabei wird eine Phosphatgruppe von Phosphoenolpyruvat (PEP) auf ADP übertragen, wodurch **ATP und Pyruvat** entstehen.

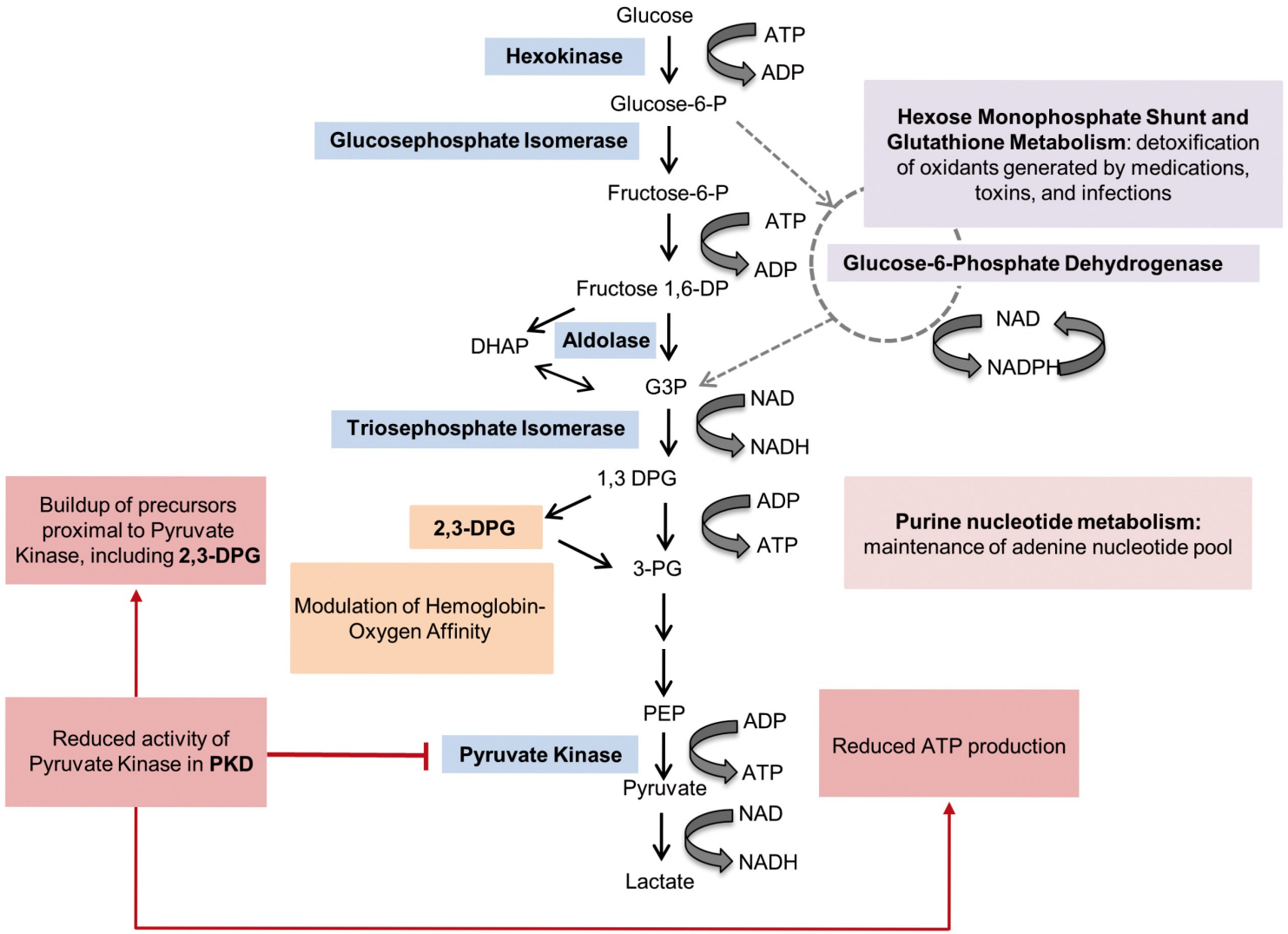

Pyruvatkinase (PK)-Inhibitoren sind chemische Verbindungen, welche die Aktivität des Enzyms Pyruvatkinase blockieren, das den letzten, geschwindigkeitsbestimmenden Schritt der Glykolyse katalysiert: die Umwandlung von Phosphoenolpyruvat (PEP) in Pyruvat unter gleichzeitiger Gewinnung von ATP. Die Forschung konzentriert sich primär auf Inhibitoren der **PKM2-Isoform**, da diese in fast allen Krebszellen hochreguliert ist und eine Schlüsselrolle beim **Warburg-Effekt** (aerobe Glykolyse) spielt, der das Tumorwachstum fördert.

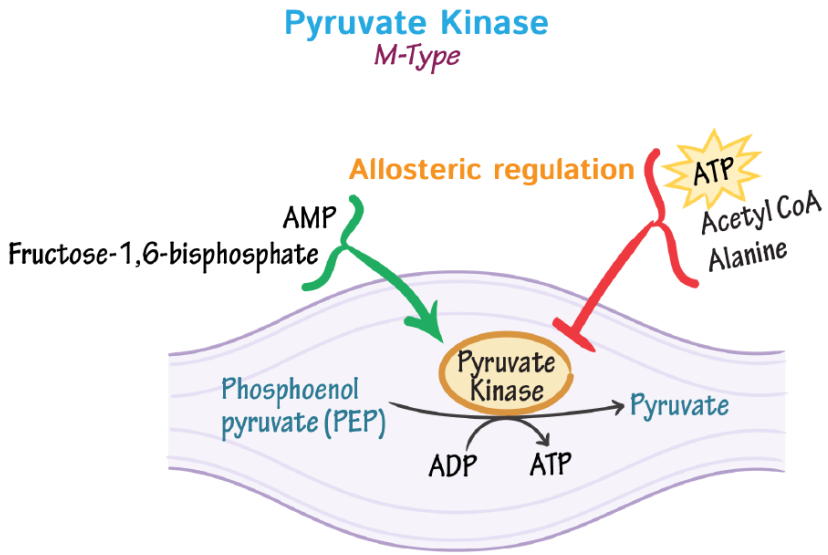

Pyruvate-Kinase-Aktivatoren sind eine neue Klasse von Medikamenten, die die Glykolyse in roten Blutkörperchen (Erythrozyten) stimulieren, um die ATP-Produktion zu erhöhen und den 2,3-Diphosphoglycerat-Spiegel (2,3-DPG) zu senken. Sie werden primär zur Behandlung seltener Erbkrankheiten eingesetzt, bei denen der Energiestoffwechsel der Blutzellen gestört ist.

Therapeutische Anwendungsgebiete

Diese Medikamente zeigen Potenzial bei einer Vielzahl von hämolytischen Anämien, da sie auch die Aktivität des Wildtyp-Enzyms steigern können:

- **Pyruvatkinase-Mangel (PKD)**: Erhöht den Hämoglobinwert und reduziert die Notwendigkeit von Bluttransfusionen.
- **Sichelzellkrankheit (SCD)**: Durch die Senkung von 2,3-DPG wird die Sauerstoffaffinität von Hämoglobin S erhöht, was die Polymerisation und Sichelbildung der Zellen verzögert.
- **Thalassämie**: Verbessert die ineffektive Erythropoese und reduziert die Eisenüberladung durch gesteigerten Energiestoffwechsel.
- **Andere Anämien**: Es laufen Untersuchungen zur Anwendung bei Membrandefekten (z. B. hereditäre Sphärozytose) und bestimmten Formen von MDS.

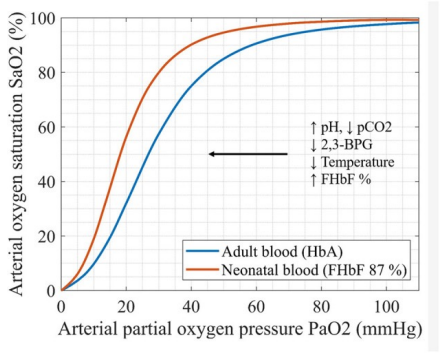

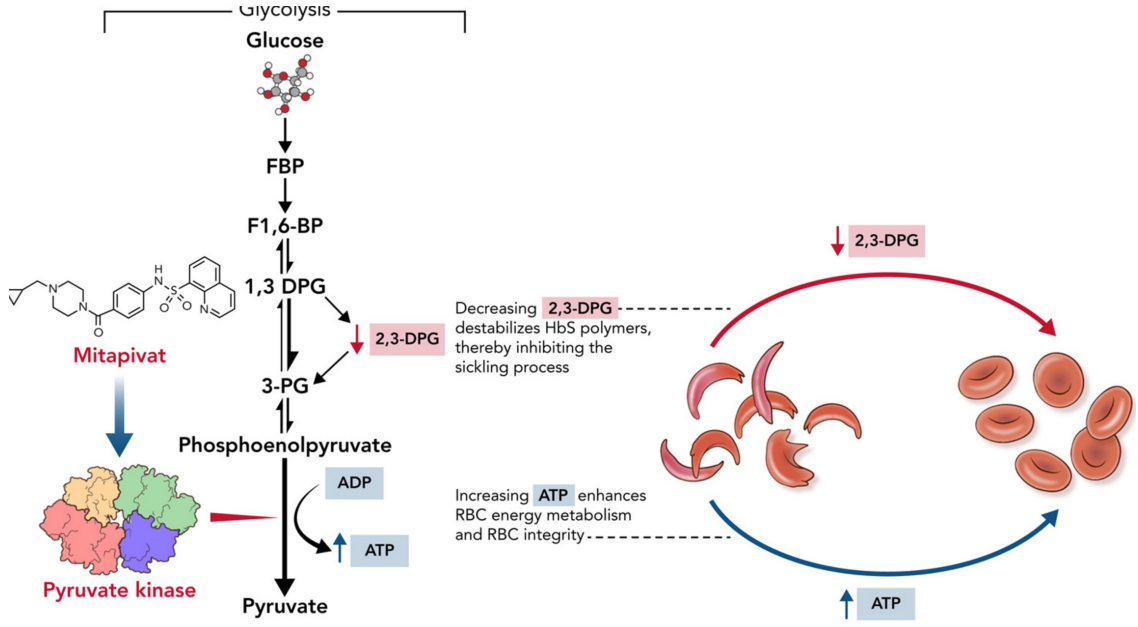

Pyruvate kinase activators in hereditary haemolytic anaemias: current evidence and clinical potential

Hereditary haemolytic anaemias represent the most prevalent group of genetic disorders worldwide and have a substantial impact on global health. Current treatments are few and primarily supportive. Recent studies suggest a crucial and overlapping role of metabolic impairment of red blood cells in these diseases, extending beyond the primary genetic defect. Pyruvate kinase activators enhance glycolysis, thereby targeting this shared metabolic impairment by increasing ATP production and improving cellular homeostasis. The first pyruvate kinase activator has been approved for the treatment of pyruvate kinase deficiency. Clinical trials evaluating pyruvate kinase activators in other haemolytic disorders, including thalassaemia, sickle cell disease, and red blood cell membrane disorders have provided evidence of clinical efficacy by ameliorating haemolytic anaemia and improving other disease-related outcomes, while maintaining a generally favourable safety profile. Ongoing preclinical and translational research continues to provide further insights into other potential indications for pyruvate kinase activators.

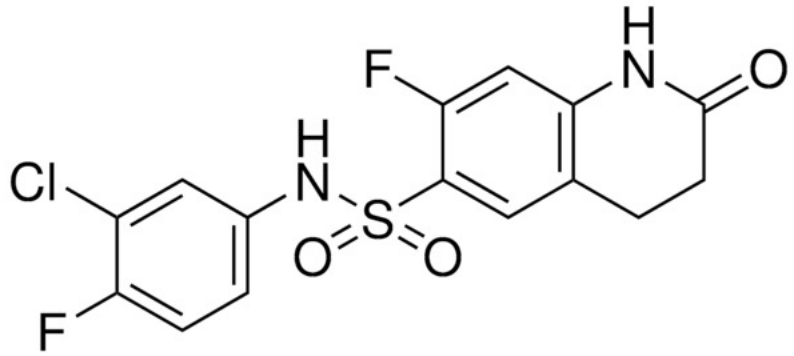

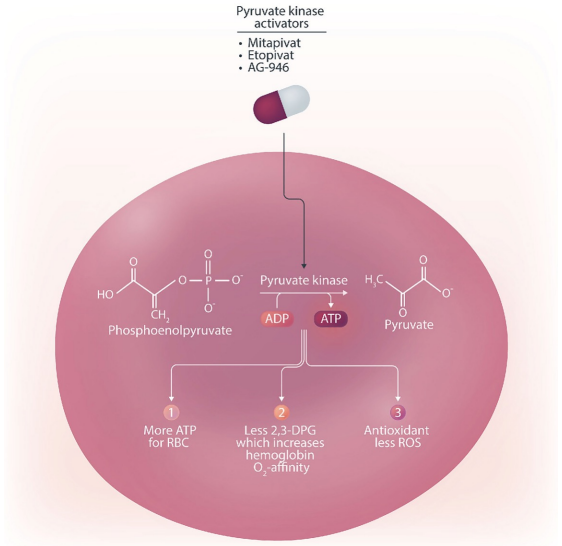

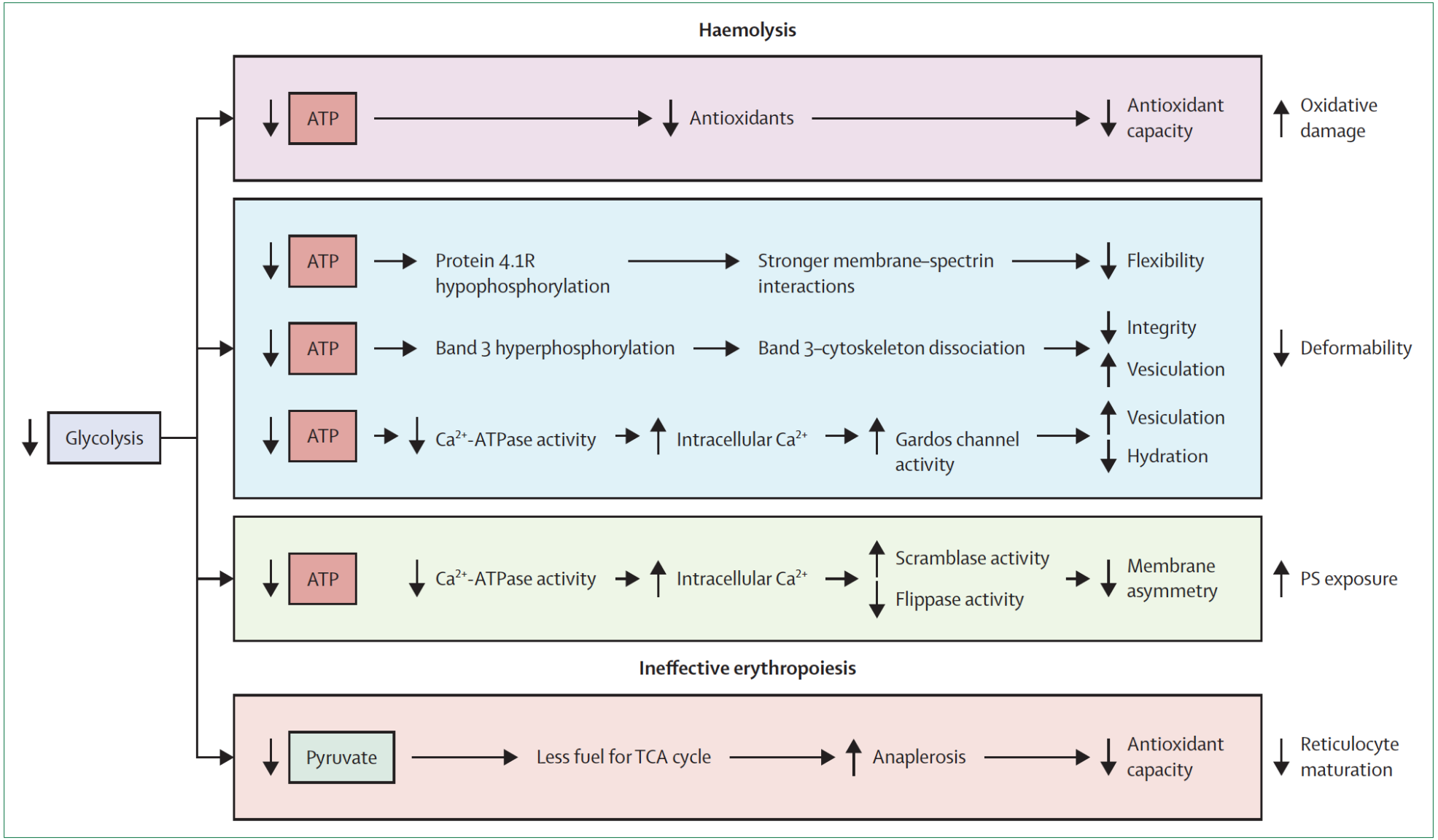

Figure 1: **Pathways through which glycolytic dysfunction causes anaemia**
Impaired glycolytic function leads to anaemia through several mechanisms affecting red blood cell function, homeostasis, production, and survival. PS=phosphatidylserine. TCA=tricarboxylic acid. Figure created using biorender.com.

	Mechanism of action	Diseases investigated in clinical trials	Dosages in phase 2/3 clinical trials, mg	Median range t_{max}, h* (min, max)	Mean range $t_{½}$, h* (±SD)	Bioavailability† (%)	Metabolism	Elimination
Mitapivat (AG-348)[13,40,41]	Allosteric activator of PKR, PKM2, and PKL	PKD, SCD, thalassaemia, RBC membrane disorders, and CDA II	5–200 BID	0·77 (0·48, 2·00)–1·01 (0·50, 3·00)‡	17·8 (3·3)–20·4 (3·6)‡	72·7	CYP3A4, CYP3A5, CYP1A2, CYP2C8, CYP2C9	Primarily via hepatic metabolism (1·1–2·4% renal clearance)
Etavopivat (FT-4202)[38,42]	Selective allosteric PKR activator	SCD and thalassaemia	200–400 QD	0·50 (0·5, 3·0)–1·5 (0·5, 4·0)	10·6 (2·4)–13·8 (3·9)	..	CYP3A4, CYP3A5, CYP2C9	Primarily via hepatic metabolism (0·8–1·7% renal clearance)
Tebapivat (AG-946)[39]	Allosteric activator of PKR and PKM2	SCD and MDS	2·5–20 QD	..	..	..	..	..

t_{max}=time to maximum concentration. $t_{½}$=estimated terminal elimination half-life. PKR=pyruvate kinase R. PKD=pyruvate kinase deficiency. SCD=sickle cell disease. RBC=red blood cell. CDA II=congenital dyserythropoietic anaemia type 2. BID=twice daily. QD=once daily. MDS=myelodysplastic syndrome. *Results displayed are based on single dosage of either 30 mg, 120 mg, or 360 mg mitapivat or 200 mg, 400 mg, 700 mg, or 1000 mg etavopivat. †After administration of a single dose of 120 mg mitapivat. ‡Accuracy and reliability at higher dose levels (700–2500 mg) were influenced by duration of sampling and were therefore not included.

Table 1: **Pharmacodynamic and pharmacokinetic properties of current pyruvate kinase activators**

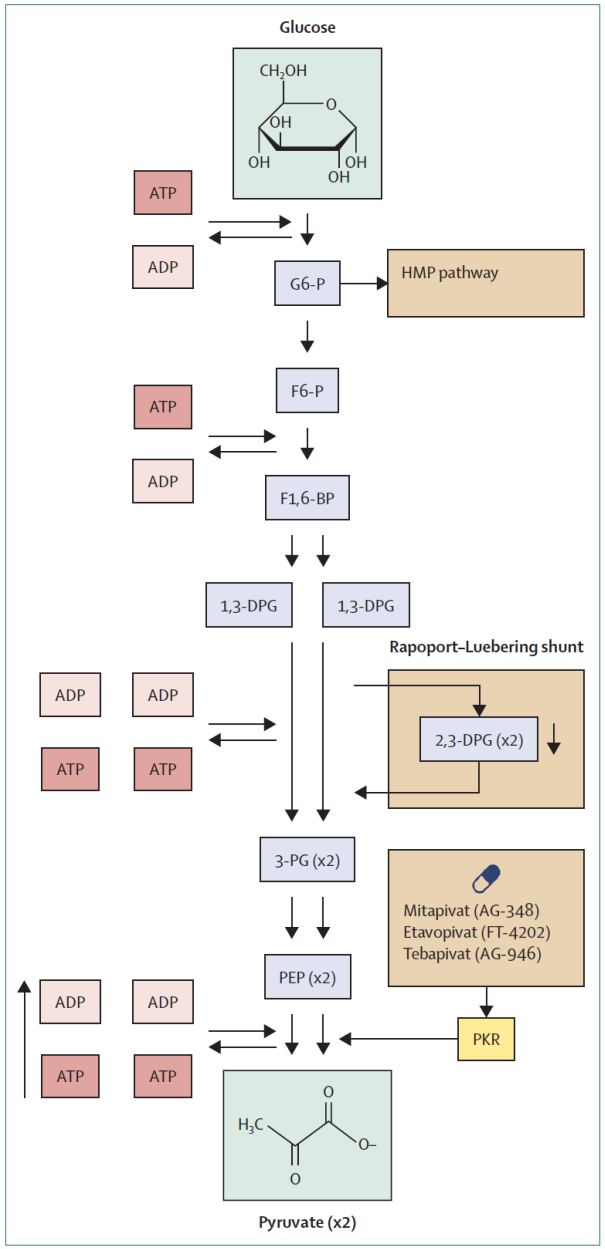

Figure 2: **Effects of PK activation on glycolytic flux**
A simplified overview of the glycolytic pathway, highlighting the effects on ATP and 2,3-DPG following PK activation. G6-P=glucose-6-phosphate. HMP=hexose monophosphate. F6-P=fructose-6-phosphate. F1,6-BP=fructose-1,6-biphosphate. 1,3-DPG=1,3-diphosphoglycerate. 2,3-DPG=2,3-diphosphoglycerate. 3-PG=3-phosphoglycerate. PEP=phosphoenolpyruvate. PK=pyruvate kinase. PKR=pyruvate kinase R. Figure created using biorender.com.

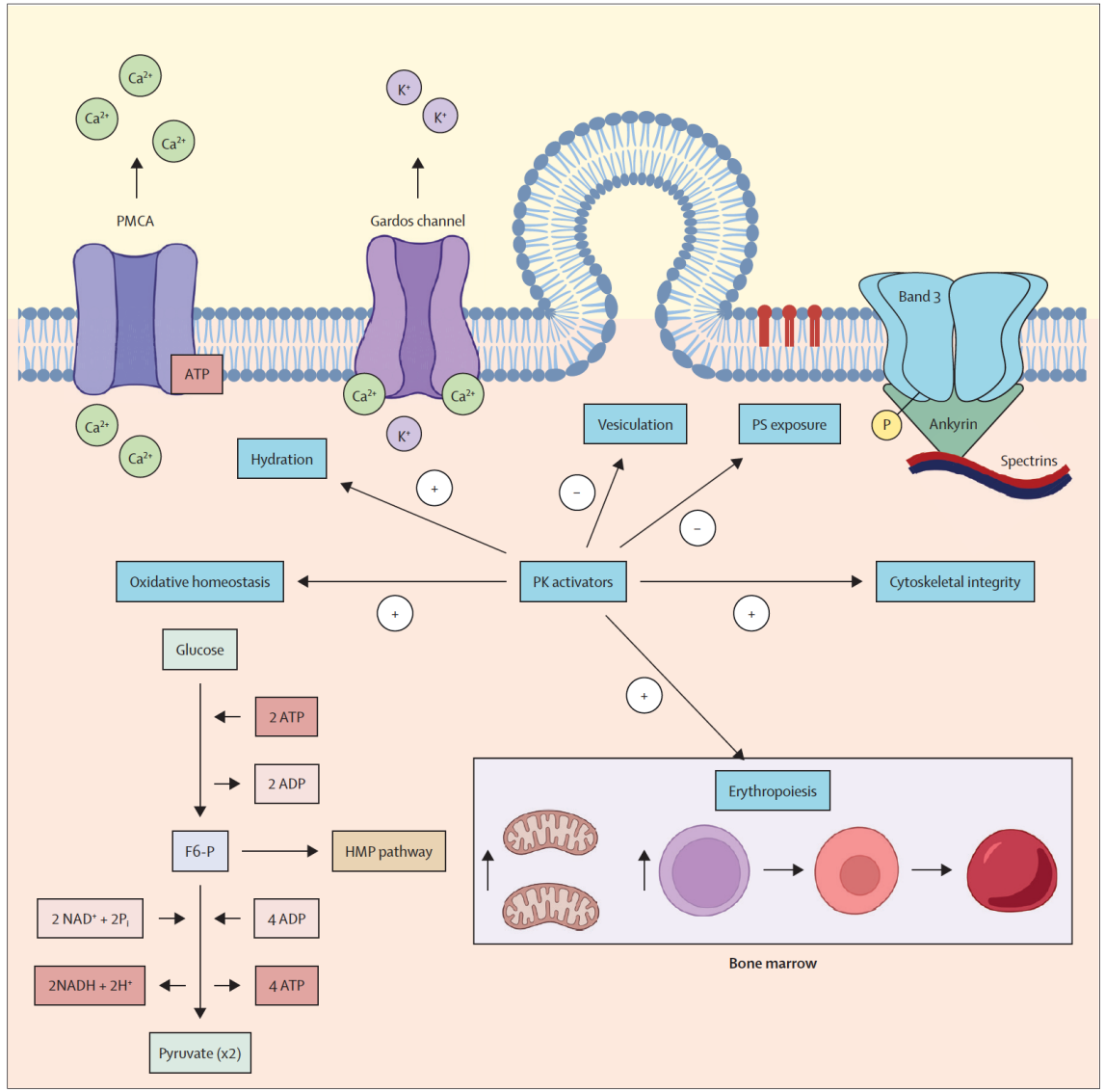

Figure 3: **Effect of PK activators on cellular mechanisms that influence cell survival**
Intracellular and intramedullary pathways improved by PK activation across hereditary haemolytic anaemias. Mechanisms described from left to right. PK activators enhance glycolytic flux, thereby increasing ATP production, decreasing glycolytic intermediates, including 2,3-diphosphoglycerate, and restoring the metabolic and oxidative homeostasis. Consequently, less oxidative stress-related protein denaturation and band 3 phosphorylation occur. Increased ATP availability following PK activation might lead to enhanced PMCA-mediated Ca^{2+} efflux. As a result, decreased intracellular Ca^{2+} concentrations prevent Gardos channel activation, thereby reducing K^+ efflux and cellular dehydration. Moreover, decreased intracellular Ca^{2+} concentrations prevent membrane vesiculation, and enable the maintenance of membrane asymmetry, including less PS exposure. Increased ATP generation resulting from PK activation boosts protein phosphatase activity, thereby preventing the phosphorylation of band 3. This effect leads to enhanced cytoskeleton–membrane interactions, preventing membrane vesiculation and improving membrane integrity and flexibility. During erythropoiesis, PK activators increase glycolytic flux in the erythroblasts, enhancing the oxidative stress response and promoting erythroid maturation. Additionally, PK activators enhance mitochondrial biogenesis and promote mitochondrial clearance, thereby ameliorating mitochondrial dysfunction. Both mechanisms contribute to improved erythropoiesis. F6-P=fructose-6-phosphate. HMP=hexose monophosphate. P=phosphate. PK=pyruvate kinase. PMCA=plasma membrane Ca^{2+}-ATPase. PS=phosphatidylserine. Figure created using biorender.com.

	Design	Dosage	Population, n	Treatment period	Safety outcomes*	Key efficacy outcomes
Mitapivat						
Yang et al[40] (NCT0210810)PK	Phase 1, randomised, double-blind, placebo-controlled, single ascending dose	30–2500 mg, single dose	Healthy volunteers, 36	Single dose	Headache (16·7%); nausea (13·9%); AE ≥grade 3 (0%)	ATP ↑; 2,3-DPG decrease
Yang et al[40] (NCT0214996)	Phase 1, randomised, double-blind, placebo-controlled, multiple ascending dose	15–700 mg BID	Healthy volunteers, 36	2 weeks	Headache (13·9%); nausea (13·9%); AE ≥grade 3 (2%)	ATP ↑; 2,3-DPG decrease
Grace et al[58] (NCT02476916): DRIVE PK	Phase 2, open-label, single-arm	50 mg or 300 mg BID	PKD, not receiving regular RBC transfusions, 52	24 weeks (core); up to 8·5 years (extension)	Headache (44%); insomnia (40%); nausea (38%); AE ≥grade 3 (21%)	20 (38%) participants with Hb response ≥1·0 g/dL
Al-Samkari et al[59] (NCT03548220): ACTIVATE	Phase 3, randomised, placebo-controlled	Dose escalation from 5 mg to 50 mg BID	PKD, not receiving regular RBC transfusions, 40	24 weeks (core); 192 weeks (open-label extension)	Nausea (18%); headache (15%); AE ≥grade 3 (25%)	16 (40%) participants with sustained Hb response ≥1·5 g/dL
Glenthøj et al[60] (NCT03559699): ACTIVATE-T	Phase 3, open-label, single-arm	Dose escalation from 5 mg to 50 mg BID	PKD, receiving regular RBC transfusions, 27	40 weeks (core); 192 weeks (open-label extension)	ALT increase (37%); headache (37%); nausea (19%); AST increase (19%); fatigue (19%); AE ≥grade 3 (30%)	10 (37%) participants with transfusion reduction ≥33%
van Beers et al[61] (NCT03853798) ACTIVATE extension	Phase 3, open-label, single-arm	Dose escalation from 5 mg to 50 mg BID	PKD, not receiving regular RBC transfusions, 78	96 weeks	..	Improvements in laboratory markers of erythropoiesis and iron overload reduction in MRI liver iron content
Kuo et al[8] (NCT0369205)	Phase 2, open-label, single-arm	Dose escalation from 50 mg to 100 mg BID	α or β-NTDT, 20	24 weeks (core); 10 years (extension)	Insomnia (50%); dizziness (30%); headache (25%); AE ≥grade 3 (25%)	16 (80%) participants with Hb response of ≥1·0 g/dL
Taher et al[62] (NCT04770753): ENERGIZE	Phase 3, double-blind, randomised, placebo-controlled	100 mg BID	α or β-NTDT, 129	24 weeks (core); 5 years (open-label extension)	Headache (22%); insomnia (15%); nausea (12%); AE ≥grade 3 (14%)	55 (42%) participants with Hb response of ≥1·0 g/dL *vs* 1 (2%) participant in the placebo group
Xu et al[63] (NCT0400016)	Phase 1, open-label, single-arm	Dose escalation from 5 mg to 100 mg BID	SCD HbSS, 17	2 weeks each dose (core); up to 6 years (extension)	Insomnia (41%); hyperglycaemia (29%); pain (29%); AE ≥grade 3 (41%)	9 (56·3%) participants with Hb response ≥1·0 g/dL
Conrey et al[64] (NCT04000165) and Xu et al[63] extension	Phase 2, open-label, single-arm	Dose escalation from 50 mg to 100 mg BID	SCD HbSS, 15	Up to 144 weeks	VOCs (66·7%); estradiol ↓ (53·3%); esterone ↓ (46·7%); AE ≥grade 3 (73·3%)	14 (93%) participants with Hb response ≥1·0 g/dL
van Dijk et al[65] (EudraCT 2019-003438-18): ESTIMATE	Phase 2, open-label, single-arm	Dose escalation from 20 mg to 100 mg BID	SCD (HbSS, HbS-β^0 thal, or HbS-β$^+$ thal), 10	8 weeks	Headache (44%); ALT ↑ (44%); AST ↑ (22%); dyspepsia (22%); AE ≥grade 3 (not specified)	Mean reduction in point of sickling of 9·7 ±6·2 mmHg (p=0·0032) from baseline
van Dijk et al[7] (EudraCT 2019-003438-18): ESTIMATE extension	Phase 2, open-label, single-arm	Dose escalation from 20 mg to 100 mg BID	SCD (HbSS, HbS-β^0 thal, or HbS-β$^+$ thal), 9	52 weeks (core); 2 + 2 years (extension)[66]	ALT ↑ (70%); AST ↑ (60%); headache (40%); AE ≥grade 3 (20%)	Mean reduction in point of sickling of 4·1 ± 5·6 mm Hg (p=0·0802) from baseline
Idowu et al[67] (NCT05031780): RISE UP	Phase 2/3, double-blind, randomised, placebo-controlled	50 mg or 100 mg BID	SCD (any genotype), 52	12 weeks (phase 2); 52 weeks (phase 3); 216 weeks (open-label extension)	Headache (23%); arthralgia (15%); AE ≥grade 3 (15%)	12 (46%) participants with Hb response ≥1·0 g/dL in the 50 mg group and 13 (50%) in the 100 mg group *vs* one (4%) in the placebo group after 12 weeks of treatment

(Table 2 continues on next page)

(Continued from previous page)

	Design	Dosage	Population, n	Treatment period	Safety outcomes*	Key efficacy outcomes
Etavopivat						
Forsyth et al[42] (NCT0381569)	Phase 1, randomised, placebo-controlled, double-blind, single ascending dose	200–1000 mg, single dose	Healthy volunteers, 24	Single dose	Each reported event occurred once; AE ≥grade 3 (4%)	..
Forsyth et al[42] (NCT0381569)	Phase 1, randomised, placebo-controlled, double-blind, multiple ascending dose	100, 200, 300 BID or 400 mg QD	Healthy volunteers, 36	2 weeks	Headache (28%); all other events occurred once; AE ≥grade 3 (0%)	ATP ↑; 2,3-DPG decrease; p50 decrease
Saraf et al[68] (NCT0381569)	Phase 1, randomised, placebo-controlled, single dose	700 mg, single dose	SCD (HbSS, HbS-β^0 thal, HbS-β$^+$ thal, or HbSC), 5	Single dose	Each reported event occurred once; AE ≥grade 3 (0%)	..
Saraf et al[68] (NCT0381569)	Phase 1, randomised, placebo-controlled, double-blind, multiple ascending dose	300 mg or 600 mg QD	SCD (HbSS, HbS-β^0 thal, HbS-β$^+$ thal, HbSC), 16	2 weeks	Headache (37·5%); nausea (37·5%); dizziness (25%); AE ≥grade 3 (12·5%)	11 (73%) participants with a Hb response ≥1·0 g/dL; p50 decrease
Saraf et al[68] (NCT0381569)	Phase 1, open-label, single-arm	400 mg QD	SCD (HbSS, HbS-β^0 thal, HbS-β$^+$ thal, or HbSC), 15	12 weeks	Headache (46·7%); nausea (26·7%); dizziness (20%); upper respiratory infection (20%); AE ≥grade 3 (40%)	11 (73%) participants with a Hb response ≥1·0 g/dL; p50 decrease

Safety and efficacy results correspond to the core period specified for each study. Results from the extension periods are listed where available. n=number of patients treated with pyruvate kinase activator (placebo not included). AE=adverse event. 2,3-DPG=2,3-diphosphoglycerate. BID=twice daily. PKD=pyruvate kinase deficiency. RBC=red blood cell. Hb=haemoglobin. ALT=alanine aminotransferase. AST=aspartate aminotransferase. NTDT=non-transfusion dependent thalassaemia. SCD=sickle cell disease. VOC=vaso-occlusive crisis. Thal=thalassaemia. QD=once daily. *Percentages represent the proportion of patients in whom the corresponding events occurred. Only safety outcomes from the intervention arm are displayed in the case of placebo-controlled trials. For each study, the three most frequent reported events (occurring in ≥10% of participants) are presented.

Table 2: **Clinical trials with completed and published results**

	Design	Dosage	Population	Treatment period	Key outcome measures
Mitapivat					
NCT05175105: ACTIVATE-Kids	Phase 3, double-blind, placebo-controlled	Dose escalation from 1 mg to 50 mg BID	Paediatric (age <18 years) patients with non-transfusion-dependent PKD	20 weeks (core); 5 years (extension)	Hb response; sex hormones and BMD; haemolytic and erythropoietic markers; iron markers; patient-reported outcomes; pharmacokinetics and pharmacodynamics
NCT05144256: ACTIVATE-KidsT	Phase 3, double-blind, placebo-controlled	Dose escalation from 1 mg to 50 mg BID	Paediatric (age <18 years) patients with transfusion-dependent PKD	32 weeks (core); 5 years (open-label extension)	Transfusion reduction response; Hb response; sex hormones and BMD; iron markers; patient-reported outcomes; pharmacokinetics and pharmacodynamics
NCT04770779: ENERGIZE-T	Phase 3, double-blind, randomised, placebo-controlled	100 mg BID	Transfusion dependent α or β-thal	48 weeks (core); 5 years (open-label extension)	Transfusion reduction response; iron markers; safety; pharmacokinetics and pharmacodynamics
NCT06286046: RESIST	Phase 2, open-label, single-arm	100 mg BID	SCD (HbSS or HbS-β^0 thal)	6 months	Kidney function and markers; hospitalisation rate; safety
NCT05935202: SATISFY	Phase 2, open-label, single-arm	Dose escalation from 50 mg to 100 mg BID	RBC membranopathies or CDA II	32 weeks (core); 1 year (extension)	Safety; Hb response; haemolytic and erythropoietic markers; iron markers; patient-reported outcomes
Etavopivat					
NCT04987489: GLADIOLUS	Phase 2, open-label	400 mg QD	SCD (cohort A); transfusion-dependent thal (cohort B); non-transfusion dependent thal (cohort C)	48 weeks	Hb response; transfusion reduction response; iron markers and overload
NCT06609226: FLORAL	Phase 3, open-label, roll-over	400 mg QD	SCD or thal who completed at least one treatment period in the parent study	264 weeks	Annualised rate of VOCs; Hb response; transfusion reduction response; hospitalisation rate; safety
NCT04624659: HIBISCUS	Phase 2/3, randomised, double-blind, placebo-controlled	200 mg or 400 mg QD	SCD (any genotype)	52 weeks (core); 112 weeks (open-label extension)	Hb response; annualised rate of VOCs; haemolytic and erythropoietic markers; patient-reported outcomes
NCT06612268: HIBISCUS 2	Phase 3, randomised, double-blind, placebo-controlled	400 mg QD	Patients aged ≥12 years with SCD (HbSS, HbS-β^0 thal, or other syndrome)	52 weeks	VOC rate; Hb response; haemolytic and erythropoietic markers; patient-reported outcomes; kidney function
NCT05953584: HIBISCUS 3	Phase 2, open-label, single-arm	400 mg QD	Children with SCD (HbSS or HbS-β^0 thal) who are at increased risk of stroke	52 weeks (core); 48 weeks (extension)	Timed average mean maximum velocity of the internal carotid artery and middle cerebral artery
NCT06198712: HIBISCUS KIDS	Phase 1/2, open-label, single-arm	400 mg QD	Paediatric (age 12–18 years) patients with SCD (any genotype)	24 weeks (core); 72 weeks (extension)	Pharmacokinetics and pharmacodynamics; Hb response; annualised rate of VOCs; patient-reported outcomes; timed average mean maximum velocity; safety
NCT05725902	Phase 2, open-label, single-arm	400 mg QD	Children with SCD (HbSS or HbS-β^0 thal)	24 weeks	Cerebral blood flow; oxygen ejection fraction; cerebral metabolic rate of oxygen; safety
NCT05568225: FORTITUDE	Phase 2, open-label	400 mg QD	Very low, low, and intermediate risk MDS	48 weeks	Transfusion reduction response; Hb response; iron markers; platelet and neutrophil response; overall survival; safety

(Table 3 continues on next page)

(Continued from previous page)

	Design	Dosage	Population	Treatment period	Key outcome measures
Tebapivat					
NCT04536792	Phase 1, randomised, double-blind, placebo-controlled, SAD and MAD	1 mg to 100 mg (SAD); 1 mg to 20 mg QD (MAD)	Healthy volunteers	Single dose (SAD); 2 weeks (MAD)	Safety; pharmacokinetics and pharmacodynamics
NCT04536792	Phase 1, open-label	2 mg or 5 mg QD	SCD (HbSS or HbS-β^0 thal)	4 weeks (core); 2 years (extension)	Safety; pharmacokinetics and pharmacodynamics; Hb response; haemolytic and erythropoietic markers
NCT06924970	Phase 2, double-blind, randomised, placebo-controlled	2·5 mg, 5 mg, or 7 mg QD	SCD (HbSS, HbSC, HbS-β^0 thal or other syndrome)	12 weeks (core); 52 weeks (extension)	Hb response; haemolytic and erythropoietic markers; patient-reported outcomes; safety
NCT05490446	Phase 2, open-label, single-arm (phase 2A)	5 mg QD	Lower-risk MDS*	16 weeks (core); 156 weeks (extension)	Hb response; transfusion independence; transfusion reduction response; safety; pharmacokinetics and pharmacodynamics
NCT05490446	Phase 2, open-label (phase 2B)	10 mg, 15 mg, or 20 mg QD	Lower-risk MDS*	24 weeks (core); 156 weeks (extension)	Transfusion reduction response; Hb response; safety; pharmacokinetics and pharmacodynamics

Safety measured as number and severity of treatment-emergent adverse events. BID=twice daily. PKD=pyruvate kinase deficiency. Hb=haemoglobin. BMD=bone mineral density. Thal=thalassaemia. SCD=sickle cell disease. RBC=red blood cell. CDA II=congenital dyserythropoietic anaemia type 2. QD=once daily. VOC=vaso-occlusive crisis. SAD=single ascending dose. MAD=multiple ascending dose. MDS=myelodysplastic syndrome. *Lower-risk MDS defined as Revised International Prognostic Scoring System risk score ≤3·5 and <5% blasts.

Table 3: **Ongoing clinical trials without completed and published core period results**

Future directions

Many other red blood cell enzyme disorders could benefit from PK activation due to enhancement of glycolytic flux and restoration of metabolic and antioxidative homeostasis. A case report of a patient with phosphofructokinase deficiency described symptom improvement of muscle disease and improvements in haemoglobin following mitapivat treatment, supporting further exploration in other red cell enzymopathies, such as glucose-6-phosphate isomerase deficiency.[97] Ongoing trials of PK activators in haematological conditions, such as myelodysplastic syndrome, are expected to provide important insights that might support expanding their use to other hypoproliferative anaemias or bone marrow failure syndromes, such as Diamond-Blackfan anaemia.[87]

Ongoing evaluation in the paediatric population is important, as early initiation of treatment might prevent the development of long-term complications associated with haemolysis, blood transfusions, and iron overload. Most importantly, effective symptom management is crucial given the substantial disease burden during childhood, and this could prevent unnecessary splenectomy and its associated complications and risks.

Conclusions

PK activators represent a novel, oral, and generally well tolerated therapeutic approach for hereditary haemolytic anaemias, offering a mechanism-based alternative to supportive care. Clinical trials have shown meaningful improvements in key disease markers, with potential benefits in reducing complications and improving quality of life. An expanding number of red blood cell disorders could benefit from PK activation, supported by preclinical research suggesting a role of glycolytic disturbances in their pathophysiology. Early results of PK activation in children with PK deficiency suggest a favourable safety profile, supporting the expansion to early treatment, which remains an area of substantial unmet need. Second-generation PK activators with improved pharmacokinetic properties could optimise treatment further, and ongoing research underscores the expanding role of PK activation and its potential applications in other haematological conditions. Collectively, these recent advances have the potential to transform the clinical management of patients with hereditary haemolytic anaemias, particularly in diseases with few effective oral options, including sickle cell disease and thalassaemia.

Das Fibroblasten-Aktivierungsprotein (FAP) ist eine Serinprotease, die in atherosklerotischen Plaques exprimiert wird und Entzündungsprozesse sowie den Umbau der extrazellulären Matrix fördert, was zu Plaque-Instabilität beiträgt. FAP-Defizienz schützt vor Atherosklerose, indem sie die Plaquebildung reduziert, die fibröse Kappe stabilisiert und Entzündungszellen verringert. FAP gilt als potenzielles Ziel für die Bildgebung (FAPI-PET) und therapeutische Ansätze.

Wichtige Zusammenhänge zwischen FAP und Atherosklerose:

- **Rolle in der Plaque:** FAP wird in menschlichen atherosklerotischen Läsionen gefunden, insbesondere in aktivierten vaskulären glatten Muskelzellen (VSMCs), und fördert dort Entzündungen.
- **Auswirkung auf Plaques:** Eine Deletion oder Hemmung von FAP führt in Mausmodellen zu einer verringerten Plaquebildung (Atheroprotektion) und einer Zunahme von fibrillärem Kollagen, was die Stabilität erhöht.
- **Bildgebung:** Die FAP-Inhibitor (FAPI)-PET-Bildgebung wird genutzt, um aktivierte Fibroblasten in Plaques sichtbar zu machen und könnte zur Identifizierung von Hochrisiko-Läsionen dienen.
- **Therapeutisches Potenzial:** Da FAP die Plaque-Progression fördert, könnte die Hemmung von FAP eine Behandlungsoption zur Stabilisierung von Plaques darstellen.

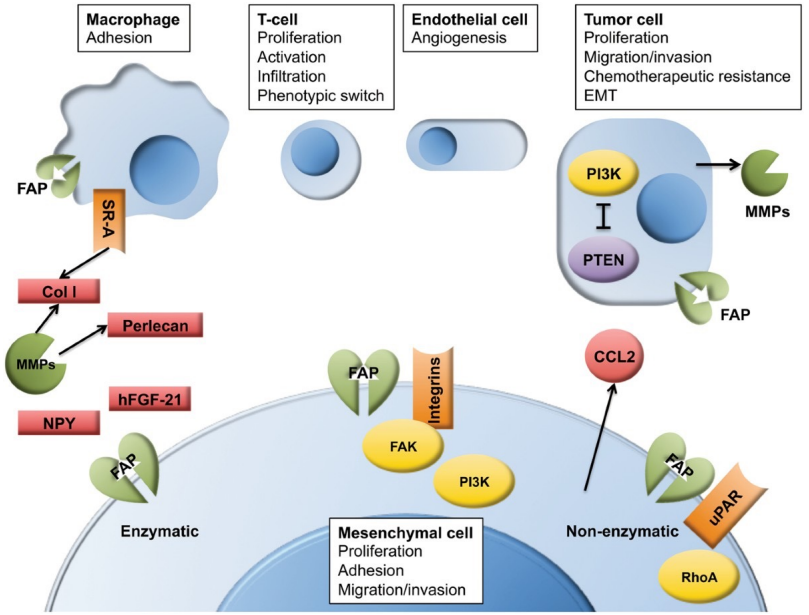

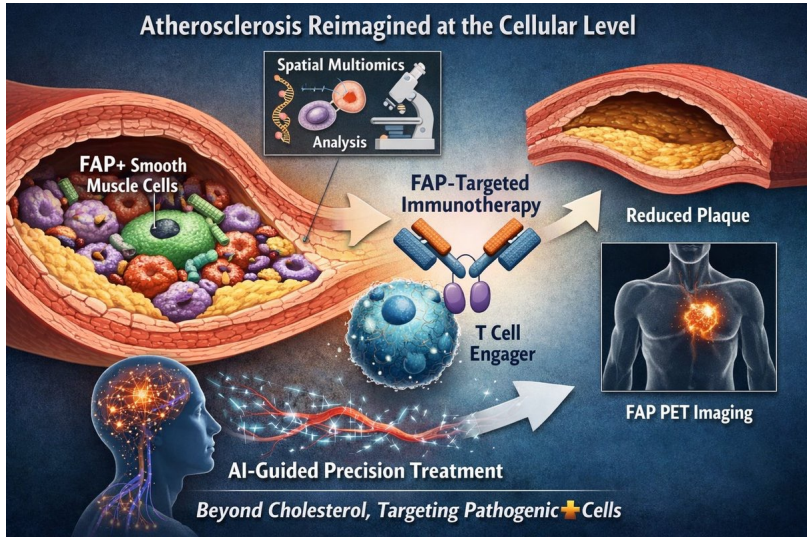

Targeting modulated vascular smooth muscle cells in atherosclerosis via FAP-directed immunotherapy

Editor's summary

Atherosclerosis is characterized by the buildup of lipid-containing plaque in blood vessels including coronary arteries and is a leading cause of death worldwide. The mainstay of therapy is lipid-lowering agents such as statins, which help but do not always fully prevent disease progression and mortality. To gain further insight into the biology of atherosclerotic plaques, Amrute *et al*. performed single-cell spatial transcriptomics on coronary arteries from people with and without atherosclerosis. This analysis helped identify smooth muscle cells expressing fibroblast activation protein as a major culprit in blood vessel plaque formation. Immunotherapy using a bispecific T cell engager (BiTE) against this protein reduced the atherosclerotic plaque burden in mouse models, suggesting a potential therapeutic strategy. —

BiTE (Bispecific T-cell Engager) therapy is a form of immunotherapy that acts as a bridge between a patient's immune system (T-cells) and cancer cells, directing the immune system to destroy the tumor.

Structured Abstract

INTRODUCTION

Atherosclerosis is a leading cause of cardiovascular disease and mortality, which is characterized by accumulation of lipid-rich vascular plaques that contain diverse populations of stromal and immune cells. Preclinical studies have demonstrated that during atherogenesis, vascular smooth muscle cells (VSMCs) undergo a phenotypic shift and give rise to populations of modulated SMCs (modSMCs) that comprise the neo-intima. Genome-wide association studies have identified numerous genetic variants linked to coronary artery disease, many of which regulate genes expressed in VSMCs, highlighting the therapeutic potential of targeting VSMCs and their phenotypic transitions. Notably, major gaps remain in the field's mechanistic understanding of modSMC specification and contribution to plaque progression.

RATIONALE

Advances in single-cell multiomics and spatial transcriptomics have enabled high-resolution profiling of healthy and diseased human tissues and provided an opportunity to map cell types within their anatomical context. During atherosclerosis progression, immune infiltration and VSMC diversification reshape the media and intimal compartments and drive neointimal growth and plaque instability. Comprehensive single-cell and spatial datasets of human coronary artery disease capturing these events are lacking. We performed cellular indexing of transcriptomes and epitopes by sequencing and single-cell spatial transcriptomics on healthy and diseased human coronary arteries. We further leveraged mouse models and antibody-based therapeutics to dissect the origin of and target modSMCs in vivo.

RESULTS

We identified fibroblast activation protein (FAP) as a marker of modSMCs located within the neo-intima in humans and mice. Using spatial transcriptomics, we revealed that FAP^+ modSMCs reside within a macrophage-rich cellular neighborhood, which contributes to their specification. Genetic lineage tracing demonstrated that FAP^+ modSMCs arise from quiescent VSMCs. To explore the therapeutic potential of targeting FAP^+ modSMCs in atherosclerosis, we developed a half-life extended anti-FAP bispecific T cell–engaging antibody (BiTE) that harnesses T cell cytotoxicity with optimized pharmacodynamics to selectively eliminate FAP-expressing cells. Although BiTE technology has been extensively investigated in oncology to direct T cells against tumor-associated antigens, its application to cardiovascular disease is unexplored. BiTE treatment resulted in a marked reduction in plaque burden across mouse atherosclerosis models, suggesting that immunotherapeutic depletion of FAP^+ modSMCs may be a viable therapeutic strategy for atherosclerosis. Finally, by leveraging single cell RNA sequencing, we observed that anti-FAP BiTEs favorably remodeled the cellular and immune cell architecture of the plaques, which was associated with emergence of clonal T cell populations.

CONCLUSION

Collectively, this work provides a comprehensive single-cell and spatially resolved map of human coronary artery disease, identifies FAP as a marker of modSMCs, and introduces BiTE-based immunotherapy as a potential strategy for targeting atherosclerotic plaques by selectively depleting precise disease-associated VSMC states.

Targeting FAP⁺ VSMCs reduces plaque burden. (**A**) Single-cell and spatial multiomics map of human coronary arteries in health and disease. (**B**) FAP⁺ cells in the plaque can be noninvasively imaged in patients and are derived from VSMCs. (**C**) In vivo anti-FAP BiTE therapy remodels the vascular microenvironment and reduces atherosclerotic plaque burden. FAP, fibroblast activation protein; VSMCs, vascular smooth muscle cells; BiTE, bi-specific T cell engager. [Figure created with BioRender.com]

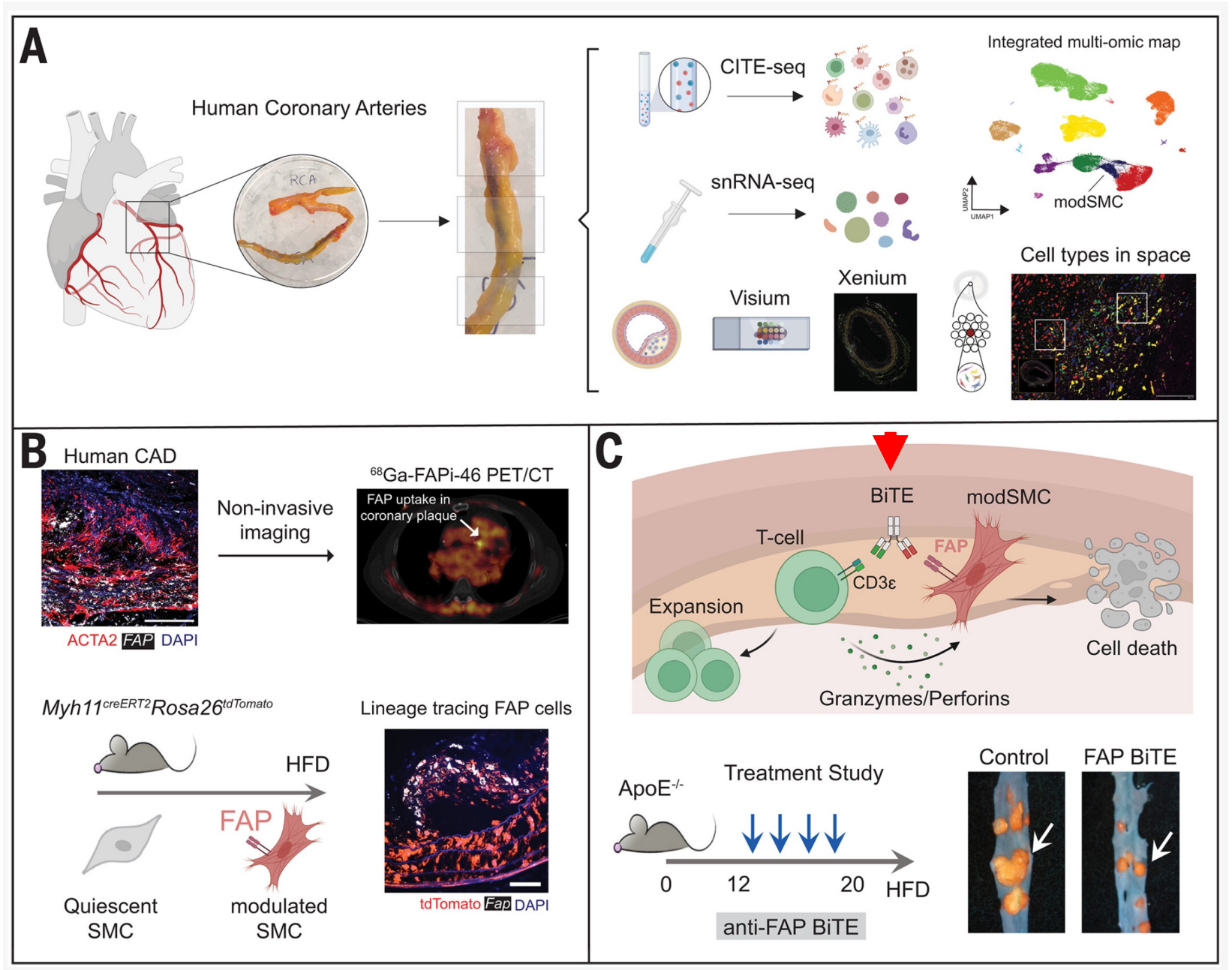

The secrets of the sex lives of octopuses, revealed

Harvard postdoctoral researcher Pablo Villar started studying how octopuses use receptors in their arms to “taste by touch” while hunting prey and exploring. In doing so, his team in a molecular and cellular biology lab eventually stumbled on answers to the birds and the bees of cephalopods getting busy.

Their discovery, outlined in a paper published Thursday in the journal Science, revealed how octopuses essentially have a tongue, an arm, a penis and a sperm cell all rolled into one appendage.

This octopus arm, known as a hectocotylus, looks just like the mollusk’s other seven arms — and also acts like a penis. It delivers a package of sperm directly to the female in a sac containing her internal organs, including ovaries.

You rarely see an octopus use that arm to explore the seafloor or hunt. But the Harvard researchers noticed sensory receptors were present in the mating arm, too, raising the question: Why?

Octopuses are solitary and rarely encounter each other in the wild. So the researchers set out to observe them mate in the lab to monitor their behavior in a more controlled manner.

They placed a male and female California two-spot octopus in a tank divided by an opaque barrier, uncertain whether they’d get aggressive and fight rather than getting intimate. They planned to remove the barrier if all was going well.

What happened next surprised them.

The male wiggled its hectocotylus through an eight-millimeter barrier hole, reaching through the female's mantle cavity.

Scientists did not expect this sight-unseen mating. They saw this with other pairs, even in the dark — but not when both octopuses were male.

The mystery of how octopuses identify females and locate their ovaries unraveled.

The hectocotylus appeared drawn to progesterone, an ovarian hormone.

When two-inch tips of mating arms were severed, they still moved when exposed to the ovarian hormone.

When scientists placed three chemical-coated tubes on the other side of the tank, the male inserted its arm into the one containing progesterone.

Researchers identified a receptor in the arm highly sensitive to progesterone. When making contact with the female's hormone, the arm's sensors activate, charting a path through the oviduct to release sperm.

Tests on other cephalopods, including a squid, found similar hectocotylus responses to the ovarian hormone.

"It's very uncommon that animals merge sensation and reproduction in a single organ," Villar said.

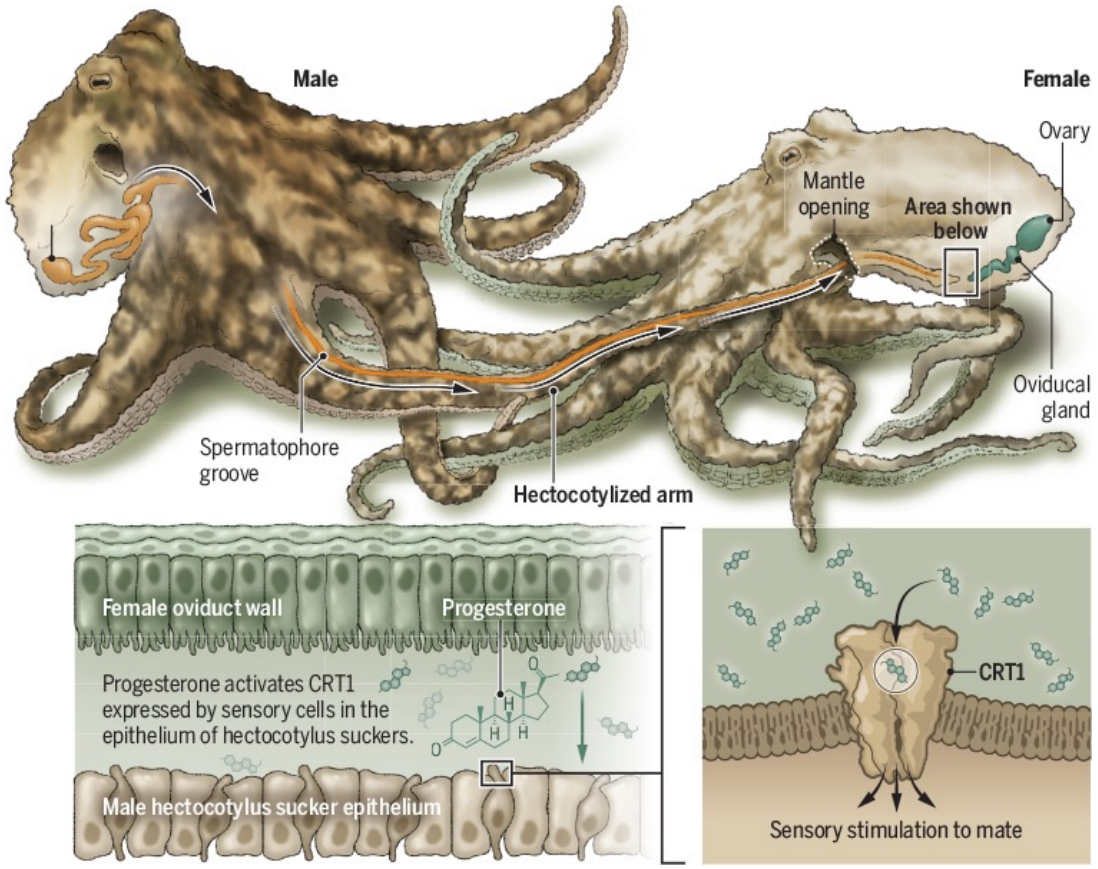

Als Hectocotylus (Plural: Hectocotyli; nach altgriechischen ἑκᾰτόν (hekatón): „hundert“ und κότυλος (kótulos): „Schüssel“, „Napf“) wird ein zum Fortpflanzungsorgan umgebildeter Arm bei männlichen Kopffüßern bezeichnet.

Analyses indicated that chemotactic receptor 1 (CRT1), a ligandgated ion channel, is expressed in the surface epithelium of suckers at the tip of the hectocotylus where it binds to progesterone. CRT1 is also expressed on the nonmating arms of octopus and binds to metabolites such as norharmane, which is produced by microbes on the surface of certain prey. Structural analysis revealed that hectocotylus CRT1 has residues that enable high-affinity binding to progesterone. Progesterone is a conserved hormone, having remained similar across diverse species throughout evolution. The findings of Villar et al. suggest that it became a target of lineage-specific receptor innovation. Thus, a receptor evolved altered specificity. A mating interaction is biased, and if such bias persists across generations, then gene flow may decline. Villar et al. provide a bridge from molecular receptor evolution to mating behavior and potentially to reproductive isolation, the foundation of speciation.